DANIELA ANDRADE FERRARO

Desempenho do ^{68}Ga-PSMA-11 PET/RM em comparação com a ressonância magnética multiparamétrica na biópsia de próstata guiada em pacientes com antígeno prostático específico elevado

(Versão corrigida. Resolução CoPGr 6018/11, de 13 de novembro de 2011. A versão original está disponível na Biblioteca da FMUSP)

São Paulo

2023

DANIELA ANDRADE FERRARO

Desempenho do ^{68}Ga-PSMA-11 PET/RM em comparação com a ressonância magnética multiparamétrica na biópsia de próstata guiada em pacientes com antígeno prostático específico elevado

Tese apresentada à Faculdade de Medicina da Universidade de São Paulo para obtenção do título de Doutor em Ciências.

Programa de Radiologia

Orientador: Prof. Dr. Marcelo Tatit Sapienza

São Paulo

2023

Dados Internacionais de Catalogação na Publicação (CIP)

Preparada pela Biblioteca da
Faculdade de Medicina da Universidade de São Paulo

©reprodução autorizada pelo autor

Ferraro, Daniela Andrade

Desempenho do ^{68}Ga-PSMA-11 PET/RM em comparação com a ressonância magnética multiparamétrica na biópsia de próstata guiada em pacientes com antígeno prostático específico elevado / Daniela Andrade Ferraro. -- São Paulo, 2023.

Tese(doutorado)--Faculdade de Medicina da Universidade de São Paulo. Programa de Radiologia.

Orientador: Marcelo Tatit Sapienza.

Descritores: 1.Tomografia por emissão de pósitrons 2.Imageamento por ressonância magnética multiparamétrica 3.Neoplasias da próstata 4.Biópsia guiada por imagem.

USP/FM/DBD-455/23

Responsável: Erinalva da Conceição Batista, CRB-8 6755

Ferraro DA. Desempenho do ^{68}Ga-PSMA-11 PET/RM em comparação com a ressonância magnética multiparamétrica na biópsia de próstata guiada em pacientes com antígeno prostático específico elevado [doutorado]. São Paulo: Faculdade de Medicina, Universidade de São Paulo; 2023.

Aprovada em: 31/01/2024

BANCA EXAMINADORA

Prof. Dr. Carlos Alberto Buchpiguel

Instituição: Faculdade de Medicina da Universidade de São Paulo

Dra. Lilian Yuri Itaya Yamaga

Instituição: Hospital Israelita Albert Einstein

Dr. Ronaldo Hueb Baroni

Instituição: Hospital Israelita Albert Einstein

Prof. Dr. Marcelo Tatit Sapienza

Instituição: Faculdade de Medicina da Universidade de São Paulo

AGRADECIMENTOS

Aos meus pais, por terem sempre tido como máxima prioridade a educação minha e do meu irmão e pelo maior incentivo que posso ter que é ver o orgulho nos olhos deles a cada conquista minha.

Ao meu irmão, pelo companheirismo desde sempre e todo o apoio durante meu tempo em Zurique.

Aos meus queridos orientadores, Profa. Dra. Irene A. Burger e Prof. Dr. Marcelo Tatit Sapienza, por tudo que me ensinaram nessa jornada e por todo apoio e paciência, com quem divido o mérito de cada linha desse trabalho.

Ao meu amigo e mentor Prof. Dr. Gustav von Schulthess, pela confiança que depositou em mim desde o primeiro momento.

Ao Prof. Dr. Carlos Alberto Buchpiguel pela oportunidade de realizar esse trabalho na Faculdade de Medicina da Universidade de São Paulo.

RESUMO

Ferraro DA. Desempenho do ^{68}Ga-PSMA-11 PET/RM em comparação com a ressonância magnética multiparamétrica na biópsia de próstata guiada em pacientes com antígeno prostático específico elevado [tese]. São Paulo: Faculdade de Medicina, Universidade de São Paulo; 2023.

Introdução: o diagnóstico de câncer de próstata é estabelecido por histologia, sendo necessária biópsia de próstata para a confirmação diagnóstica nos casos com suspeita clínica. A biópsia pode ser sistemática ou guiada por imagem e o método de imagem de escolha é a ressonância multiparamétrica da próstata (RMmp). A tomografia por emissão de pósitrons com antígeno prostático específico de membrana associada à ressonância magnética (^{68}Ga-PSMA-11 PET/RM) tem alta acurácia na detecção do tumor primário da próstata. O ^{68}Ga-PSMA-11 PET/RM pode apresentar maior acurácia para guiar biópsia do que a RMmp. O objetivo desse trabalho foi determinar a acurácia do ^{68}Ga-PSMA-11 PET/RM para guiar biópsia da próstata e comparar seu desemprenho com a RMmp. Métodos: estudo prospectivo incluindo 42 pacientes com antígeno prostático específico (PSA) elevado e ao menos uma lesão suspeita na RMmp (PIRADS ≥3). Os pacientes realizaram ^{68}Ga-PSMA-11 PET/RM e biópsia da próstata consistindo em biópsia guiada por imagem com lesões-alvo apontadas pelo ^{68}Ga-PSMA-11 PET/RM e biópsia sistemática por saturação. O resultado da biópsia foi usado como referência. Posteriormente, em análise retrospectiva, o ^{68}Ga-PSMA-11 PET/RM e a RMmp foram lidos por dois leitores e feita análise comparativa por quadrantes quanto a acurácia na detecção e localização do tumor primário. Também foram coletados parâmetros semiquantitativos no ^{68}Ga-PSMA-11 PET/RM (valor de captação padronizado máximo (SUVmax) e volume tumoral de PSMA [PSMAvol]) e na RMmp (maior diâmetro tumoral e coeficiente de difusão aparente [ADC]). A acurácia do ^{68}Ga-PSMA-11 PET/RM para guiar biópsia e a comparação entre ^{68}Ga-PSMA-11 PET/RM e a RMmp quanto à localização das lesões foi analisada por lesão e por paciente usando tabelas de contingência 2 x 2. A concordância interobservador foi analisada usando o coeficiente kappa de Cohen para localização de lesões e coeficiente de correlação intraclasse para os parâmetros semiquantitativos. Correlação entre o escore de Gleason das lesões e os parâmetros semiquantitativos foi calculado usando a correlação de Spearman. Foram investigados os casos falso-positivos e falso-negativos do ^{68}Ga-PSMA-11 PET/RM e da RMmp com peça cirúrgica quando disponível. Resultados: a acurácia do ^{68}Ga-PSMA-11 PET/RM para guiar biópsia foi de 90% com sensibilidade de 96% e especificidade de 81%. Trinta e cinco porcento dos pacientes tiveram tumor diagnosticado somente pela biópsia por saturação e 8% somente pela biópsia guiada pelo ^{68}Ga-PSMA-11 PET/RM. A análise por quadrantes demonstrou acurácia de 83,3 % para o ^{68}Ga-PSMA-11 PET/RM e 81,4 % para a RMmp (p = 0,56). A concordância interobservador para localização de lesões foi substancial para os dois métodos e quase perfeita para os parâmetros

semiquantitativos do ^{68}Ga-PSMA-11 PET e diâmetro tumoral e moderada para ADC. Houve correlação do grau tumoral com os parâmetros semiquantitativos do ^{68}Ga-PSMA-11 PET, mas não com os da RMmp. Conclusão: o ^{68}Ga-PSMA-11 PET/RM tem boa acurácia para guiar biópsia da próstata. ^{68}Ga-PSMA-11 PET/RM e RMmp apresentam acurácia semelhante na localização do tumor primário da próstata e são métodos complementares na detecção de tumores perdidos por um dos métodos. ^{68}Ga-PSMA-11 PET/RM e RMmp apresentam concordância interobservador substancial. Os parâmetros semiquantitativos do ^{68}Ga-PSMA-11 PET apresentaram correlação com o grau do tumor primário de próstata, ao contrário dos parâmetros da RMmp, que não apresentaram correlação.

Palavras-chave: Tomografia por emissão de pósitrons. Imageamento por ressonância magnética multiparamétrica. Neoplasias da próstata. Biópsia guiada por imagem.

ABSTRACT

Ferraro DA. Diagnostic performance of ^{68}Ga-PSMA-11 PET/MR in comparison to multiparametric magnetic resonance imaging for prostate biopsy-guidance in patients with elevated prostate specific antigen [thesis]. São Paulo: “Faculdade de Medicina, Universidade de São Paulo”; 2023.

Introduction: prostate cancer diagnosis is stablished by histopathology through biopsy. Prostate biopsy can be systematic or guided by imaging and multiparametric resonance magnetic imaging (mpMRI) is the method of choice for the latter. Positron emission tomography with prostate specific membrane antigen associated with resonance magnetic imaging (^{68}Ga-PSMA-11 PET/MR) has high accuracy for the detection of the primary tumor. ^{68}Ga-PSMA-11 PET/MR has the potential to guide prostate biopsy. Methods: this is a prospective study including 42 patients with high prostate specific antigen (PSA) and at least one suspicious lesion on mpMRI (PIRADS ≥3). Patients underwent ^{68}Ga-PSMA-11 PET/MR and saturation and ^{68}Ga-PSMA-11 PET/MR-guided prostate biopsy. Biopsy result was used as standard reference. In a later retrospective analysis ^{68}Ga-PSMA-11 PET/MR and mpMRI were read by two readers for a comparative quadrant-based analysis for detection and localization of the primary lesion. Semiquantitative parameters were collected for ^{68}Ga-PSMA-11 PET (maximum standardized uptake value (SUVmax) and PSMA tumor volume [PSMAvol]) and for mpMRI (maximum tumor length and apparent diffusion coefficient [ADC]). ^{68}Ga-PSMA-11 PET/MR accuracy to guide biopsy and the comparison of ^{68}Ga-PSMA-11 PET/MR and mpMRI for localization of lesions were done in a patient-based and quadrant-based analysis using 2 x 2 contingency tables. Interobserver agreement was analysed using Cohen´s kappa coefficient for lesion localization and intraclass correlation coefficient for semiquantitative parameters. Correlation of Gleason score and semiquantitative parameters was calculated using Spearman’s rank correlation. False-positive and false-negative findings of ^{68}Ga-PSMA-11 PET/MR and mpMRI were investigated using the prostatectomy specimen when available. Results: ^{68}Ga-PSMA-11 PET/MR accuracy to guide biopsy was 90%, sensitivity of 96% and specificity of 81%. Thirty-five percent of patients had tumor diagnosed only by systematic biopsy and 8% only by image-guided biopsy. Quadrant-based analysis showed accuracy of 83,3% for PET-PSMA/MR and 81,4% for mpMRI ($p = 0,56$). Interreader agreement for lesion localization was substantial for both methods and almost perfect for ^{68}Ga-PSMA-11 PET semiquantitative parameters and tumor length and moderate for ADC. ^{68}Ga-PSMA-11 PET semiquantitative parameters correlated with Gleason score whilst mpMRI parameters did not. Conclusion: ^{68}Ga-PSMA-11 PET/MR has good accuracy for prostate biopsy-guidance. ^{68}Ga-PSMA-11 PET/MR and mpMRI have similar accuracy for tumor localization and are complementary methods for the detection of lesions missed by one of the methods. ^{68}Ga-PSMA-11 PET/MR and mpMRI have substantial interreader agreement. ^{68}Ga-PSMA-11 PET semiquantitative parameters correlate with Gleason score whilst mpMRI parameters do not.

Key words: Positron-emission tomography. Multiparametric magnetic resonance imaging. Prostatic neoplasms. Image-guided biopsy.

LISTA DE ABREVIATURAS E SIGLAS

AJCC	-	Comitê Conjunto Americano de Câncer
CT	-	Tomografia computadorizada
GS	-	Escore de Gleason
ISUP	-	Sociedade Internacional de Uropatologia
PET	-	Tomografia por emissão de pósitrons
PET/CT	-	Tomografia por emissão de pósitrons/Tomografia computadorizada
PET-PSMA	-	Tomografia por emissão de pósitrons com antígeno prostático específico de membrana
PSA	-	Antígeno prostático específico
PSMA	-	Antígeno prostático específico de membrana
PSMAvol	-	Volume tumoral de PSMA
RM	-	Ressonância magnética
RMmp	-	Ressonância magnética multiparamétrica
SUVmax	-	Valor de captação padronizado máximo
US	-	Ultrassonografia

SUMÁRIO

1 INTRODUÇÃO 11
1.1 CÂNCER DE PRÓSTATA 12
1.2 BIÓPSIA DA PRÓSTATA 14
1.2.1 Biópsia sistemática 16
1.2.2 Biópsia guiada por imagem 20
1.2.3 PET com ligantes de PSMA (PET-PSMA) 21
1.2.4 PET/RM 22
1.3. JUSTIFICATIVA 23
2 OBJETIVOS 24
2.1 OBJETIVO PRIMÁRIO 25
2.2 OBJETIVOS SECUNDÁRIOS 25
3 TEXTO SISTEMATIZADO 26
3.1 ORGANIZAÇÃO DO TEXTO SISTEMATIZADO 27
3.2 PUBLICAÇÃO 1 28
3.3 PUBLICAÇÃO 2 57
4 ANÁLISE CRÍTICA E PERSPECTIVAS 82
5 CONCLUSÕES 86
REFERÊNCIAS 88
ANEXOS 94

1 INTRODUÇÃO

1.1 CÂNCER DE PRÓSTATA

O câncer de próstata representa a neoplasia maligna mais comum entre os homens no Brasil, tendo sido responsável por 15.841 óbitos em 2020 e com uma incidência estimada de 71.730 casos em 2022 (INCA, 2022). Além da mortalidade, a morbidade relacionada ao câncer e ao seu tratamento tem impacto negativo na qualidade de vida dos pacientes, com sintomas relacionados principalmente à disfunção sexual e urinária (Lardas et al., 2017).

O tipo histológico mais comum é o adenocarcinoma acinar, que se desenvolve em 70% das vezes na zona periférica da próstata (Robbins; Kumar; Cotran, 2010). Mais da metade dos tumores são multifocais, com relatos de 60% a 90% de multifocalidade na literatura sendo comum a ocorrência de tumores concomitantes com graus histológicos variados na glândula. Da mesma maneira, as lesões são heterogêneas quanto ao grau histológico, podendo haver regiões de graus histológicos diferentes dentro de uma mesma lesão (Arora et al., 2004; Andreoiu; Cheng, 2010).

A suspeita clínica do tumor é geralmente levantada por aumento nos níveis séricos de antígeno prostático específico (PSA) e/ou exame físico de toque retal alterado e o diagnóstico é feito por amostragem histológica (Mottet et al., 2017; Moses et al., 2023). As principais diretrizes atuais concordam que apenas um dos parâmetros pode ser suficiente para justificar a biópsia caso traga suspeita alta de câncer, como pacientes com PSA > 10 ou pacientes com toque retal com alta suspeição mesmo que com PSA < 3 (Mottet et al., 2017, Moses et al., 2023).

O grau histológico tumoral proveniente da biópsia é definido pelo escore de Gleason (GS) e classificação mais recente proposta pela Sociedade Internacional de Uropatologia (ISUP) (Iczkowski; van Leenders; van der Kwast, 2021). Ambos escores dividem as neoplasias de acordo com suas características histológicas e atribuem a elas uma numeração. Essa numeração é crescente conforme o aumento de atipias no tumor e conforme o distanciamento das suas características histológicas do tecido glandular normal. O GS é calculado pela soma dos dois padrões histológicos dominantes em um tumor, sendo atualmente aceita uma escala que varia de 3 a 5 (menor grau 3+3=6 e maior grau 5+5=10). Já a classificação de ISUP propõe uma escala crescente de grau tumoral que varia de 1 a 5, que tem correspondência com o GS.

O grau histológico tem correlação com prognóstico e definição de tratamento. Pacientes com tumores com graus mais altos tem maior chance de recorrência de doença após o tratamento (Epstein et al., 2016). Por este motivo é fundamental que a biópsia seja acurada e consiga identificar o foco tumoral mais agressivo no caso de tumores multifocais e, dentro de uma mesma lesão, a região mais agressiva do tumor.

Levando em consideração parâmetros histológicos, as neoplasias podem ser divididas em clinicamente significantes e clinicamente insignificantes. Essa classificação baseia-se no fato de que pacientes com tumores clinicamente significantes têm maior risco de metástases, menor sobrevida e maior frequência de eventos adversos relacionados ao câncer em relação aos pacientes com tumores clinicamente insignificantes, e, por isso, a classificação é um dos parâmetros utilizados para discriminar os pacientes que devem ser tratados e aqueles que podem ficar em vigilância (Mottet et al., 2017), evitando sobrediagnóstico e tratamento desnecessário em pacientes que provavelmente não teriam morbimortalidade significativa relacionada à doença. A classificação de tumor clinicamente significante não é consenso, com algumas definições levando em consideração apenas o grau histológico do tumor, enquanto outras consideram além disso o tamanho do tumor na amostra da biópsia (Ahmed et al., 2011). Ainda que essa definição varie entre os centros, uma definição comumente utilizada atualmente é a de que tumores com escore de GS maior ou igual que 3 + 4 = 7 / ISUP 2 são clinicamente significantes e tumores com GS de 3 + 3 = 6 / ISUP 1 são clinicamente insignificantes. Essa definição também foi adotada em comum pelos principais ensaios clínicos recentes que avaliaram métodos de imagem para guiar biópsia de próstata, como o PRECISION, PROMIS e MRI-FISRT (Ahmed et al., 2017; Rouvière et al., 2019; Emmett et al., 2021).

O estadiamento da neoplasia de próstata segue o padrão TNM do Comitê Conjunto Americano de Câncer (AJCC). Em sua edição mais recente publicada em 2017, a neoplasia primária de próstata (T) é classificada de acordo com a extensão do envolvimento da glândula prostática e presença de extensão extraprostática ou invasão de órgãos adjacentes, sendo essa informação especialmente importante para a definição da abordagem cirúrgica nos casos com indicação de prostatectomia radical (Byrd et al., 2017).

1.2 BIÓPSIA DA PRÓSTATA

O diagnóstico de câncer de próstata é estabelecido por histologia, sendo necessária biópsia de próstata para a confirmação diagnóstica nos casos com suspeita clínica. A técnica de biópsia pode variar em relação à via de acesso à glândula, ao número de amostras retiradas, à abordagem podendo ser sistemática ou guiada por métodos de imagem e, nesse último caso, também em relação ao método utilizado para guiar a biópsia.

O acesso à glândula é mais comumente realizado por via transretal ou transperineal. Os métodos acessam a próstata por vias diferentes, ambos com auxílio do ultrassom com probe endorretal. A via transretal é realizada com agulhas que atravessam o reto enquanto na transperineal as agulhas acessam a próstata por via transcutânea pelo períneo com auxílio de uma grade localizatória com coordenadas (Figuras 1 e 2). Trabalhos anteriores não mostraram diferença entre as duas vias em termos de eficiência diagnóstica quando o mesmo número de amostras é retirado (Hara et al., 2008; Takenaka et al., 2008; Abdollah et al., 2011; Grummet, 2017). Estudos mais recentes mostram desvantagem da via transretal por complicações sangramento retal e infecção de forma que, em biópsias com amostragem extensa, a via transperineal é geralmente preferida pelo baixo risco de sepse (Mottet et al., 2017; Xiang et al., 2019).

Figura 1 - Esquema de biópsia transperineal usando grade localizatória com matriz quadriculada com coordenadas para orientação da posição e furos para inserção das agulhas de biópsia. De acordo com a região da próstata ao ultrassom que se pretende atingir, o sistema informa ao médico em qual coordenada a agulha deve ser inserida

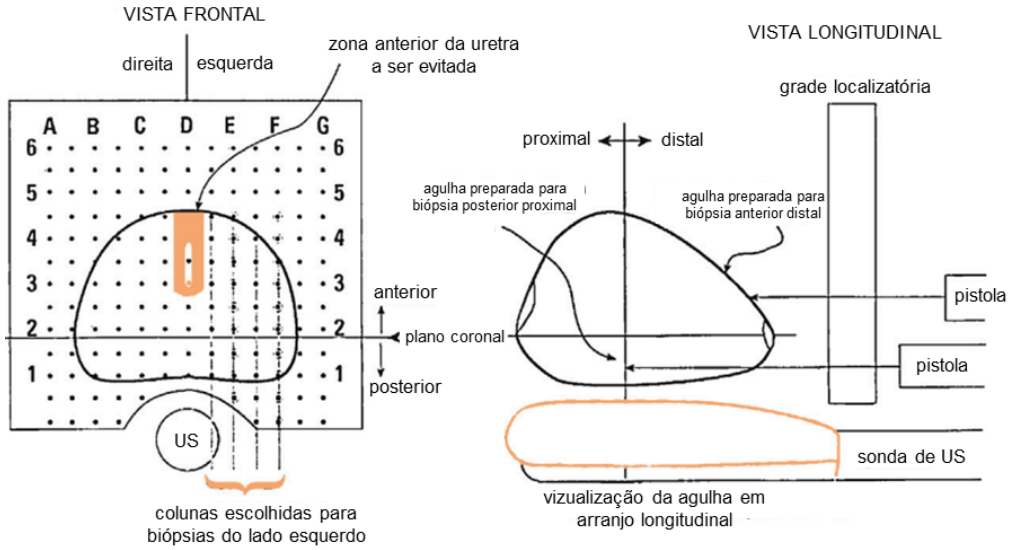

Fonte: adaptado de Singh et al. (2014).

Figura 2 - Sistema de hardware de aparelho usado para biópsia de próstata guiada por ultrassonografia. À esquerda na figura sistema de hardware de biópsia guiada por ultrassonografia consistindo de sonda de ultrassom retal, grade localizatória e aparelho de ultrassonografia portátil. À direita na figura o sistema posicionado com phantom representando a posição da próstata do paciente (*prostate*), grade localizatória (*needle guide*), sonda de ultrassonografia retal (*probe*) e dispositivo de fixação acoplado à mesa cirúrgica e à sonda para localização nos três eixos da agulha de biópsia (*stepper*)

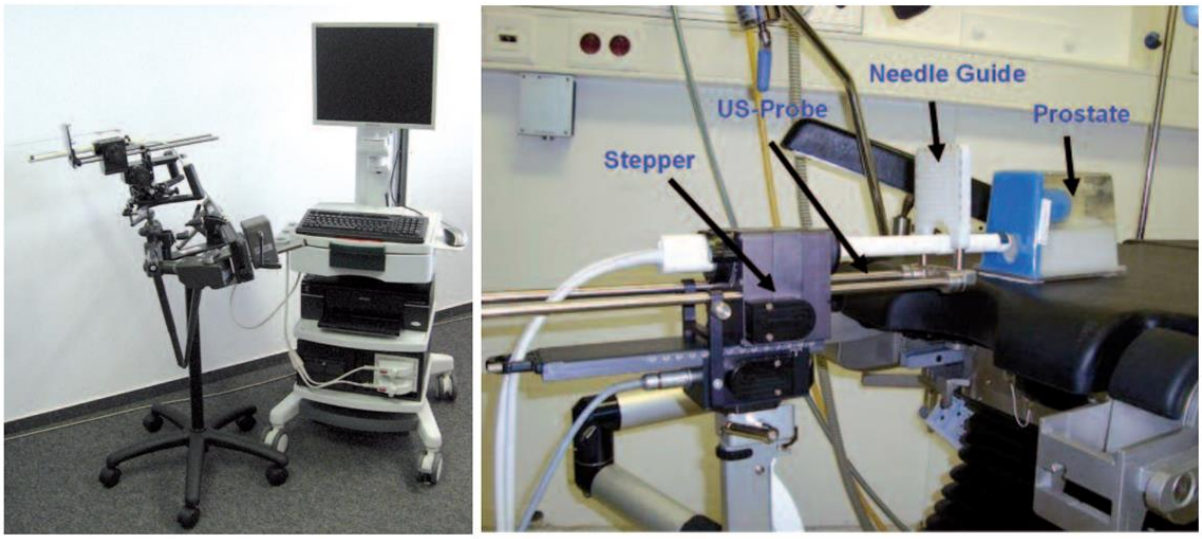

Fonte: Zogal et al. (2011).

As principais possíveis complicações do procedimento são sangramento (hematúria, hematospermia e sangramento retal), sintomas de trato urinário baixo incluindo retenção urinária, disfunção erétil, infecção e dor. A ocorrência de complicações pode estar relacionada a diversos fatores como idade e comorbidades do paciente, tamanho da próstata, técnica de biópsia e número de biópsias prévias.

Medidas para diminuir o risco de complicações incluem analgesia adequada, suspensão de medicações anticoagulantes quando possível e profilaxia com antibióticos. De qualquer maneira, a maioria dos sintomas relacionados a complicações de biópsia de próstata são leves e autolimitados, com casos raros de necessidade de internação hospitalar (Borghesi et l., 2017), havendo vantagem da via transperineal em relação à via transretal pelo menor risco de complicação infecciosa (Mottet et al., 2017; Roberts et al., 2017; Xiang et al., 2019).

Na biópsia sistemática, amostras são retiradas de áreas pré-determinadas de acordo com a segmentação da glândula na tentativa de encontrar um tumor de localização desconhecida, já na guiada por imagem uma lesão suspeita identificada por algum método de imagem é alvo da biópsia. Os dois métodos também podem ser empregados juntos no mesmo procedimento, na tentativa de aumentar a chance de diagnosticar um tumor clinicamente significante. Cada um desses métodos é explicado em mais detalhes a seguir.

1.2.1 Biópsia sistemática

A biópsia sistemática da próstata, como já citado anteriormente, não tem como alvo uma lesão específica, mas consiste em retirar amostras de diversas áreas da próstata para tentar identificar uma neoplasia de localização desconhecida na glândula. A ultrassonografia é utilizada para guiar essa biópsia, auxiliando na correta identificação das áreas da glândula a serem amostradas e na localização das agulhas. É importante que as zonas prostáticas de interesse sejam representadas na biópsia e por isso as áreas a serem biopsiadas são pré-definidas com base na segmentação da próstata. De acordo com a segmentação usada pelo *Prostate Imaging Reporting and Data System* (PIRADS v 2.1) (Turkbey et al., 2019), a glândula é dividida em ápice, terço médio e base, e cada uma dessas regiões é subdividida em zonas periférica, central, de transição e estroma anterior e, ainda, em lados direito e esquerdo com base na linha média da próstata, além de subdivisões das zonas periférica e central, determinando 38 áreas. Além disso, a divisão inclui, ainda, duas áreas para as vesículas seminais direita e esquerda e uma para a uretra, totalizando 41 áreas (Figura 3).

Figura 3 - Segmentação prostática

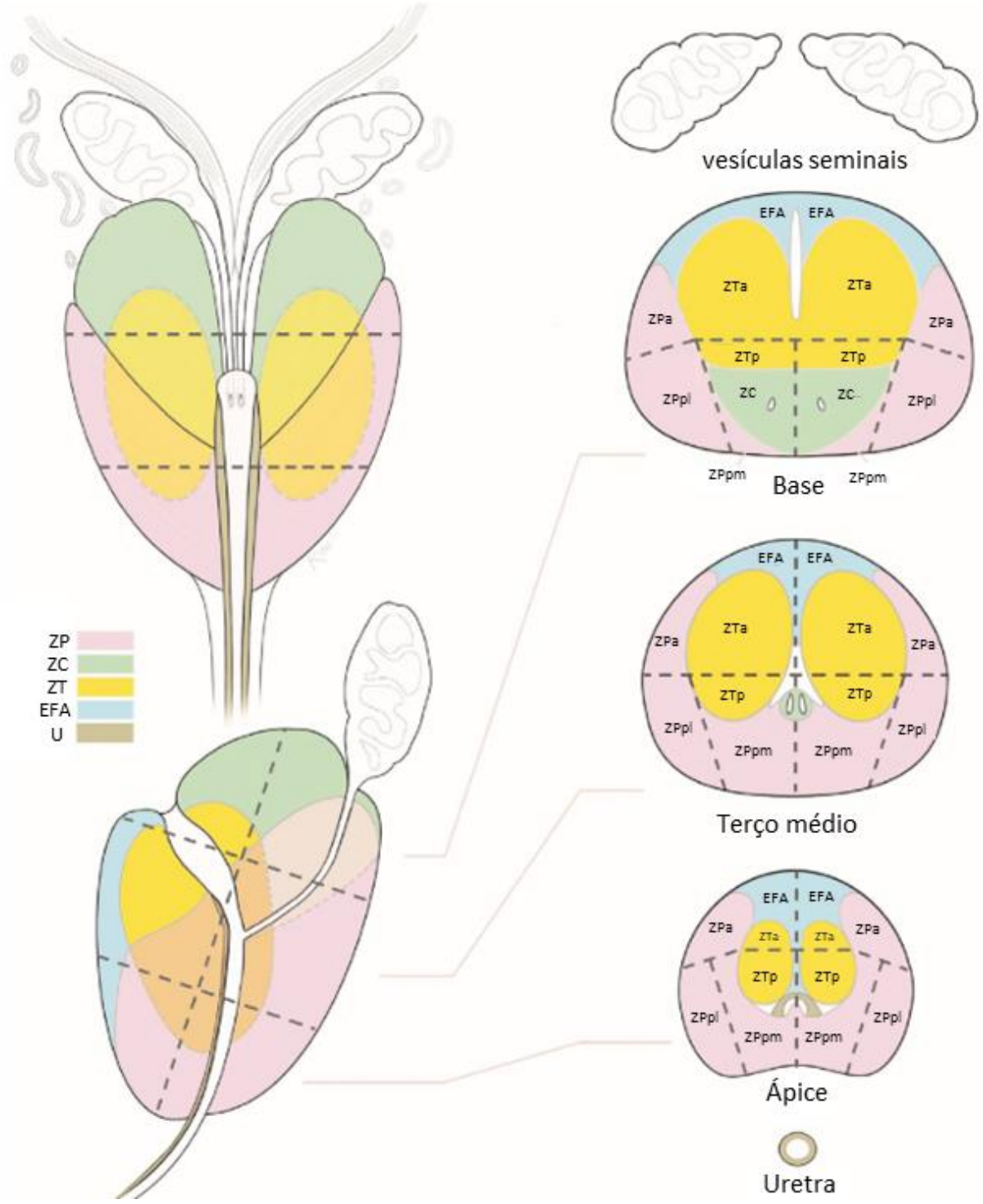

ZP: zona periférica; ZC: zona central; ZT: zona de transição; U: uretra; EFA: estroma fibromuscular anterior.
Fonte: adaptado de Turkbey et al. (2019).

O número de amostras retiradas no procedimento é variável dependendo da técnica e tamanho da glândula. Segundo diretriz europeia conjunta da Associação Europeia de Urologia, Sociedade Europeia de Radioterapia e Oncologia e Sociedade Internacional de Oncogeriatria para rastreio, diagnóstico e tratamento do câncer de

próstata clinicamente localizado, as amostras devem incluir ambos os lados da próstata, da base ao ápice e o número mínimo recomendado é de 12 amostras (Eichler et al., 2006; Mottet et al., 2017). No esquema padrão de 12 amostras sistemáticas a glândula é dividida em seis regiões (ápice, terço médio e base, cada uma delas subdividida em direita e esquerda), com duas amostras de cada uma delas. Porém, a sensibilidade para a detecção de câncer clinicamente significante de próstata desse esquema de biópsia é baixa, num estudo prospectivo recente com 576 pacientes a sensibilidade foi de 48% (Ahmed et al., 2017), existindo a possibilidade de erros de amostragem e falha no diagnóstico da neoplasia clinicamente significante. Dentre as falhas diagnósticas possíveis encontram-se falha em atingir qualquer tumor com as agulhas resultando numa biópsia falso-negativa, falha em alcançar o tumor mais agressivo no cenário de doença multifocal e falha em alcançar a região mais agressiva dentro do tumor principal (Figura 4). Como o grau tumoral é definidor de prognóstico e tratamento do paciente, é fundamental que seja identificada pela biópsia a lesão de maior grau, no caso de pacientes com tumores multifocais, e a área de maior grau dentro da lesão principal. Por esse motivo, visando uma maior acurácia da biópsia, foram desenvolvidos métodos de biópsia sistemática com amostragem extensa da próstata como a biópsia por saturação e mapeamento.

Figura 4 - Representação dos possíveis erros de amostragem da neoplasia de próstata pela biópsia. À esquerda na figura a biópsia atinge apenas tecido não-neoplásico e perde o tumor. Na imagem do meio a biópsia atinge apenas foco de neoplasia clinicamente insignificante e perde o foco mais agressivo numa próstata com tumor multifocal. À imagem da direita a biópsia atinge o foco tumoral principal porém apenas na sua região de menor agressividade, perdendo a região do tumor de maior grau

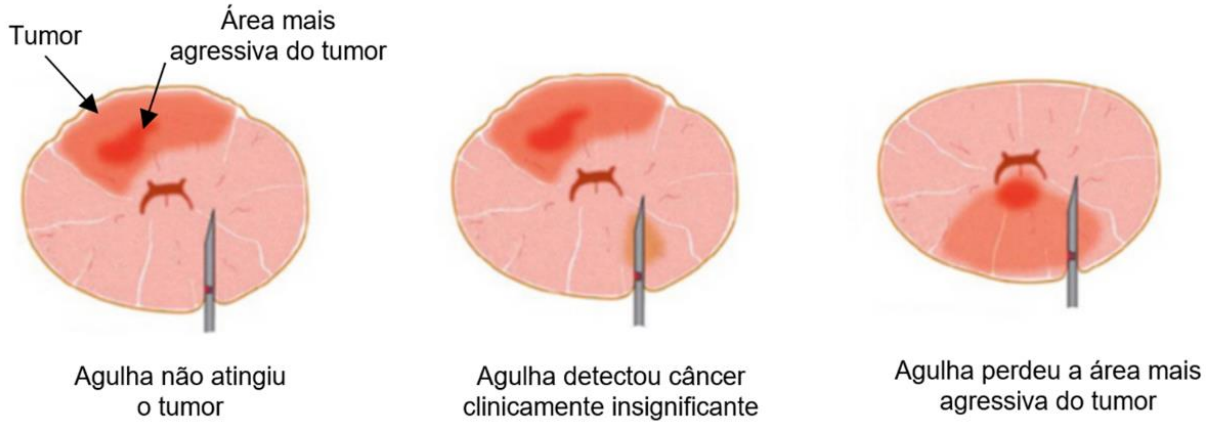

Fonte: adaptado de Goldberg (2023).

A biópsia de próstata por saturação é caracterizada pela retirada de múltiplas amostras em número maior do que na biópsia padrão, sendo 18 ou 20 amostras comumente aceito como número mínimo, que pode ainda ser adaptado ao volume glandular com mais amostras retiradas. O método visa abranger todo tecido prostático com representação extensa de todos os segmentos da glândula diminuindo a probabilidade de um resultado falso-negativo. Uma metanálise demonstrou haver vantagem da biópsia inicial por saturação em relação à biópsia padrão na detecção de câncer, principalmente em próstatas com volume acima de 40 mL (Jiang et al., 2013), o que já havia sido demonstrado usando o corte de volume prostático de 55 mL, com taxas de detecção de 31,5% da biópsia com 18 amostras contra 24,8% da biópsia com 12 amostras (Scattoni et al., 2008).

Outro método de biópsia com amostragem extensa é a biópsia por mapeamento. Nesse tipo de biópsia a abordagem é usualmente transperineal e uma grade localizatória de braquiterapia com furos distando 5 mm entre eles é usada para posicionar as agulhas e retirar amostras a cada 5 mm do tecido prostático. Nesse tipo de biópsia o número de amostras colhidas depende do volume prostático e a taxa de detecção pode chegar a 92% e a sensibilidade na detecção de neoplasia clinicamente significante encontrada num estudo com média de 54 amostras foi de 95% (Crawford et al., 2005).Entretanto, existem considerações importantes a respeito de abordagens mais invasivas com maior número de amostras, como a necessidade de anestesia geral ou raquidiana para maior conforto do paciente e o maior potencial de complicações destacando-se infecções e retenção urinária (Pepe; Aragona, 2013). Além disso, a detecção de tumores clinicamente insignificantes é maior nesse tipo de abordagem (Crawford et al., 2005). Uma alternativa é guiar a biópsia por métodos de imagem, atingindo lesões-alvo suspeitas aos métodos na tentativa de aumentar a eficiência do procedimento para a detecção de câncer clinicamente significante sem a necessidade de coleta de um número alto de amostras.

1.2.2 Biópsia guiada por imagem

A biópsia guiada por imagem consiste no uso de método de imagem para detectar as lesões suspeitas, permitindo direcionar a retirada de amostras de cada lesão-alvo detectadas pela imagem. Atualmente, o exame de escolha para guiar a biópsia é a ressonância magnética multiparamétrica (RMmp).

Para evitar as dificuldades da realização da biópsia no equipamento de ressonância magnética (RM), em geral é feita a correlação da localização das lesões-alvo apontadas pela RM com a ultrassonografia (US). A US endorretal auxilia a localizar a glândula e averiguar a posição da agulha, mas, devido a sua limitada sensibilidade para o câncer de próstata, não é usado para identificar as lesões suspeitas (Onur et al., 2004; Smeenge et al., 2012; Rouvière et al., 2019) e por este motivo, deve ser aplicado método que permita transpor a informação da RMmp para o US.

O método mais simples é a correlação visual das imagens pelo médico responsável pela biópsia, que irá identificar as lesões suspeitas detectadas na RMmp e identificar as áreas correspondentes na US (“fusão” cognitiva), para, a seguir, proceder a biópsia das lesões-alvo. A fusão também pode ser feita com auxílio de softwares, que transpõem a posição da lesão na RM para a imagem do US, baseado em marcos anatômicos ou no delineamento da glândula pelo próprio médico (Zogal et al., 2011).

A RM tem sensibilidade e especificidade para câncer clinicamente significante entre 58 e 96% e 23% e 87%, respectivamente (Fütterer et al., 2015). Num estudo prospectivo com 576 pacientes a especificidade por paciente encontrada para tumores clinicamente significantes variou entre 41% e 47% (Ahmed et al., 2017). A sensibilidade por lesão levando em conta cada foco de neoplasia clinicamente significante é estimada em 65% (Johnson et al., 2019) e a realização exclusiva da biópsia guiada por RM leva a perda de lesões clinicamente significantes, seja por limitação de sensibilidade do método ou por discordância entre a posição da lesão na imagem de RM e o tecido efetivamente biopsiado no procedimento guiado por US.

A literatura mostra que os dados de biópsia guiada por ressonância magnética não são suficientes para dispensar a biópsia sistemática e que 14% a 20% das lesões clinicamente significantes são perdidas se somente uma das

técnicas for utilizada (Rouvière et al., 2019). Por esse motivo, diversos centros usam a combinação das técnicas de biópsia guiada por ressonância e biópsia sistemática no mesmo procedimento, com em geral três a cinco amostras de cada lesão suspeita associada a retirada de 10 a 12 amostras sistemáticas para cobrir o restante da glândula. Ainda assim, um estudo prospectivo mostrou que cerca de 14,4% dos pacientes são subclassificados com escores de Gleason menores do que o real encontrado na peça cirúrgica de prostatectomia (Ahdoot et al., 2020).

1.2.3 PET com ligantes de PSMA (PET-PSMA)

O antígeno prostático específico de membrana (PSMA) é uma proteína transmembrana expressa no tecido prostático normal e com intensidade de expressão de 100 a 1000 vezes maior no câncer de próstata. Apenas cerca de 6% dos adenocarcinomas de próstata se mostram PSMA-negativos na imunohistoquímica (Minner et al., 2011). Além disso, a expressão de PSMA nos tumores de próstata tem correlação com o grau tumoral, sendo maior nos tumores de grau mais alto (Bravaccini et al., 2018).

O desenvolvimento de ligantes de PSMA marcados com radioisótopos emissores de pósitron permite a caracterização *in vivo* do câncer de próstata por meio da tomografia por emissão de pósitrons com antígeno prostático específico de membrana (PET-PSMA). As moléculas ligantes de PSMA mais amplamente utilizadas atualmente são marcadas com ^{68}Ga ou, mais recentemente, ^{18}F. Apesar de diferenças na biodistribuição e forma de excreção entre os traçadores, ambos são considerados equivalentes em termos de prática clínica e os centros de medicina nuclear tendem a optar por um deles de acordo com questões práticas e de disponibilidade (Diesel et al., 2017; Eiber et al., 2017) Alguns dos traçadores mais utilizados para imagem são o ^{18}F-DCFPyL, ^{18}F-PSMA-1007, ^{68}Ga-PSMA-11 ou ^{68}Ga-PSMA-HBED-CC, ^{68}Ga-PSMA I&T, entre outros (Eiber et al., 2017). Ao longo da última década o PET-PSMA tem sido empregado de forma crescente na investigação do câncer de próstata em diferentes cenários clínicos, com destaque para o estadiamento e reestadiamento em casos de recorrência bioquímica.

No estadiamento, apesar da sensibilidade ainda limitada demonstrada em metanálises, o PET-PSMA é o método de imagem com maior capacidade de detecção de disseminação para linfonodos e ossos (Perera et al., 2020; Tu et al., 2020). Os

estudos incluídos nas metanálises foram realizados utilizando traçadores marcados com ^{68}Ga, notadamente ^{68}Ga-PSMA-11. O método é considerado por alguns autores como a modalidade de imagem de primeira linha para estadiamento do câncer de próstata de alto risco no momento do diagnóstico. Estudo prospectivo mostrou que o PET/CT com ^{68}Ga-PSMA-11 traz informações com impacto de mudança de conduta em 27% dos pacientes em relação à imagem de estadiamento convencional (Hofman et al., 2020).

Metanálise sobre o impacto do PET-PSMA em pacientes com recorrência bioquímica (11 estudos, 908 pacientes) mostrou mudança de conduta em 54% dos pacientes, apesar da heterogeneidade de cenários clínicos (Han et al., 2018), sendo indicado na investigação de pacientes com PSA superior a 0,2 ng/mL após a prostatectomia radical (Cornford et al., 2021).

Ao lado de seu emprego mais frequente para estadiamento e reestadiamento do câncer de próstata, o PET-PSMA apresenta também alta acurácia para detecção do tumor primário da próstata clinicamente significante, com sensibilidade de 90% encontrada em metanálise que incluiu estudos usando traçadores marcados com ^{68}Ga (Perera et al., 2020).

A maioria dos estudos que avaliaram acurácia e impacto na conduta do PET-PSMA foram realizados com PET/CT. Entretanto, a RM é superior à tomografia computadorizada (CT) na avaliação da próstata, fornecendo maior detalhamento anatômico que permite diferenciação entre as zonas prostáticas e identificação de lesões. Nesse sentido, a combinação do PET com a RM (PET/RM) tem potencial de ser superior ao PET/CT na avaliação de pacientes com câncer de próstata diagnosticado ou suspeitado.

1.2.4 PET/RM

O PET/RM é uma modalidade de imagem relativamente recente, com o primeiro escâner integrado disponível no mercado em 2011. O desenvolvimento da técnica com a possibilidade de aquisição simultânea de imagens de PET e de RM em protocolos otimizados tornaram o estudo factível num tempo tolerável para o paciente e vantajoso em termos de detalhamento anatômico e avaliação funcional, além de menor exposição à radiação ionizante em comparação com o PET/CT (Evangelista et al., 2021). O PET/MRI é superior ao PET/CT para estadiamento local

de neoplasias pélvicas (Catalano et al., 2013). Estudo com ^{68}Ga-PSMA-11 PET/RM mostrou especificidade do método de até 97% na detecção do tumor primário de próstata (Eiber et al., 2016) Isso foi confirmado em uma metanálise que mostrou que a especificidade do PET/RM com ligante de PSMA, medida por lesão na próstata, é de 90,9% (Evangelista et al., 2021). Num estudo prospectivo que comparou achados do PET/RM com a peça cirúrgica de prostatectomia, os autores encontraram forte correlação da captação de ^{18}F-DCFPyL e alterações na RM com a lesão prostática dominante (Bauman et al., 2018).

Dessa maneira, a união da alta sensibilidade e especificidade para detecção de câncer de próstata clinicamente significante do PET-PSMA com a resolução anatômica da RM fazem com que a técnica tenha o potencial de aprimorar a seleção de pacientes para realização de biópsia de próstata e ser o método de imagem ideal para guiar a biópsia nos casos em que for indicada. A alta acurácia do PET/RM com PSMA na detecção do tumor primário clinicamente significante idealmente permitiria poupar da biópsia pacientes com imagem negativa. Em contrapartida, o exame poderia ser usado para guiar a biópsia em pacientes com imagem positiva. Isso reduziria a necessidade da biópsia sistemática, bem como a chance de biópsia falso-negativa ou com grau tumoral subestimado.

1.3. JUSTIFICATIVA

Com base nos dados disponíveis na literatura, levantou-se a hipótese que o PET-PSMA possa aumentar a acurácia diagnóstica da investigação de câncer de próstata clinicamente significante em relação a investigação utilizando a RMmp. A associação do PET-PSMA à RM em um único procedimento (PET-PSMA/RM) tem o potencial de guiar a biópsia da próstata, combinando a alta acurácia do PET-PSMA para neoplasia de próstata com a resolução anatômica da RM. Esta associação de métodos com a finalidade de guiar biópsia de tumores de próstata não foi estudada de forma prospectiva até o início do presente trabalho.

2 OBJETIVOS

2.1 OBJETIVO PRIMÁRIO

- Determinar a acurácia do ^{68}Ga-PSMA-11 PET/RM para guiar biópsia da próstata usando o resultado da biópsia de saturação como padrão-ouro.

2.2 OBJETIVOS SECUNDÁRIOS

- Comparar o desempenho do ^{68}Ga-PSMA-11 PET/RM com a RMmp na localização do tumor primário de próstata.
- Investigar os casos falsos-negativos e falsos-positivos do ^{68}Ga-PSMA-11 PET/RM bem como os casos de discordância entre o ^{68}Ga-PSMA-11 PET e a RMmp pela análise da peça cirúrgica da prostatectomia quando disponível.
- Comparar a análise da concordância interobservador para o ^{68}Ga-PSMA-11 PET/RM e RMmp na localização do tumor primário de próstata.
- Investigar a correlação dos parâmetros semiquantitativos do ^{68}Ga-PSMA-11 PET/RM e RMmp com o grau tumoral.

3 TEXTO SISTEMATIZADO

3.1 ORGANIZAÇÃO DO TEXTO SISTEMATIZADO

O texto sistematizado refere-se às seguintes publicações, que cobrem os objetivos desta tese:

Publicação 1: **FERRARO DA**, Becker AS, Kranzbühler B, Mebert I, Baltensperger A, Zeimpekis KG, Grünig H, Messerli M, Rupp NJ, Rueschoff JH, Mortezavi A, Donati OF, Sapienza MT, Eberli D, Burger IA. Diagnostic performance of 68Ga-PSMA-11 PET/MRI-guided biopsy in patients with suspected prostate cancer: a prospective single-center study. Eur J Nucl Med Mol Imaging. 2021 Sep;48(10):3315-3324.

Objetivo principal: determinar a acurácia do ^{68}Ga-PSMA-11 PET/RM para guiar biópsia da próstata usando o resultado da biópsia de saturação como padrão-ouro.

Objetivo secundário: investigar os casos falsos-negativos e falsos-positivos do ^{68}Ga-PSMA-11 PET/RM.

Status: publicado em 23 de fevereiro de 2021.

Publicação 2: **FERRARO DA**, Hötker AM, Becker AS, Mebert I, Laudicella R, Baltensperger A, Rupp NJ, Rueschoff JH, Müller J, Mortezavi A, Sapienza MT, Eberli D, Donati OF, Burger IA. 68Ga-PSMA-11 PET/MRI versus multiparametric MRI in men referred for prostate biopsy: primary tumour localization and interreader agreement. Eur J Hybrid Imaging. 2022 Jul 18;6(1):14.

Objetivo principal: comparar o desempenho do ^{68}Ga-PSMA-11 PET/RM com a RMmp na localização do tumor primário de próstata.

Objetivos secundários: investigar os casos de discordância entre o ^{68}Ga-PSMA-11 PET e a RMmp pela análise da peça cirúrgica da prostatectomia quando disponível; comparar a análise da concordância interobservador para o ^{68}Ga-PSMA-11 PET/RM e RMmp na localização do tumor primário de próstata; investigar a correlação dos parâmetros semiquantitativos do ^{68}Ga-PSMA-11 PET/RM e RMmp com o grau tumoral.

Status: publicado em 18 de julho de 2022.

3.2 PUBLICAÇÃO 1

FERRARO DA, Becker AS, Kranzbühler B, Mebert I, Baltensperger A, Zeimpekis KG, Grünig H, Messerli M, Rupp NJ, Rueschoff JH, Mortezavi A, Donati OF, Sapienza MT, Eberli D, Burger IA. Diagnostic performance of 68Ga-PSMA-11 PET/MRI-guided biopsy in patients with suspected prostate cancer: a prospective single-center study. Eur J Nucl Med Mol Imaging. 2021 Sep;48(10):3315-3324.

O estudo teve por objetivo avaliar a acurácia da biópsia guiada pelo ^{68}Ga-PSMA-11 PET/RM no diagnóstico do câncer primário da próstata clinicamente significante, usando como método de referência o escore de Gleason da biópsia por saturação. Também permitiu investigar os casos falsos-negativos ou falsos-positivos do ^{68}Ga-PSMA-11 PET/RM, com análise da peça cirúrgica derivada da prostatectomia, quando disponível. Para isso, foram incluídos pacientes com suspeita de câncer de próstata devido a elevação de PSA e alteração suspeita na RMmp. Esses pacientes realizaram ^{68}Ga-PSMA-11 PET/RM para identificação das lesões suspeitas, essas posteriormente submetidas a biópsia guiada, associada a biópsia sistemática por saturação. A escolha da biópsia por saturação como método de referência se deve ao fato dos pacientes incluídos não obrigatoriamente terem câncer confirmado pela biópsia e, naqueles com câncer confirmado, nem todos terem indicação de cirurgia da próstata, inviabilizando a análise da peça cirúrgica como padrão-ouro. A acurácia foi calculada por paciente e por lesão e, para fins de comparação com a literatura, foram estabelecidas duas definições de câncer clinicamente significante: 1) ISUP ≥ 3 ou tamanho ≥ 6mm na biópsia e 2) ISUP ≥ 2.

Em uma coorte final de 42 pacientes, a acurácia do ^{68}Ga-PSMA-11 PET para câncer clinicamente significante por paciente, usando-se a localização da lesão na imagem e todas as biópsias retiradas dessa região, foi de 90%, com sensibilidade de 96% e especificidade de 81% (pela definição 1 de câncer significante). Quando foram consideradas apenas as amostras provenientes das biópsias guiadas, houve uma queda de acurácia, o que significa que lesões-alvo vistas ao ^{68}Ga-PSMA-11 PET não foram atingidas pela biópsia guiada. O fato de lesões-alvo vistas no ^{68}Ga-PSMA-11 PET e transpostas para a biópsia com auxílio do software de fusão serem perdidas na biópsia guiada e detectadas na biópsia sistemática da mesma região merece uma melhor análise

crítica.

A maioria dos tumores clinicamente significantes foi detectada tanto pela biópsia sistemática por saturação quanto pela biópsia guiada pelo ^{68}Ga-PSMA-11 PET, porém 35% dos pacientes tiveram tumor diagnosticado somente pela biópsia sistemática por saturação e 8% tiveram o câncer diagnosticado somente pela biópsia guiada pelo ^{68}Ga-PSMA-11 PET. Ressalta-se que foi retirado um elevado número de amostras sistemáticas neste estudo (mediana de 43) e que a biópsia sistemática por saturação também encontrou um maior número câncer clinicamente insignificante, podendo levar a *overdiagnosis* e *overtreatment*.

A análise de falso-positivos e falso-negativos ao ^{68}Ga-PSMA-11 PET mostrou que quase a totalidade dos falso-positivos tratava-se de tumores clinicamente insignificantes que poderiam ser classificados como verdadeiros positivos dependendo da definição de tumor clinicamente significante. Houve um único paciente com resultado falso-negativo ao ^{68}Ga-PSMA-11 PET, relacionado a um tumor sem expressão de PSMA na imunohistoquímica da amostra de biópsia.

Em relação à RMmp de inclusão dos pacientes, o ^{68}Ga-PSMA-11 PET discriminou o único paciente com câncer clinicamente significante classificado como PIRADS 3 e discriminou quase todos os pacientes sem câncer clinicamente significante que haviam sido classificados como PIRADS 4.

Em conclusão, o estudo mostrou que o ^{68}Ga-PSMA-11 PET/RM mostrou alta acurácia na detecção de câncer de próstata clinicamente significante e é uma ferramenta promissora que pode ajudar na seleção de pacientes para biópsia, bem como para guiá-la.

Segue-se o texto do artigo conforme publicado originalmente em inglês na referência acima mencionada:

Diagnostic performance of 68Ga-PSMA-11 PET/MRI-guided biopsy in patients with suspected prostate cancer: a prospective single-center study

Daniela A. Ferraro[1,2], Anton S. Becker[3,4], Benedikt Kranzbühler[5], Iliana Mebert[1,5], Anka Baltensperger[1,5], Konstantinos G. Zeimpekis[1], Hannes Grünig[1], Michael Messerli[1], Niels J. Rupp[6], Jan H. Rueschoff[6], Ashkan Mortezavi[5], Olivio F. Donati[3], Marcelo T. Sapienza[2], Daniel Eberli[5], Irene A. Burger[1,7,8]

1 Department of Nuclear Medicine, University Hospital Zurich, University of Zurich, Zurich, Switzerland
2 Department of Radiology and Oncology, Faculdade de Medicina FMUSP, Universidade de Sao Paulo, Sao Paulo, Brazil
3 Institute of Interventional and Diagnostic Radiology, University Hospital Zurich, University of Zurich, Zurich, Switzerland
4 Department of Radiology, Memorial Sloan Kettering Cancer Center, New York City, NY, USA
5 Department of Urology, University Hospital Zürich, University of Zurich, Zurich, Switzerland
6 Department of Pathology and Molecular Pathology, University Hospital Zurich, University of Zurich, Zurich, Switzerland
7 Department of Nuclear Medicine, Kantonsspital Baden, Baden, Switzerland
8 Department of Nuclear Medicine, University Hospital Zürich, Rämistrasse 100, 8091 Zürich, Switzerland

Corresponding author: Irene A. Burger, irene.burger@usz.ch

Abstract

Purpose Ultrasound-guided biopsy (US biopsy) with 10–12 cores has a suboptimal sensitivity for clinically significant prostate cancer (sigPCa). If US biopsy is negative, magnetic resonance imaging (MRI)–guided biopsy is recommended, despite a low specificity for lesions with score 3–5 on Prostate Imaging Reporting and Data System (PIRADS). Screening and biopsy guidance using an imaging modality with high accuracy could reduce the number of unnecessary biopsies, reducing side effects. The aim of this study was to assess the performance of positron emission tomography/MRI with 68Ga-labeled prostate-specific membrane antigen (PSMA-PET/MRI) to detect and localize primary sigPCa (ISUP grade group 3 and/or cancer core length ≥ 6 mm) and guide biopsy. **Methods** Prospective, open-label, single-center, non-randomized, diagnostic accuracy study including patients with suspected PCa by elevation of prostate-specific antigen (PSA) level and a suspicious lesion (PIRADS ≥3) on multiparametric MRI (mpMRI). Forty-two patients underwent PSMA-PET/MRI followed by both PSMA-PET/MRI-guided and section-based saturation

template biopsy between May 2017 and February 2019. Primary outcome was the accuracy of PSMA-PET/MRI for biopsy guidance using section-based saturation template biopsy as the reference standard. **Results** SigPCa was found in 62% of the patients. Patient-based sensitivity, specificity, negative and positive predictive value, and accuracy for sigPCa were 96%, 81%, 93%, 89%, and 90%, respectively. One patient had PSMA-negative sigPCa. Eight of nine false-positive lesions corresponded to cancer on prostatectomy and one in six false-negative lesions was negative on prostatectomy. **Conclusion** PSMA-PET/MRI has a high accuracy for detecting sigPCa and is a promising tool to select patients with suspicion of PCa for biopsy. **Trial registration** This trial was retrospectively registered under the name “Positron Emission Tomography/Magnetic Resonance Imaging (PET/MRI) Guided Biopsy in Men with Elevated PSA” (NCT03187990) on 06/15/2017 (https://clinicaltrials.gov/ct2/show/NCT03187990).

Introduction

Assessment of histological tumor grade on biopsy is needed for diagnosis and risk classification of prostate cancer (PCa). The updated European Association of Urology (EAU) guideline recommends ultrasound-guided systematic prostate biopsy (US biopsy) in patients with suspicion of PCa [1, 2]. Magnetic resonance imaging (MRI)–guided biopsy is considered for cases in which no cancer was detected [2]. The PROMIS trial revealed sensitivity of only 48% for their primary definition of clinically significant cancer (sigPCa) using 10–12 cores US biopsy and suggested that, instead, multiparametric MRI (mpMRI) should be used to reduce the number of unnecessary biopsies. However, if all lesions with a score ≥ 3 on Prostate Imaging Reporting and Data System (PIRADS) are targeted, the specificity of mpMRI is only 41% [3]. Several other studies also showed superior detection rates of sigPCa in MRI-guided biopsy compared to US biopsy [4–7]. Nevertheless, false-negative results or histological upgrade after surgery are found in 21% of patients [8–10]. The most reliable method to reduce undersampling and false-negative results is transperineal saturation biopsy (template biopsy) with samples taken from all 20 Barzell zones, leading to organ coverage of approximately 95% [10]. Screening and imaging-guided biopsy could potentially reduce side effects of saturation prostate biopsies [11], but recent studies suggest that a template-based systematic approach should not be omitted despite mpMRI [6, 12]. Positron emission tomography

(PET)/MRI targeting prostate-specific membrane antigen (PSMA) could be an ideal technique to improve the accuracy of imaging-guided biopsies, combining the high sensitivity and specificity of PSMA-PET for PCa with the high anatomical contrast and spatial resolution of MRI [13–15]. Despite promising results in PSMA-PET/computed tomography (CT) for biopsy targeting [16], with an accuracy of 80.6% for sigPCa [17], the diagnostic accuracy of PSMA-PET/MRI-guided biopsy has not yet been prospectively assessed. Therefore, the aim of this study is to assess the performance of 68Ga-PSMA-11 PET/MRI (PSMA-PET/MRI) to detect and localize primary sigPCa for accurate prostate biopsy guidance.

Patients and methods

Study design

The study was designed as an open-label, single-center, non-randomized, prospective diagnostic accuracy study including patients with suspected PCa. Patients without biopsy-proven sigPCa but suspicion of cancer due to persistently elevated prostate-specific antigen (PSA) (PSA > 2.5 ng/ml if age 30– 50 years and PSA > 4 ng/ml if age 50–80 years) and at least one suspicious lesion on mpMRI clinical report (PIRADS ≥3) were included. All patients underwent PSMA-PET/MRI followed by both PSMA-PET/MRI-guided and section-based saturation template biopsy of the prostate between May 2017 and February 2019. Exclusion criteria were age < 30 and > 80, previous biopsy within 8 weeks prior to imaging, previous pelvic irradiation, prostatectomy, transurethral resection of the prostate (TURP) or androgen deprivation hormonal therapy (ADT), and any contra-indication to MRI or prostate biopsy as well active urinary tract infection or indwelling catheter. PSMA-PET/MRI and biopsy were performed with an interval of up to 30 weeks from mpMRI (median 2.7 weeks, IQR 0.4–12). Figure 1 illustrates patient selection. This study was approved by the institutional review board (BASEC Nr: 2017-00016), was carried out in accordance with the Declaration of Helsinki, and is registered in the international trial registry ClinicalTrials.gov (NCT03187990).

68Ga-PSMA-11 PET/MRI imaging acquisition and analysis

All patients underwent a pelvic PET/MRI on a hybrid scanner (SIGNA PET/MR, GE Healthcare, Waukesha, WI, USA) 60 min after injection of 85 MBq of 68Ga-PSMA-11. A 15- min frame over the prostate was recorded, allowing reducing

the dose since patients without confirmed cancer were included. For biopsy targeting, suspected lesions were delineated on PSMA-PET/MRI by a double-board-certified nuclear medicine physician and radiologist, specialist in pelvic imaging, with 10 and 5 years of experience (IAB,MM), with a maximum of three target lesions. Imaging protocol and analysis are given in the supplements (Online Resource 1).

Biopsy

Biopsies were performed under general anesthesia by specialized urologists with US-MRI software fusion (BiopSee®). Axial fused PSMA-PET/MRI images in DICOM format were uploaded to BiopSee® instead of T2w MRI sequences. Standard transperineal template biopsy with number of cores adapted to prostate volume as well as PSMA-PET/MRI-targeted biopsy was performed with a maximum of three cores per target lesion (Online Resource 2). Patients with no suspicious uptake on PSMA-PET/MRI or with discordant lesions between PSMA-PET/MRI and mpMRI underwent template biopsy and the urologist was free to target any suspicious lesion on mpMRI.

Clinically significant cancer definition

SigPCa was defined as International Society of Urological Pathology (ISUP) grade group 3 and/or cancer core length ≥ 6 mm [18]. Conversely, clinically insignificant cancer (insigPCa) was defined as ISUP 1 or 2 lesions with cancer core length < 6 mm. Biopsies with the latter characteristics were classified as negative for further analysis. Results based on other definition of sigPCa (ISUP ≥2) are in Table S3 (Online Resource 1).

Reference standard

Results of PSMA-PET/MRI-targeted biopsies were compared to template biopsies regarding presence of sigPCa on histopathology. All patients classified as having a false-positive or false-negative 68Ga-PSMA-11 PET/MRI result had the biopsy samples, or radical prostatectomy (RPE) specimens if available, reevaluated on histopathology for possible explanations including PSMA immunohistochemistry (IHC). Biopsies and RPE specimens were evaluated by two board-certified genitourinary pathologists (NR, JR) with 8–10 years of experience.

Data analysis

Study results were analyzed using descriptive statistics and frequency tables in Excel (Excel2016, Microsoft, USA). Accuracy was assessed on 2 × 2 contingency tables on patient and lesion basis. For lesion-based analysis, the number of lesions was defined as number of PSMA-positive lesions added to number of PSMA-negative lesions with sigPCa found on biopsy. For patient-based analysis in patients with more than one lesion and different classifications (for example, one true-positive and one false-negative lesion), we considered whether PSMA-PET/MRI correctly staged the patient regarding the presence or absence of sigPCa according to Table S1 (Online Resource 1). We also assessed patient-based accuracy for PET/MRI-targeted cores.

Results General

Forty-nine patients met the inclusion criteria and were included between May 2017 and January 2020. Seven patients withdrew participation before the PSMA-PET/MRI scan or the biopsy was performed; therefore, data from 42 patients were analyzed (descriptive characteristics in Table 1). Median interval between PSMA-PET/MRI and biopsy was 12 days (interquartile range (IQR) 6–18)

Biopsy

Based on template and targeted biopsy, 26 of 42 (62%) patients had sigPCa. While there was no malignancy in seven of 42 patients (17%), in the remaining nine patients (21.4%), cancer detected on biopsy did not meet the criteria of sigPCa. Fifteen cases of sigPCa were detected by both template and targeted biopsies (58%, 15/26), nine only by template (35%) and two only by targeted (8%). Two cases of insigPca were detected by both biopsy methods (22%, 2/9), six only by template (67%) and one only by targeted. Table 2 and Fig. 2 show the distribution of sigPCa, insigPCa, and no disease, in correlation to PIRADS, ISUP, and PSMA-PET/MRI result. Eighteen patients had one lesion, seven patients had two, and one patient had three lesions, resulting in 35 sigPCa lesions in total. The median number of positive cores per patient was three (IQR 2–6). The median number of samples taken per patient was 43 (IQR 36–44). Eight patients (19%, 8/42) had biopsy procedure complications, none life-threatening. Six patients presented to the emergency department for acute urinary retention, one patient had postinterventional bleeding with need of catheter irrigation, and one patient with anesthesia complications was

admitted for observation and released the day after.

68Ga-PSMA-11 PET/MRI

Table 3 shows sensitivity, specificity, positive predictive value (PPV), negative predictive value (NPV), and accuracy of PSMA-PET/MRI per patient and per lesion. PSMA-PET/MRI was positive in 28 patients (66.7%, 28/42), of which 25 had sigPCa on biopsy (89%, 25/28) and negative in 14 patients (33.3%, 14/42), of which only one had sigPCa (7%, 1/14) (Figs. 2b and 3a). Nineteen patients had one PSMA-positive lesion, eight patients had two lesions, and one patient had three lesions, resulting in 38 PSMA-positive lesions. One patient had a lesion without PSMA uptake but clear PIRADS 5 features on MRI, confirmed as sigPCa by MRI-targeted biopsy and classified as negative PSMA-PET/MRI for further analysis. Figure 3b shows PSMA-PET/MRI results in relation to PIRADS. The accuracy of PSMA-targeted cores was lower compared to PSMA-PET/MRI imaging findings. In eight cases with PSMA uptake in the sigPCa lesion, the three target needles were negative, but additional adjacent template needles confirmed sigPCa. Per lesion, 44 lesions were detected in 29 patients (38 on PSMA-PET/MRI and 35 on biopsy, with 29 concordant lesions). Six sigPCa lesions and 24 insigPCa lesions were not detected by PSMA-PET/MRI.

False-positive PSMA-PET/MRI

Three patients had a false-positive PSMA-PET/MRI, but insigPCa on biopsy in at least one of the PSMA uptake areas (ISUP grade group 2 with cancer length of 1.5–5 mm). Relevant cancer was confirmed on RPE specimen in all three cases (Fig. 4). Per lesion, nine lesions were false-positive (Online Resource 3). In all patients, RPE was available and showed cancer in eight lesions (Table 4). In the case without cancer, additional pathology workup showed clear PSMA overexpression on IHC, but no benign or malignant alterations. Interval between biopsy and RPE in these patients ranged from 1 to 3.8 months.

False-negative PSMA-PET/MRI

68Ga-PSMA-11 PET/MRI was false-negative in one patient with sigPCa, who had two positive cores with ISUP grade group 2 and lengths of 9 and 10 mm. Despite no PSMA uptake, the lesion was easily appreciated on T2- and diffusion-weighted sequences of the MRI component (Fig. 5). Per lesion, six were false-negatives

(Online Resource 4). In four lesions, ISUP grade was low or tumor volume small (up to 3 mm) on biopsy. In one case, there was no cancer on RPE in the corresponding location of the positive biopsy core (Table 4). One lesion with positive cores of ISUP grade group 4 (6 mm) was downgraded to ISUP grade 2 on RPE and in one lesion (ISUP 2, 10 mm) biopsy cores stained for PSMA on IHC showed a PSMA-negative tumor (Fig. 5). The interval between biopsy and RPE in these patients ranged from 1.4 to 3.7 months.

Discussion

PSMA-PET/MRI showed a patient-based accuracy of 90% for detecting sigPCa in our cohort, with a sensitivity of 96% and specificity of 81%. This is higher than the mpMRI accuracy reported in most studies using template biopsy as reference standard [19], including the PROMIS trial, which reported sensitivity and specificity of 93% and 41%, respectively [3]. Our improved specificity was mainly due to PSMA-PET mitigating false-positive mpMRI PIRADS 3 and 4 lesions harboring no sigPCa (Fig. 3b). The PROMIS authors conclude that screening by mpMRI prior to biopsy could reduce the number of unnecessary biopsies. Our study suggests PSMA-PET/MRI could further improve on mpMRI patient selection. In our cohort, 16 patients (38%) without sigPCa underwent biopsy based on equivocal or suspicious lesions on mpMRI (PIRADS 3 to 5). Omitting biopsy in patients with negative PSMA-PET/MRI would have spared 13 (13/16, 81%), without missing any patient with sigPCa. Only one patient had a false-negative PSMA-PET result; however, his ISUP 2 tumor would not have been missed due to clear PIRADS 5 features on MRI. The tumor was PSMA-negative on IHC, which is in accordance with the reported rate of around 5% of PSMA-negative tumors in the literature [20]. For the three patients with false-positive PSMA-PET/MR results, insigPCa was present on template biopsy, and cancer with Gleason 4 pattern was confirmed on RPE in each case. Interestingly, despite PET findings confirmed by biopsy in 90% of the cases, the accuracy of 71% with a sensitivity of 65% for PET-targeted biopsy shows that some of the sigPCa lesions seen on PET are actually missed by the three targeted cores. This was already reported by van der Leest et al. [9] in a study comparing transrectal US-guided biopsy versus MRI-guided biopsy. They found that positive TRUS cores were obtained from the mpMRI lesion area or its neighboring and suggested that four additional perilesional cores greatly improved sigPCa detection with MRI-guided biopsy. They concluded that the majority of sigPCa missed by targeted biopsy was

probably due to sampling errors related to spatial heterogeneity of the tumor [9]. False-negative and false-positive lesions in our study were often lesions with borderline characteristics regarding clinical significance. The lower PSMA expression in Gleason pattern 3 compared to 4 has been demonstrated on IHC [20–22] and our results probably reflect it: most false-negative lesions corresponded to low-grade groups (ISUP 1 and 2) or small volume tumors and, in only one case, a significant PSMA-negative tumor. Omitting template biopsy in our cohort would leave undetected six sigPCa, but also 24 lesions with insigPCa, mitigating overdiagnosis. On the other hand, eight of nine false-positive lesions based on biopsy were insigPCa, with only one showing no cancer on RPE specimen. This case was previously published as a case report with extensive histopathology workup excluding inflammation, pre-cancerous lesions, or other malignancies [23]. Therefore, template and targeted biopsies were false-negative for significant disease for eight lesions. The definition of sigPCa is not standardized among centers; therefore, we chose the definition used in the PROMIS trial [3] to allow a direct comparison of our results. We recognize that other definitions can be found in the literature and that more recent guidelines of the EAU suggest considering any ISUP grade group 2 biopsy as sigPCa [1, 2]. Incorporating this cutoff, we would have had only one false-positive PET in our cohort on per-patient analysis, but four false-negative PET scans. Therefore, we also give the results using this other definition of sigPCa in Tables S2 and S3 (Online Resource 1). There is sparse literature on PSMA-PET/CT-guided biopsy. Recently, PSMA-PET/CT was compared, for biopsy purposes, to micro-ultrasound, a novel imaging technique with promising results when added to mpMRI [24]. PSMA-PET/CT yielded an accuracy of 83% versus 61% of micro-ultrasound [25]. No study so far compared PSMA-PET/CT to PET/MRI for biopsy guidance. In our limited experience (anecdotal data not included in present study), delineating the prostate and PSMA-positive lesions on non-contrast-enhanced CT using US-fusion-software is feasible but cumbersome. In a study with 31 patients, sensitivity and specificity for sigPCa of PSMA-PET/CT-guided biopsy was 100% and 68% [17]. The higher sensitivity and lower specificity compared to our study may be explained by the approach to biopsy the prostate area with highest PSMA uptake if no suspicious lesion was reported. This probably led to false-positives, which could be ruled out by MRI but not by CT, such as activity in the central zone [26]. Another study found a region-based sensitivity of PET/CT for sigPCa of 61%, lower than our lesion-based

sensitivity (83%). However, patients did not undergo mpMRI so no insights on PET/CT limitations compared to PET/MRI could be drawn [27]. A prospective study showed higher detection rate of sigPCa for PET/CT compared to 12- core TRUS biopsy; however, biopsies were performed within the CT scanner, and again mpMRI was not performed routinely [28]. In a study with 97 patients that compared PSMA-PET/CT with mpMRI, PSMA-PET/CT identified 25% of patients with Gleason 7 tumors missed by mpMRI [29]. Due to their inclusion criteria, around half of the patients that were biopsied had contra-indications to mpMRI or PIRADS 1 or 2; what makes it difficult to compare their results to ours but rather offers nice complementary data. Interestingly, these results are similar to the results found by the same group in a smaller cohort using 11CCholine PET/CT, with 26% of patients with Gleason 7 tumors detected by PET in patients with negative or contra-indication to mpMRI [30]. Advantages of PET/MRI over PET/CT are that surgeons are already used to delineate prostate and target lesions based on MRI and that they can target lesions by both PSMA-PET and MRI in case of discordance. That a combination of these both methods could further improve the sensitivity for detecting PCa was already shown by Eiber et al. [13]. While PET/ MRI profits from the higher soft tissue contrast, studies performing head-to-head comparisons are needed to investigate whether this offsets the higher general availability and lower cost of PET/CT. Moreover, post hoc image fusion of MRI and PSMA-PET (from PET/CT) may be a viable option for centers without a dedicated PET/MRI device. Despite the good coverage of template biopsy, absence of RPE specimen as reference standard in some cases is a limitation of this study. Given that RPE specimen were not available for all patients, we opted to use RPE results only to investigate false-positive or false-negative lesions on PSMA-PET/MRI. Another limitation is pre-selection of patients based on mpMRI results. The aim of this proof-of-mechanism study was to assess whether PSMA-PET/MR could add value to mpMRI. Given that the probability of sigPCa in patients with PIRADS 1–2 is very low, we opted to exclude those patients in a first step. However, this limits the conclusion about the accuracy of PET scans in an mpMRI naïve population.

Conclusions

PSMA-PET/MRI has a high accuracy for detecting sigPCa and is a promising tool to select patients for biopsy as well as to guide it, with the potential to

substantially reduce unnecessary biopsies compared to mpMRI and might even improve the detection of sigPCa in comparison to systematic template biopsies.

Declarations

Ethics approval This study was performed in line with the principles of the Declaration of Helsinki. Approval was granted by the Cantonal Ethics Committee of Zurich (Date: 03/23/2017/ BASEC Nr: 2017-00016).

Consent to participate Informed consent was obtained from all individual participants included in the study.

Conflict of interest I. A. B. has received research grants and speaker honorarium from GE Healthcare, research grants from Swiss Life, and speaker honorarium from Bayer Health Care and Astellas Pharma AG. M. M. received speaker fees from GE Healthcare. The Department of Nuclear Medicine holds an institutional Research Contract with GE Healthcare. N. J. R. has provided consultancy services (advisory board member) to F. Hoffmann- La Roche AG. A. S. B. received research grants from the Prof. Dr. Max Cloëtta Foundation, medAlumni UZH, and the Swiss Society of Radiology. All other authors declare no competing interests.

Open Access This article is licensed under a Creative Commons Attribution 4.0 International License, which permits use, sharing, adaptation, distribution and reproduction in any medium or format, as long as you give appropriate credit to the original author(s) and the source, provide a link to the Creative Commons licence, and indicate if changes were made. The images or other third party material in this article are included in the article's Creative Commons licence, unless indicated otherwise in a credit line to the material. If material is not included in the article's Creative Commons licence and your intended use is not permitted by statutory regulation or exceeds the permitted use, you will need to obtain permission directly from the copyright holder. To view a copy of this licence, visit http://creativecommons.org/licenses/by/4.0/.

References

1. Cornford P, Bellmunt J, Bolla M, Briers E, De Santis M, Gross T, et al. EAU-ESTRO-SIOG guidelines on prostate cancer. Part II: treatment of relapsing, metastatic, and castration-resistant prostate cancer. Eur Urol. 2017;71:630–42.

https://doi.org/10.1016/j. eururo.2016.08.002.

2. Mottet N, Bellmunt J, Bolla M, Briers E, Cumberbatch MG, De Santis M, et al. EAU-ESTRO-SIOG guidelines on prostate cancer. Part 1: screening, diagnosis, and local treatment with curative intent. Eur Urol. 2017;71:618–29. https://doi.org/10.1016/j.eururo. 2016.08.003.
3. Ahmed HU, El-Shater Bosaily A, Brown LC, Gabe R, Kaplan R, Parmar MK, et al. Diagnostic accuracy of multi-parametric MRI and TRUS biopsy in prostate cancer (PROMIS): a paired validating confirmatory study. Lancet. 2017;389:815–22. https://doi.org/10. 1016/S0140-6736(16)32401-1.
4. Schoots IG, Roobol MJ, Nieboer D, Bangma CH, Steyerberg EW, Hunink MG. Magnetic resonance imaging-targeted biopsy may enhance the diagnostic accuracy of significant prostate cancer detection compared to standard transrectal ultrasound-guided biopsy: a systematic review and meta-analysis. Eur Urol. 2015;68:438–50. https://doi.org/10.1016/j.eururo.2014.11.037.
5. Valerio M, Donaldson I, Emberton M, Ehdaie B, Hadaschik BA, Marks LS, et al. Detection of clinically significant prostate cancer using magnetic resonance imaging-ultrasound fusion targeted biopsy: a systematic review. Eur Urol. 2015;68:8–19. https://doi.org/10. 1016/j.eururo.2014.10.026.
6. Ahdoot M, Wilbur AR, Reese SE, Lebastchi AH, Mehralivand S, Gomella PT, et al. MRI-targeted, systematic, and combined biopsy for prostate cancer diagnosis. N Engl J Med. 2020;382:917–28. https://doi.org/10.1056/NEJMoa1910038.
7. Kasivisvanathan V, Rannikko AS, Borghi M, Panebianco V, Mynderse LA, Vaarala MH, et al. MRI-targeted or standard biopsy for prostate-cancer diagnosis. N Engl J Med. 2018;378:1767–77. https://doi.org/10.1056/NEJMoa1801993.
8. Kasivisvanathan V, Dufour R, Moore CM, Ahmed HU, Abd-Alazeez M, Charman SC, et al. Transperineal magnetic resonance image targeted prostate biopsy versus transperineal template prostate biopsy in the detection of clinically significant prostate cancer. J Urol. 2013;189:860–6. https://doi.org/10.1016/j.juro.2012.10.009.
9. van der Leest M, Cornel E, Israel B, Hendriks R, Padhani AR, Hoogenboom M, et al. Head-to-head comparison of transrectal ultrasound-guided prostate biopsy versus multiparametric prostate resonance imaging with subsequent magnetic resonance-guided biopsy in biopsy-naive men with elevated prostate-specific

antigen: a large prospective multicenter clinical study. Eur Urol. 2019;75: 570–8. https://doi.org/10.1016/j.eururo.2018.11.023.

10. Mortezavi A, Marzendorfer O, Donati OF, Rizzi G, Rupp NJ, Wettstein MS, et al. Diagnostic accuracy of multiparametric magnetic resonance imaging and fusion guided targeted biopsy evaluated by Transperineal template saturation prostate biopsy for the detection and characterization of prostate cancer. J Urol. 2018;200:309–18. https://doi.org/10.1016/j.juro.2018.02.067.
11. Loeb S, Vellekoop A, Ahmed HU, Catto J, Emberton M, Nam R, et al. Systematic review of complications of prostate biopsy. Eur Urol. 2013;64:876–92. https://doi.org/10.1016/j.eururo.2013.05.049.
12. Rouviere O, Puech P, Renard-Penna R, Claudon M, Roy C, Mege-Lechevallier F, et al. Use of prostate systematic and targeted biopsy on the basis of multiparametric MRI in biopsy-naive patients (MRI-FIRST): a prospective, multicentre, paired diagnostic study. Lancet Oncol. 2019;20:100–9. https://doi.org/10.1016/S1470-2045(18) 30569-2.
13. Eiber M, Weirich G, Holzapfel K, Souvatzoglou M, Haller B, Rauscher I, et al. Simultaneous (68)Ga-PSMA HBED-CC PET/ MRI improves the localization of primary prostate cancer. Eur Urol. 2016;70:829–36. https://doi.org/10.1016/j.eururo.2015.12. 053.
14. Donato P, Morton A, Yaxley J, Ranasinghe S, Teloken PE, Kyle S, et al. (68)Ga-PSMA PET/CT better characterises localised prostate cancer after MRI and transperineal prostate biopsy: Is (68)Ga-PSMA PET/CT guided biopsy the future? Eur J Nucl Med Mol Imaging. 2020. https://doi.org/10.1007/s00259-019-04620-0.
15. Berger I, Annabattula C, Lewis J, Shetty DV, Kam J, Maclean F, et al. (68)Ga-PSMA PET/CT vs. mpMRI for locoregional prostate cancer staging: correlation with final histopathology. Prostate Cancer Prostatic Dis. 2018;21:204–11. https://doi.org/10.1038/ s41391-018-0048-7.
16. Lopci E, Saita A, Lazzeri M, Lughezzani G, Colombo P, Buffi NM, et al. (68)Ga-PSMA positron emission tomography/computerized tomography for primary diagnosis of prostate cancer in men with contraindications to or negative multiparametric magnetic resonance imaging: a prospective observational study. J Urol. 2018;200:95–103. https://doi.org/10.1016/j.juro.2018.01.079.
17. Liu C, Liu T, Zhang Z, Zhang N, Du P, Yang Y, et al. PSMA PET/ CT and

standard plus PET/CT-ultrasound fusion targeted prostate biopsy can diagnose clinically significant prostate cancer in men with previous negative biopsies. J Nucl Med. 2020. https://doi.org/ 10.2967/jnumed.119.235333.

18. Ahmed HU, Hu Y, Carter T, Arumainayagam N, Lecornet E, Freeman A, et al. Characterizing clinically significant prostate cancer using template prostate mapping biopsy. J Urol. 2011;186:458– 64. https://doi.org/10.1016/j.juro.2011.03.147.
19. Kasivisvanathan V, Stabile A, Neves JB, Giganti F, Valerio M, Shanmugabavan Y, et al. Magnetic resonance imaging-targeted biopsy versus systematic biopsy in the detection of prostate cancer: a systematic review and meta-analysis. Eur Urol. 2019;76:284–303. https://doi.org/10.1016/j.eururo.2019.04.043.
20. Minner S, Wittmer C, Graefen M, Salomon G, Steuber T, Haese A, et al. High level PSMA expression is associated with early PSA recurrence in surgically treated prostate cancer. Prostate. 2011;71: 281–8. https://doi.org/10.1002/pros.21241.
21. Bravaccini S, Puccetti M, Bocchini M, Ravaioli S, Celli M, Scarpi E, et al. PSMA expression: a potential ally for the pathologist in prostate cancer diagnosis. Sci Rep. 2018;8:4254. https://doi.org/10. 1038/s41598-018-22594-1.
22. Hupe MC, Philippi C, Roth D, Kumpers C, Ribbat-Idel J, Becker F, et al. Expression of prostate-specific membrane antigen (PSMA) on biopsies is an independent risk stratifier of prostate cancer patients at time of initial diagnosis. Front Oncol. 2018;8:ARTN 623. https:// doi.org/10.3389/fonc.2018.00623.
23. Ferraro DA, Rupp NJ, Donati OF, Messerli M, Eberli D, Burger IA. 68Ga-PSMA-11 PET/MR can be false positive in normal prostatic tissue. Clin Nucl Med. 2019;44:e291–3.
24. Wiemer L, Hollenbach M, Heckmann R, Kittner B, Plage H, Reimann M, et al. Evolution of targeted prostate biopsy by adding micro-ultrasound to the magnetic resonance imaging pathway. Eur Urol Focus. 2020. https://doi.org/10.1016/j.euf.2020.06.022.
25. Lopci E, Lughezzani G, Castello A, Colombo P, Casale P, Saita A, et al. PSMA-PET and micro-ultrasound potential in the diagnostic pathway of prostate cancer. Clin Transl Oncol. 2021;23:172–8. https://doi.org/10.1007/s12094-020-02384-w.
26. Pizzuto DA, Muller J, Muhlematter U, Rupp NJ, Topfer A, Mortezavi A, et al. The central zone has increased (68)Ga-PSMA-11 uptake: “Mickey Mouse ears” can

be hot on (68)Ga-PSMA-11 PET. Eur J Nucl Med Mol Imaging. 2018;45:1335–43. https://doi.org/10.1007/s00259-018-3979-2.

27. Bodar YJL, Jansen BHE, van der Voorn JP, Zwezerijnen GJC, Meijer D, Nieuwenhuijzen JA, et al. Detection of prostate cancer with (18)F-DCFPyL PET/CT compared to final histopathology of radical prostatectomy specimens: is PSMA-targeted biopsy feasible? The DeTeCT trial. World J Urol. 2020. https://doi.org/10. 1007/s00345-020-03490-8.
28. Zhang LL, Li WC, Xu Z, Jiang N, Zang SM, Xu LW, et al. (68)Ga-PSMA PET/CT targeted biopsy for the diagnosis of clinically significant prostate cancer compared with transrectal ultrasound guided biopsy: a prospective randomized single-centre study. Eur J Nucl Med Mol Imaging. 2020. https://doi.org/10.1007/s00259-020- 04863-2.
29. Lopci E, Lughezzani G, Castello A, Saita A, Colombo P, Hurle R, et al. Prospective evaluation of (68)Ga-labeled prostate-specific membrane antigen ligand positron emission tomography/ computed tomography in primary prostate cancer diagnosis. Eur Urol Focus. 2020. https://doi.org/10.1016/j.euf.2020.03.004.
30. Lazzeri M, Lopci E, Lughezzani G, Colombo P, Casale P, Hurle R, et al. Targeted 11C-choline PET-CT/TRUS software fusion-guided prostate biopsy in men with persistently elevated PSA and negative mpMRI after previous negative biopsy. Eur J Hybrid Imaging. 2017;1:9. https://doi.org/10.1186/s41824-017-0011-1.

Tables

Table 1 Characteristics of the patients at inclusion in the study (n = 42).

Characteristics	Value
Age at scan (years)	
Mean±SD	64±6
Median (IQR)	65 (59–68)
PSA at time of PET scan (ng/ml)	
Mean±SD	10±7.4
Median (IQR)	8 (7–11)
PIRADS (*n*)	
3	7 (16.7%)
4	24 (57.1%)
5	11 (26.2%)

SD = standard deviation; IQR = interquartile range

Table 2 Distribution of patients with sigPCa and insigPCa, based on biopsy, according to ISUP grade groups. Clinically significant prostate cancer defined as ISUP grade ≥ 3 and/or cancer core length ≥ 6 mm. Seven patients had no cancer on biopsy.

	sigPCa	insigPCa
ISUP		
1	1 (4%)	3 (33%)
2	6 (23%)	6 (67%)
3	9 (34%)	–
4	8 (31%)	–
5	2 (8%)	–
Total	26	9

sigPCa = clinically significant prostate cancer; insigPCa = clinically insignificant prostate cancer

Table 3 Performance of PSMA-PET/MRI for biopsy guidance, given patient-based for PSMA-PET/MRI imaging findings and PET-targeted cores, and lesion-based.

	Patient-based	Patient-based targeted cores	Lesion-based
Sensitivity	96% (25/26)	65% (17/26)	83% (29/35)
Specificity	81% (13/16)	81% (13/16)	–
PPV	89% (25/28)	61% (17/28)	76% (29/38)
NPV	93% (13/14)	93% (13/14)	–
Accuracy	90% (38/42)	71% (30/42)	–

PPV = positive predictive value; NPV = negative predictive value. For the targeted core analysis, values were calculated as if patients with a negative PSMA-PET/MRI were not submitted to biopsy and patients with a positive PSMA-PET/MRI underwent only PSMA-PET/MRI-targeted biopsy. Lesion-based specificity and NPV were not calculated since patients with negative PSMA-PET/MRI and no significant cancer on biopsy have, per definition, no lesion

Table 4 Findings on PET (SUVmax), biopsy, and radical prostatectomy (RPE) specimen of the false-positive and false-negative lesions on PSMA-PET/MRI. PSMA-PET/MRI image of each lesion can be seen in the correspondent supplementary figure (Online Resources 3 for Fig. S2 and 4 for Fig. S3) showed in the first column.

	Fig.	SUV_{max}	Biopsy			RPE specimen	
			Finding	ISUP	Length (mm)	Finding	ISUP
False-positive lesions*							
Pat. 03	S2 a	7.9	ASAP	–	–	PSMA overexpression	–
Pat. 24	S2 b	5.3	Inflammation	–	–	Cancer	3
Pat. 30	S2 c	5.4	insigPCa	2	1.0	Cancer	2
Pat. 32	S2 d	12.9	insigPCa	2	2.0	Cancer	2
Pat. 33	S2 e	9.4	insigPCa	2	1.5	Cancer	3
Pat. 35	S2 f	4.4	insigPCa	2	5.0	Cancer	2
Pat. 35	S2 g	5.7	None	–	–	Cancer	3
Pat. 38	S2 h	10.1	None	–	–	Cancer	2
Pat. 42	S2 i	8	insigPCa	2	1.5	Cancer	2
False-negative lesions*							
Pat. 05	S3 a	–	sigPCa	1	6.0	Not available	–
Pat. 07	S3 b	–	sigPCa	3	1.0	No cancer	–
Pat. 16	S3 c	–	sigPCa	3	3.0	Cancer	3
Pat. 26	S3 d	–	sigPCa	4	6.0	Cancer	2
Pat. 32	S3 e	–	sigPCa	2	6.0	Cancer	2
Pat. 39	S3 f	–	sigPCa PSMA-negative	2	10.0	Not available	–

*Based on biopsy findings

ASAP = atypical small acinar proliferation; insigPCa = clinically insignificant prostate cancer; sigPCa = clinically significant prostate cancer; SUVmax = maximum standardized uptake value

Figures

Fig. 1 Patient selection and inclusion in the study

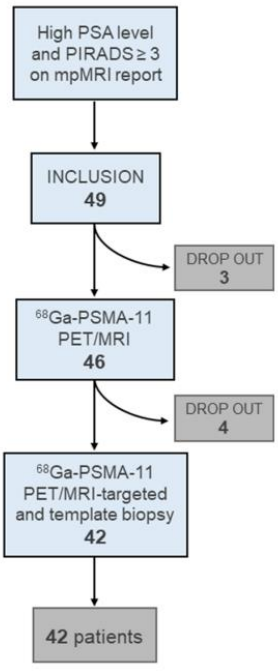

Fig. 2 Distribution of patients with clinically significant prostate cancer (sigPCa), clinically insignificant prostate cancer (insigPCa), and no evidence of disease on biopsy in correlation to PIRADS classification on multiparametric resonance magnetic imaging (a) and 68Ga-PSMA-11 PET/MRI result (b).

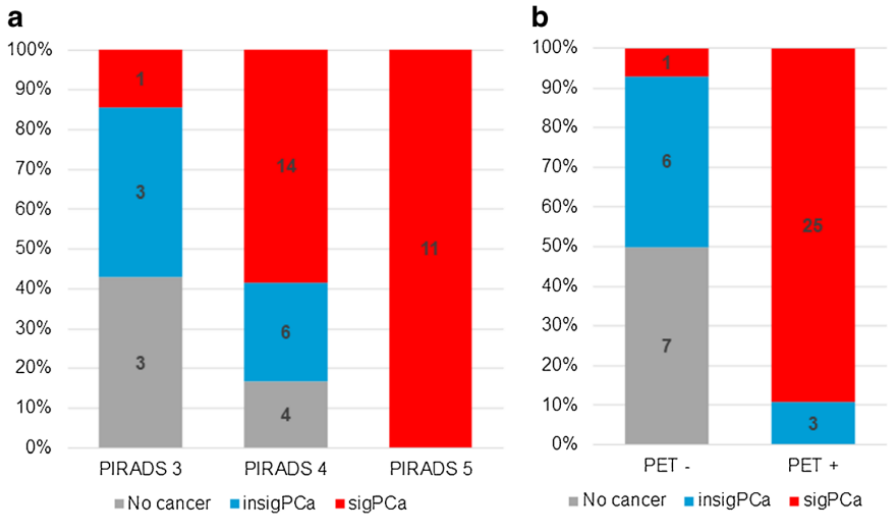

Fig. 3 Distribution of patients with clinically significant prostate cancer (sigPCa), clinically insignificant prostate cancer (insigPCa), and no evidence of disease on biopsy according to 68Ga-PSMA-11 PET/MRI results (a) and according to 68Ga-PSMA-11 PET/MRI results in correlation to PIRADS classification on multiparametric resonance magnetic imaging (b). The single false-negative case and the three false-positive cases shown in part “a” are shown in part “b” under PIRADS 5/negative PSMA-PET/ MRI and PIRADS 3/positive PSMA-PET/MRI (two cases) and 4/positive PSMA-PET/MRI (one case), respectively.

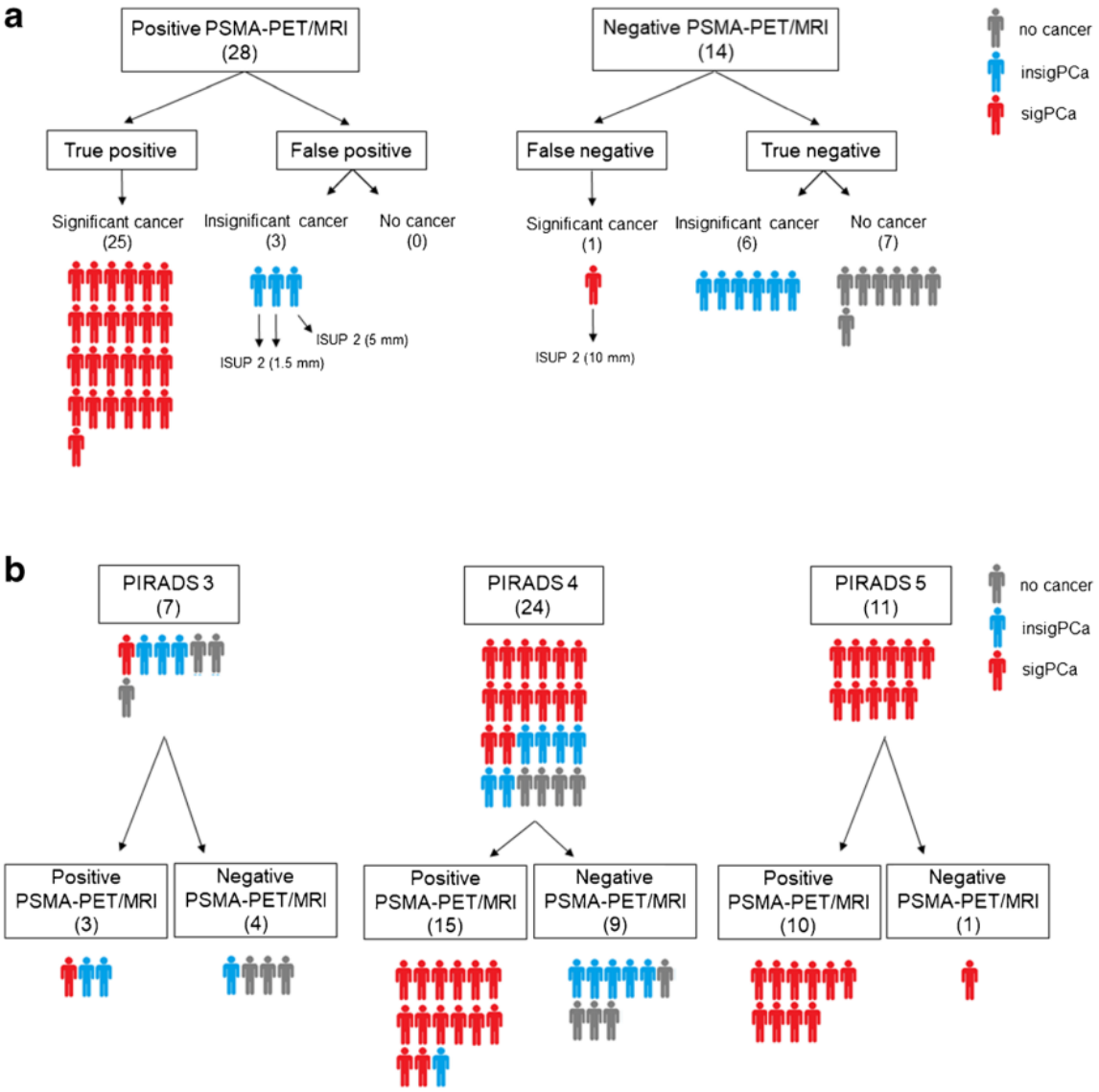

Fig. 4 All three patients with a false-positive PSMA-PET/MRI. From left to right, prostate MRI sequences T2-weighted and diffusion-weighted images (b value 1000), fused PET/MRI, representative pathology map with biopsy results, and radical prostatectomy (RPE) specimen with tumor outlined on hematoxylin and eosin staining (H&E) and PSMA-IHC (overview and magnification). Bars represent 2.5 mm in the H&E and PSMA-IHC images and 100 µm in the PSMA-IHC magnified images. Blue dots in the pathology map correspond to location of needles with clinically insignificant cancer diagnosed. a 67-year-old patient, with a PSA of 7.3 ng/ml and a PIRADS 4 lesion on mpMRI. PSMA-PET/ MRI shows one targeted lesion (arrow) in

the posterior right peripheral zone, where biopsy found ISUP grade group 2 tumor with up to 1.5-mm length. RPE specimen shows a PSMA-positive ISUP grade group 3 tumor in the PSMA uptake area. b 65-year-old patient, with a PSA of 7.18 ng/ml and a PIRADS 3 lesion on mpMRI. PSMA-PET/MRI shows one targeted lesion (arrow) in the anterior zone, where biopsy found ISUP grade group 2 tumor with up to 1.5-mm length. RPE specimen shows a PSMA-positive ISUP grade group 2 tumor in the PSMA uptake area. c 65-year-old patient, with a PSA of 48.5 ng/ml and a PIRADS 3 lesion on mpMRI. PSMA-PET/MRI shows two targeted lesions (arrows) in the transition zone corresponding on biopsy to ISUP grade group 2 tumor up to 5 mm length, and in the posterior left peripheral zone, where biopsy was negative. RPE specimen shows a PSMA-positive ISUP grade group 3 tumor in the PSMA uptake area of the posterior left peripheral zone.

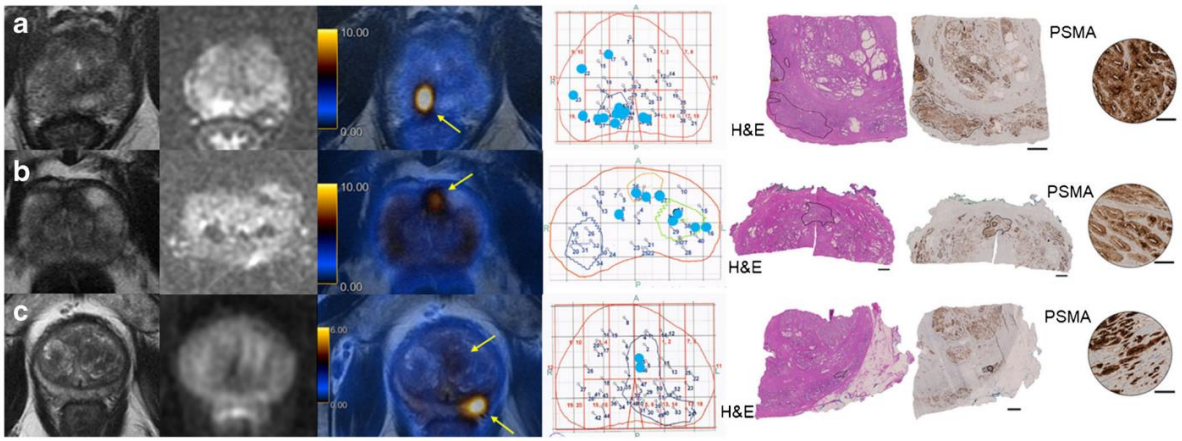

Fig. 5 The only patient with a false-negative PSMA-PET/MRI in our cohort. A 62-year-old patient with a PSA of 11.38 ng/ml. Top images from left to right are prostate MRI sequences T2-weighted and diffusion-weighted images and fused PET/MRI showing a PIRADS 5 lesion in the anterior transition zone (arrows) with no PSMA uptake. Bottom left image shows the representative pathology map with biopsy results including two cores with clinically significant cancer in the lesion area (red dots, ISUP grade group 2 tumor with length up to 10 mm) and many cores with clinically insignificant cancer (blue dots). Remaining bottom images show one of the biopsy cores with clinically significant cancer. The tumor is outlined in hematoxylin

and eosin staining (H&E) and PSMA-IHC (overview and magnification), showing a virtually PSMA-negative tumor. Bars represent 2.5 mm in the H&E and PSMA-IHC images and 100 µm in the PSMA-IHC magnified image.

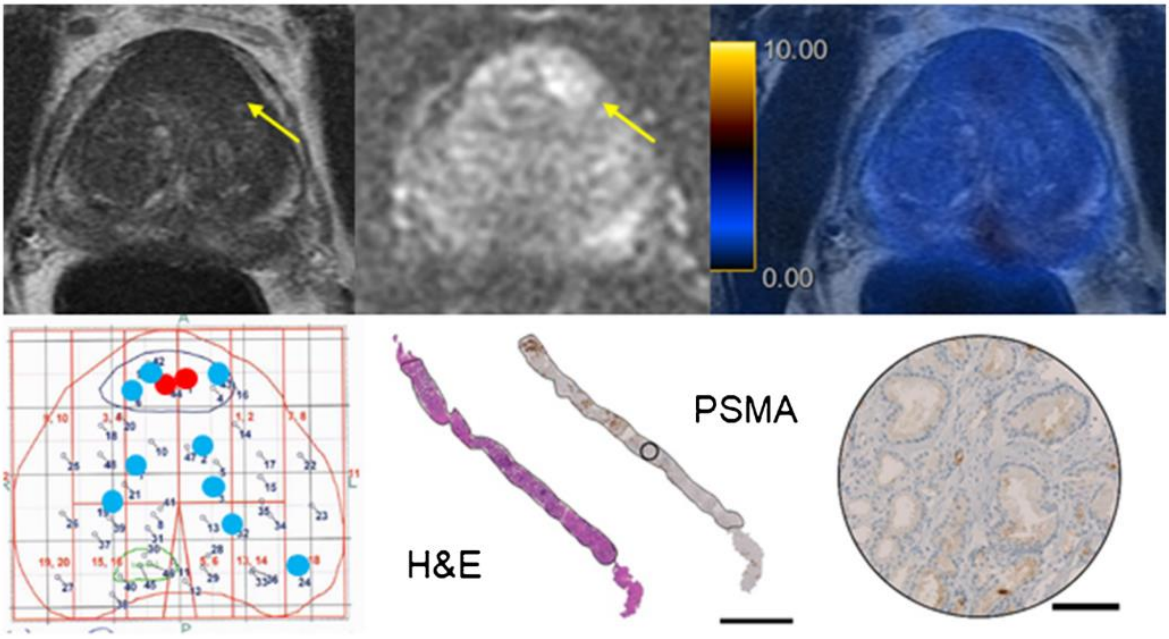

Supplementary material

Online Resource 1

Sample size calculation The sample size was calculated with the assumption that the sensitivity of PSMA PET would be 15% higher than mpMRI. We determine the number of patients required to achieve a power of 80% to prove an increase of the sensitivity by 15% on a significance level of α=5% in this paired design by utilizing the one-sided MC Nemar test. We used the statistical programming language R to perform the sample size calculation and the result is that 40 patients are needed.

Imaging protocol All patients underwent a pelvic PET/MRI on a dedicated hybrid scanner (SIGNA PET/MR, GE Healthcare, Waukesha, WI, USA) 60 minutes after injection of 85 MBq PSMA and images were transferred to a dedicated review workstation (Advantage Workstation, Version 4·6 or 4·7, GE Healthcare) for reporting. To reduce PSMA activity in the bladder, furosemide was injected intravenously 30 minutes prior to the 68Ga-PSMA-11 injection. PET acquisition for the whole-body protocol was in 3D time of flight (TOF) mode, two bed positions with 4 min acquisition time per bed position pelvis to the renal vessels. An additional pelvic frame over 15 minutes was acquired. Based on previous dose reduction

calculation we concluded that the 15 min scan would allow us to lower the injected dose to 85 MBq to minimize dose for patients without confirmed cancer (Quantitative performance and optimal regularization parameter in block sequential regularized expectation maximization reconstructions in clinical 68Ga-PSMA PET/MR. Ter Voert EEGW, Muehlematter UJ, Delso G, Pizzuto DA, Müller J, Nagel HW, Burger IA. EJNMMI Res. 2018 Jul 27;8(1):70. doi: 10.1186/s13550-018-0414-4.). Axial FOV was of 25 cm, overlap of 24%, matrix 256x256, 2 iterations, 28 subsets, with sharpIR algorithm (GE Healthcare), and 5 mm filter cutoff. To rule out lymph nodes or distant metastasis, one more frame with 4 minutes frame-time was be performed up to the renal vessels. The MRI protocol included specific sequences covering the pelvis: a high-resolution T1-weighted LAVA-FLEX sequence, T2-weighted fast recovery fast spin-echo sequence in three planes and diffusion weighted images, detailed in the table below.

	Axial DWI EPI (Focus) (Pelvis)	Axial LAVA-FLEX WB (DIXON)	Axial T1w Whole ARC (Pelvis)	Axial T2w FRFSE-XL (Pelvis)	Coronal T2w WB FRFSE-XL	Coronal T2w FRFSE-XL (Pelvis)	Axial DCE (Lava Dyn) (Pelvis)	Ax syn. DWI Focus	Sag T2w FRFSE
Repetition time, TR (ms)	4000	5·6	550	5034	5538	5034	6·361	3500	4678
Echo time, TE (ms)	67·3	1·3-2·7	8·26	120	120	120	2·376	Minimum	120
Flip angle, FA (degrees)	90	12	111	140	111	140	30	-	140
Acquisition matrix	160 x 80	344 x 256	384x384	300x280	288 x 224	300x280	160 x 80	140x70	300x272
Image size (voxels)	256 x 256	512 x 512	512 x 512	512 x 512	512 x 512	512 x 512	288 x 192	-	
Slice thickness (mm)	4	3	5	3·5	5	3·5	4	4	3·5
Signal averages	8	0·68	0·5	2	0·5	4	0·35	-	
b-values (s/mm2) and signal averages	0 (6 av.) 400 (8 av.) 700(16 av.)							0 400 1000 1500 2000	
Diffusion direction	'All'							All	
Bandwidth (Hz/pixel)	1953	166	62·5	50	90·9	50	62·5	250	50
Acquisition time (mm:ss)	5:41	0:18	1:44	3:27	0:50	3:27	3:27	4:05	3:12

Imaging analysis The acquired 68Ga-PSMA-11 PET and MRI images were transmitted to a dedicated review workstation (Advantage Workstation, Version 4.6 or 4.7, GE Healthcare), which enables the review of the 68Ga-PSMA-11 PET and the MRI images side by side and in fused mode. All scans were analysed by a double-boarded nuclear medicine physician and radiologist, specialist in pelvic imaging, with 10 and 5 years of experience (IAB, MM), incorporating both the MRI and 68Ga-

PSMA-11 PET information. The readers had access to clinical information for the readouts. Dual board certified nuclear physicians and radiologists interpreted the scans, taking zonal anatomy based on T2- MRI into account. Lesions were considered suspicious if there was focal PSMA-uptake higher than local background. Readers were aware of potential pitfalls, such as increased uptake in prostatitis or in the central zone to avoid false-positive findings (Pizzuto et al. The central zone has increased 68Ga-PSMA-11 uptake: «Mickey Mouse ears» can be hot on 68Ga-PSMA-11 PET. EJNMMI, 2018). PSMA-negative lesions seen only on the MRI component were considered as negative.

Table S1 Classification of patients that had up to three lesions with different classifications

	Lesion 1	Lesion 2	Lesion 3	Patient classification
Patients with 2 lesions	TP	FP or FN	---	TP
	FN	FP	---	FN
Patients with 3 lesions	TP	FP or FN	FP or FN	TP
	FN	FP or FN	FP or FN	FN

TP= true positive; FP= false positive; FN= false negative. Patients classified as false positive had only false-positive lesions.

Table S2 Distribution of patients with sigPCa, insigPCa and no cancer, based on biopsy, according to PIRADS, ISUP grade groups and PSMA-PET/MRI result using the criteria for clinically significant prostate cancer as tumours with ISUP grade ≥ 2.

	sigPCa	insigPCa	No cancer
PIRADS			
3	3 (10%)	1 (25%)	3 (43%)
4	17 (55%)	3 (75%)	4 (57%)
5	11 (35%)	0	0
ISUP			
1	0	4 (100%)	-
2	12 (39%)	-	-
3	9 (29%)	-	-
4	8 (26%)	-	-
5	2 (6%)	-	-
PSMA-PET/MRI			
Positive	27 (87%)	1 (25%)	0
Negative	4 (13%)	3 (75%)	7 (100%)
Total	31	4	7

sigPCa = clinically significant prostate cancer; insigPCa = clinically insignificant prostate câncer

Table S3 Performance of PSMA-PET/MRI for biopsy guidance, given patient-based for PSMA-PET/MRI imaging findings and PET-targeted cores, and lesion-based, using the criteria for clinically significant prostate cancer as tumours with ISUP grade ≥ 2.

	Patient-based	Patient-based targeted cores	Lesion-based
Sensitivity	87% (27/31)	68% (21/31)	66% (33/50)
Specificity	91% (10/11)	91% (10/11)	-
PPV	96% (27/28)	75% (21/28)	87% (33/38)
NPV	71% (10/14)	71% (10/14)	-
Accuracy	88% (37/42)	74% (31/42)	-

PPV= positive predictive value; NPV= negative predictive value. For the targeted cores analysis, values were calculated as if patients with a negative PSMA-PET/MRI were not submitted to biopsy and patients with a positive PSMA-PET/MRI underwent only PSMA-PET/MRI targeted biopsy. Lesion-based specificity and NPV cannot not be calculated since patients with negative PSMA-PET/MRI and no significant cancer on biopsy have, per definition, no lesion.

Online Resource 2

Example of PSMA -PET/MRI targeted biopsy. (A) PSMA -PET/MRI of a 57 years -old patient with prostate specific antigen (PSA) level of 15 ng/ml and a PIRADS 5 lesion on previous multiparametric resonance magnetic imaging (MRI) showing two suspicious lesions with high PSMA uptake (SUVmax 19.3 on the right and 13.5 on the left lesion) with hipointense signal on T2 -weighted MRI sequence. (B) DICOM file inserted by the urologist in the MRI -US machine, prepared by the nuclear physician who outlined the two suspicious lesions on PET for biopsy targeting. (C) Representative prostate map with targeted lesions delineated in blue and green according to the DICOM file. Each number represent a biopsy sample, the position of needles with clinically significant cancer (ISUP grade 4 on the right and 3 on the left) and clinically insignificant cancer are marked by red and blue dots, respectively.

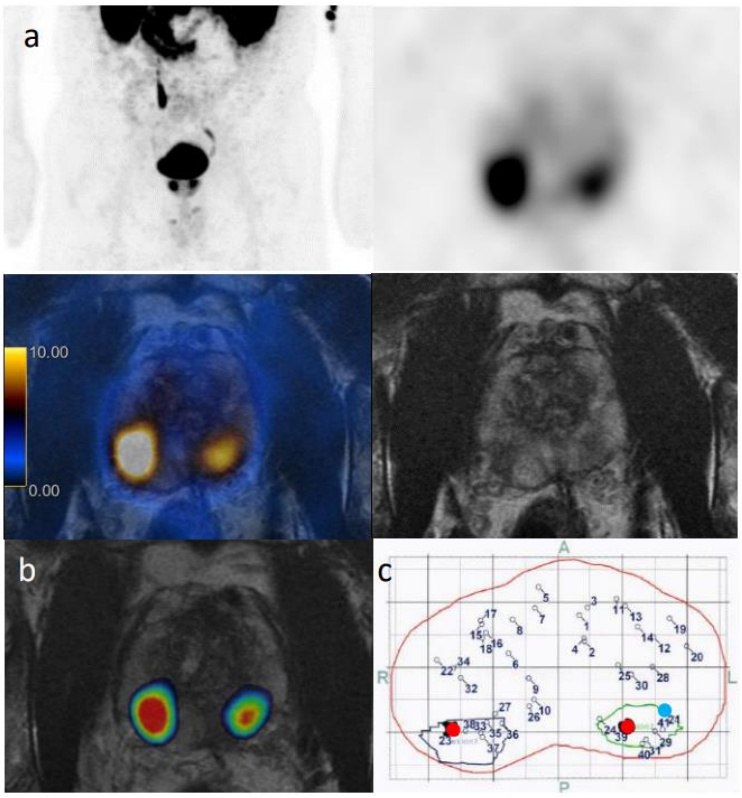

Online Resource 3

False-negative PSMA -PET/MRI lesions based on biopsy. From left to right, prostate magnetic resonance imaging (MRI) sequences diffusion - weighted T 2 - weighted images, fused PET/MRI and representative pathology map with biopsy results in which red and blue dots correspond to the location of needles with clinically significant cancer and clinically insignificant cancer, respectively. Table 4 shows the biopsy and radical prostatectomy findings for each lesion.

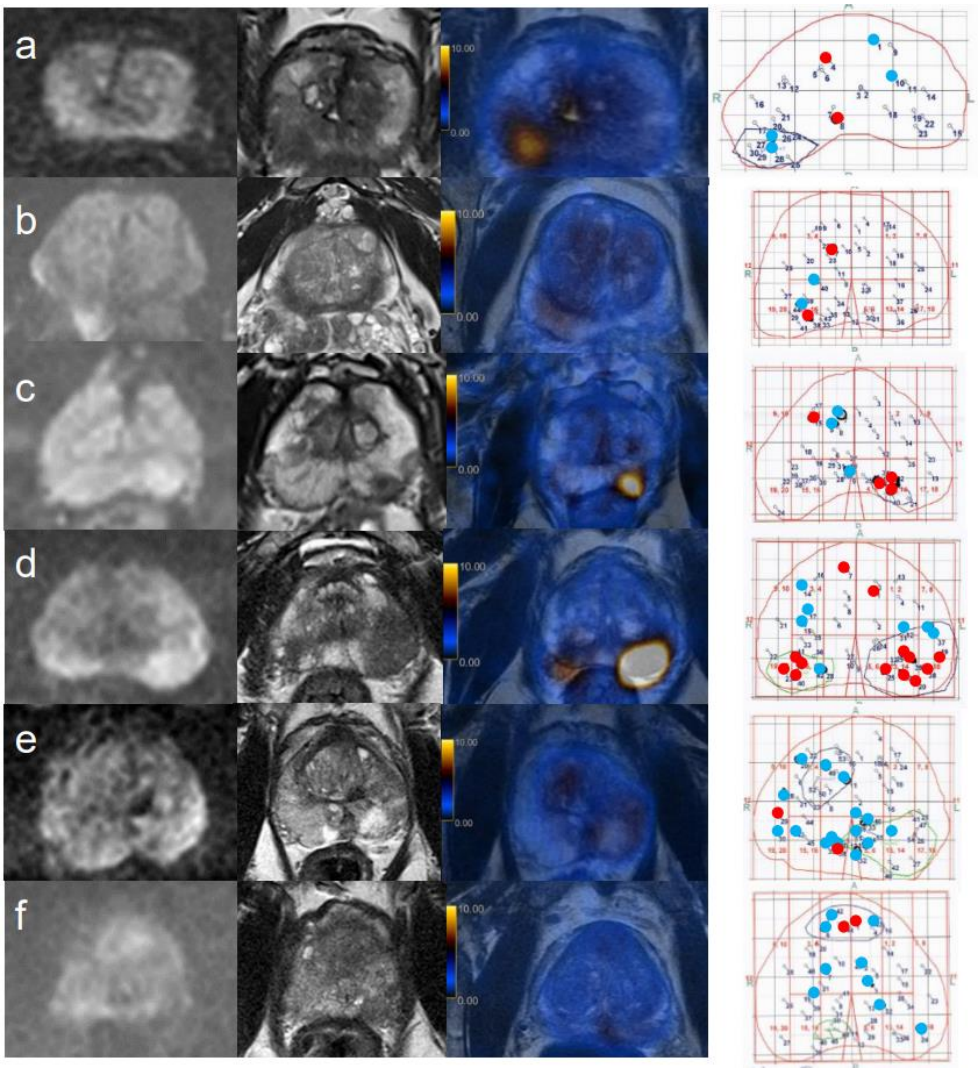

Online Resource 4

False-positive PSMA-PET/MRI lesion based on biopsy. From left to right, prostate magnetic resonance imaging (MRI) sequences diffusion-weighted T2-weighted images, fused PET/MRI, and representative pathology map with biopsy results in which red and blue dots correspond to the location of needles with clinically significant cancer and clinically insignificant cancer, respectively. False-positive target lesions are pointed out by arrows. Images F and G belong to the same patient, who had two false-positive lesions on PSMA-PET/MRI. Table 4 shows the biopsy and radical prostatectomy specimen findings, as well as the maximum standardized uptake value (SUVmax) for each lesion.

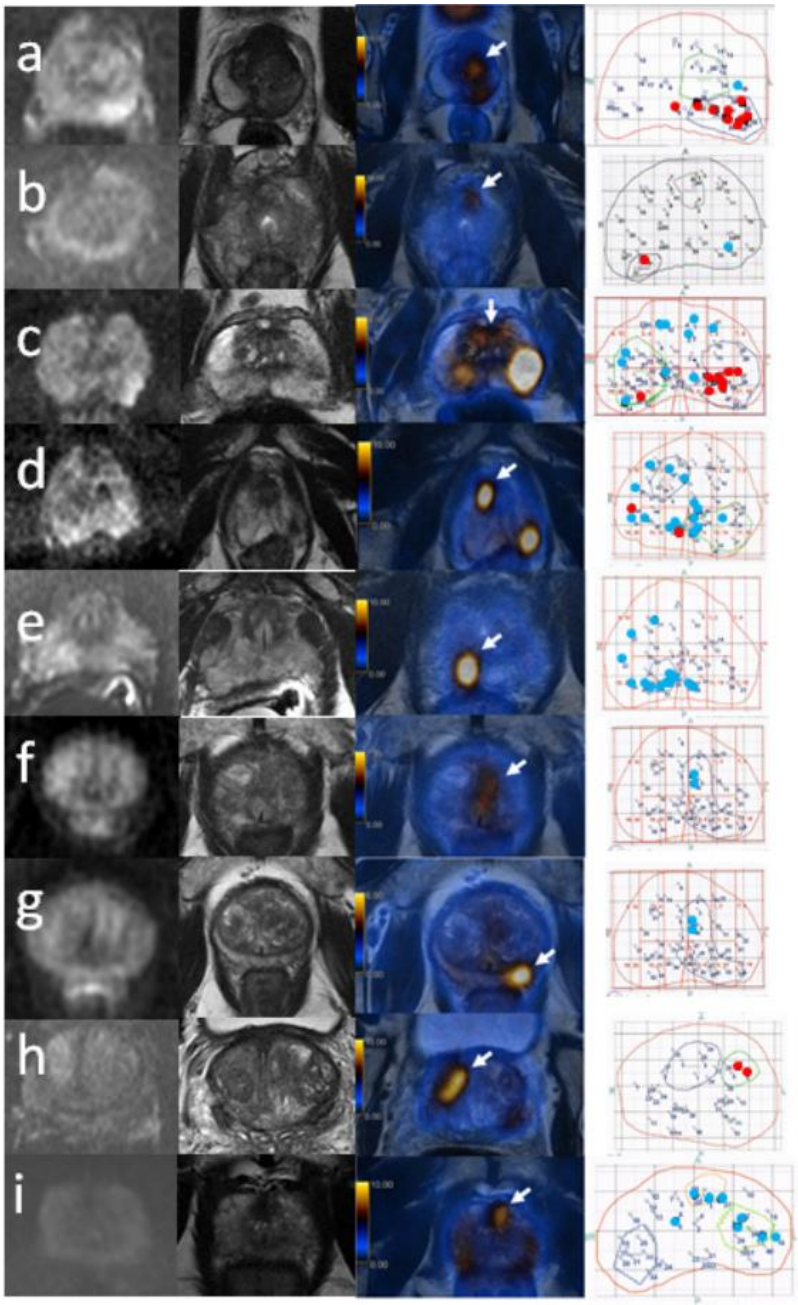
a
b
c
d
e
f
g
h
i

3.3 PUBLICAÇÃO 2

FERRARO DA, Hötker AM, Becker AS, Mebert I, Laudicella R, Baltensperger A, Rupp NJ, Rueschoff JH, Müller J, Mortezavi A, Sapienza MT, Eberli D, Donati OF, Burger IA. 68Ga-PSMA-11 PET/MRI versus multiparametric MRI in men referred for prostate biopsy: primary tumour localization and interreader agreement. Eur J Hybrid Imaging. 2022 Jul 18;6(1):14.

O estudo publicado consistiu em uma análise retrospectiva dos dados da coorte do primeiro estudo, tendo como objetivos comparar o ^{68}Ga-PSMA-11 PET/RM com a RMmp quanto a capacidade de localização do tumor primário e a concordância interobservador e investigar a correlação dos parâmetros semiquantitativos de ambos os métodos com o grau tumoral, além de investigar histologicamente os casos de discordância entre o ^{68}Ga-PSMA-11 PET e a RMmp com análise da peça cirúrgica derivada da prostatectomia, quando disponível.

Dos 42 pacientes participantes do primeiro estudo, três tiveram que ser excluídos devido a impossibilidade de análise das imagens da RMmp, sendo estudados 39 pacientes. Os exames de ^{68}Ga-PSMA-11 PET/RM e RMmp foram lidos por dois especialistas em cada modalidade que, para cada lesão, definiram uma classificação de acordo com o sistema PIRADS v2.1 para a RMmp e com uma escala adaptada para o ^{68}Ga-PSMA-11 PET e coletaram parâmetros semiquantitativos (valor de captação padronizado máximo [SUVmax] e PSMA volume para o ^{68}Ga-PSMA-11 PET e diâmetro da lesão e coeficiente de difusão aparente [ADC] para a RMmp). Para análise, o resultado da leitura foi dicotomizado em positivo e negativo e comparado com o resultado da biópsia numa análise por lesão e baseada em quadrantes da próstata. No contexto pré-biópsia considerou-se adequado privilegiar a sensibilidade mesmo que em detrimento da especificidade, portanto na dicotomização o escore 3 foi incluído junto aos escores 4 e 5 e considerado positivo, sendo os escores 1 e 2 considerados negativos para ambos os métodos.

A distribuição dos quadrantes com câncer clinicamente significante e a acurácia dos dois métodos não mostrou diferença estatisticamente significativa, com acurácia de 83,3 % para o ^{68}Ga-PSMA-11 PET e 81,4 % para a RMmp (p =

0,56) e a concordância interobservador da análise visual foi substancial em ambos os métodos. A análise dos parâmetros semiquantitativos demonstrou correlação com o grau tumoral dos parâmetros do ^{68}Ga-PSMA-11 PET mas não dos parâmetros da RMmp e houve alta concordância interobservador para os parâmetros do ^{68}Ga-PSMA-11 PET e para o diâmetro tumoral e moderada para ADC.

Em relação à análise dos casos discordantes entre os dois métodos ou destes com a biópsia, cabem os seguintes destaques:

- A maioria dos quadrantes (4/5) falso-positivos na imagem em que ^{68}Ga-PSMA-11 PET e RMmp discordaram da biópsia (negativa) consistiu na realidade em um erro do resultado da biópsia, sendo comprovada a existência de câncer na peça cirúrgica.
- A maioria dos quadrantes (9/12) falso-negativos na imagem em que ^{68}Ga-PSMA-11 PET e RMmp discordaram da biópsia (positiva) teve neoplasia confirmada na peça cirúrgica, predominantemente Gleason 3+4. Houve casos (2/12) em que a peça cirúrgica foi de acordo com os métodos de imagem e mostrou ausência de neoplasia no quadrante com biópsia positiva, o que pode ter sido causado por uma má identificação do quadrante biopsiado, por exemplo por distorção arquitetural da próstata no momento da biópsia.
- Na maioria dos quadrantes (8/9) em que a RMmp foi positiva e ^{68}Ga-PSMA-11 PET negativo, a biópsia ou peça cirúrgica confirmou a presença de câncer.
- Em todos os quadrantes (12/12) com ^{68}Ga-PSMA-11 PET positivo e RMmp negativa, a biópsia ou peça cirúrgica confirmou a presença de câncer.

Em conclusão, o estudo mostrou acurácia semelhante e alguma complementariedade entre o ^{68}Ga-PSMA-11 PET/RM e a RMmp na localização da lesão primária de câncer de próstata, bem como concordância interobservador substancial para ambos os métodos. O estudo também mostrou correlação entre os parâmetros semiquantitativos do ^{68}Ga-PSMA-11 PET e o grau tumoral, ao contrário dos parâmetros da RMmp.

Segue-se o texto do artigo conforme publicado originalmente em inglês na referência acima mencionada:

68Ga-PSMA-11 PET/MRI versus multiparametric MRI in men referred for prostate biopsy: primary tumour localization and interreader agreement

Daniela A. Ferraro[1,2,3], Andreas M. Hötker[4], Anton S. Becker[4,5], Iliana Mebert[1,6], Riccardo Laudicella[1,7], Anka Baltensperger[1,6], Niels J. Rupp[8] , Jan H. Rueschof[8] , Julian Müller[1] , Ashkan Mortezavi[6,9], Marcelo T. Sapienza[2] , Daniel Eberli[6] , Olivio F. Donati[4] and Irene A. Burger[1,3,10]

1 Department of Nuclear Medicine, University Hospital Zürich, University of Zurich, Rämistrasse 100, 8091 Zurich, Switzerland.
2 Department of Radiology and Oncology, Faculdade de Medicina FMUSP, Universidade de São Paulo, São Paulo, Brazil.
3 University of Zurich, Zurich, Switzerland.
4 Diagnostic and Interventional Radiology, University Hospital Zurich, University of Zurich, Zurich, Switzerland.
5 Department of Radiology, Memorial Sloan Kettering Cancer Center, New York City, USA.
6 Department of Urology, University Hospital Zürich, University of Zurich, Zurich, Switzerland.
7 Department of Biomedical and Dental Sciences and Morpho-Functional Imaging, Nuclear Medicine Unit, University of Messina, Messina, Italy.
8 Department of Pathology and Molecular Pathology, University Hospital Zurich, University of Zurich, Zurich, Switzerland.
9 Department of Urology, University Hospital Basel, Basel, Switzerland.
10Department of Nuclear Medicine, Kantonsspital Baden, Baden, Switzerland.

Corresponding author: Irene A. Burger, irene.burger@usz.ch

Abstract

Background: Magnetic resonance imaging (MRI) is recommended by the European Urology Association guidelines as the standard modality for imaging-guided biopsy. Recently positron emission tomography with prostate-specific membrane antigen (PSMA PET) has shown promising results as a tool for this purpose. The aim of this study was to compare the accuracy of positron emission tomography with prostate-specific membrane

antigen/magnetic resonance imaging (PET/MRI) using the gallium-labeled prostate-specific membrane antigen (68Ga-PSMA-11) and multiparametric MRI (mpMRI) for pre-biopsy tumour localization and interreader agreement for visual and semiquantitative analysis. Semiquantitative parameters included apparent diffusion coeficient (ADC) and maximum lesion diameter for mpMRI and standardized uptake value (SUVmax) and PSMA-positive volume (PSMAvol) for PSMA PET/MRI. **Results:** Sensitivity and specificity were 61.4% and 92.9% for mpMRI and 66.7% and 92.9% for PSMA PET/MRI for reader one, respectively. RPE was available in 23 patients and 41 of 47 quadrants with discrepant findings. Based on RPE results, the specificity for both imaging modalities increased to 98% and 99%, and the sensitivity improved to 63.9% and 72.1% for mpMRI and PSMA PET/MRI, respectively. Both modalities yielded a substantial interreader agreement for primary tumour localization (mpMRI kappa=0.65 (0.52–0.79), PSMA PET/MRI kappa=0.73 (0.61–0.84)). ICC for SUVmax, PSMAvol and lesion diameter were almost perfect (≥0.90) while for ADC it was only moderate (ICC=0.54 (0.04–0.78)). ADC and lesion diameter did not correlate significantly with Gleason score (ρ=0.26 and ρ=0.16) while SUVmax and PSMAvol did (ρ= −0.474 and ρ= −0.468). **Conclusions:** PSMA PET/MRI has similar accuracy and reliability to mpMRI regarding primary prostate cancer (PCa) localization. In our cohort, semiquantitative parameters from PSMA PET/MRI correlated with tumour grade and were more reliable than the ones from mpMRI.

Introduction

Precise diagnosis and risk assessment are of major importance for treatment planning of prostate cancer (PCa) (American Joint Committee on Cancer and Amin 2017). Tumour diagnosis is based on prostate biopsy (American Joint Committee on Cancer and Amin 2017; Mottet, et al. 2017). While systematic 12-core ultrasound-guided biopsy lacks accuracy, saturation biopsy (SB) has a high number of cores with increased side effects (Loeb et al. 2013). Therefore, MRI-guided biopsy has been adopted by many centers in addition to systematic biopsy (Kasivisvanathan et al. 2018; Ahdoot et al. 2020; Ahmed et al. 2017; Elkhoury et al. 2019). Magnetic resonance imaging (MRI) is recommended by the European Urology Association guidelines as the standard modality for imaging-guided biopsy (Mottet, et al. 2017) with reported sensitivity and specificity ranging between 58–96% and 23–87%, respectively (Futterer et al. 2015). Furthermore, accurate and robust lesion localization needs good interreader agreement and implementation and continuous

improvement of the PI-RADS scoring system has significantly improved MRI rates over time, achieving substantial agreement (Park et al. 2020).

Recently, positron emission tomography with prostate-specific membrane antigen (PSMA PET) has gained importance in the setting of PCa initial staging, especially because of its known high sensitivity and specificity for metastasis (Hofman et al. 2020). Lately, there is an increasing use of the method in treatment-naive patients. It was shown that staging PSMA PET has a general impact on management in about 21–29% of patients (Han et al. 2018; Ferraro et al. 2019; Grubmuller et al. 2018; Roach et al. 2018). Furthermore, studies have shown that the combination of PET and MRI in PSMA PET/ MRI may have additional value for local assessment when compared to multiparametric MRI (mpMRI) alone, including 98% sensitivity for tumour detection without missing important information such as extraprostatic extension (Muehlematter et al. 2019; Eiber et al. 2016). Primary tumour localization with PSMA PET/MRI was assessed retrospectively in patients with biopsy-proven intermediate to high-risk PCa, showing it outperforms mpMRI (Grubmuller et al. 2018; Eiber et al. 2016; Park et al. 2018; Li et al. 2019). In the pre-biopsy setting, a recent prospective trial at our institution found PSMA PET/ MRI to be negative in all seven patients with false-positive findings on mpMRI (Ferraro et al. 2021). The aim of this study was to perform a head-to-head comparison between mpMRI and PSMA PET/MR for pre-biopsy tumour localization accuracy and interreader agreement for visual and semiquantitative analysis using transperineal template saturation biopsy (TTSB) as reference standard.

Patients and methods

Study design

This is a retrospective analysis of data collected within a prospective trial (trial identification number blinded for review). The original trial aimed to assess PSMA PET/ MRI diagnostic accuracy for biopsy targeting. The aim of this study is to compare PSMA PET/MRI with 68Ga-PSMA-11 and mpMRI with respect to accuracy for primary prostate cancer detection and localization and interreader agreement, using histopathology from TTSB as reference standard. Patients with elevated PSA and at least one suspicious lesion on mpMRI (PIRADS v.2≥3) were included in the trial and underwent PSMA PET/MRI. For this analysis, only patients with available mpMRI classified as adequate by our radiologist were selected. Thirty-nine of the 42

previously published patients were included, and three patients were excluded because of mpMRI imaging not available for a second readout (15). Images were anonymized and read by four specialists at our institution. Figure 1 illustrates patient selection.

68Ga-PSMA-11 PET/MRI protocol

All patients underwent a pelvic PET/MRI on a dedicated hybrid scanner (SIGNA PET/ MR, GE Healthcare, Waukesha, WI, USA) 60 min after injection of 85 MBq PSMA. Detailed protocol has been published previously (Ferraro et al. 2021). In brief, the PET/MR protocol included specific sequences covering the pelvis: a high-resolution T1-weighted 3D-FSPGR sequence, T2-weighted fast recovery fast spin-echo sequence in three planes and diffusion-weighted images. A 15-min frame over the prostate was recorded, allowing reducing the dose since patients without confirmed cancer were included. To reduce PSMA activity in the bladder, furosemide was injected intravenously 30 min prior to the 68Ga-PSMA-11 injection.

mpMRI

MpMRI acquisition protocol at our institution was already published elsewhere (Muehlematter et al. 2019). The typical protocol included diffusion-weighted imaging, T2-weighted fast spin-echo in three planes and dynamic contrast-enhanced imaging and was in accordance with current guidelines (PI-RADS v2.1). Detailed information of the mpMRI protocol is given in the supplements.

Imaging analysis

Two readers for each modality (R1-M and R2-M for mpMRI and R1-P and R2-P for PSMA PET/MRI) analysed anonymized images, blinded for the results of the biopsy or for the other imaging modality as well as for clinical data. A double board-certified nuclear medicine physician and radiologist with 10 years of experience (R1-P) and a nuclear medicine physician with 2 years of experience (R2-P) analysed the PSMA PET/ MRI images (PET and T2 sequence), and two expert radiologists (Rooij et al. 2016) with 10 (R1-M) and 8 (R2-M) years of experience in interpretation of mpMRI of the prostate analysed the mpMRI images. Imaging findings were delineated by the readers using a transaxial prostate map and classified according to PIRADS v2.1 (Turkbey et al. 2019) for mpMRI and according to an adaptation of the same scale for focal uptake on 68Ga-

PSMA-11 PET/MRI (1 = no focal uptake; 2 = benign; 3 = undetermined; 4 = suspicious for malignancy ≤ 1.5 cm; 5 = suspicious for malignancy > 1.5 cm) as illustrated in Fig. 2. Readers also recorded quantitative parameters for suspected lesions: maximum standardized uptake value (SUVmax) and PSMA-positive volume (PSMAvol) from PSMA PET/MRI and from mpMRI diffusion restriction were assessed measuring the mean apparent diffusion coefficient (ADCmean in 10−3 mm2/s) and lesion size (maximum diameter) from mpMRI. In the case of artifacts on diffusion-weighted imaging (DWI) from the mpMRI that would affect ADC measurement, mpMRI readers were allowed to use the ADC data set from the PSMA PET/MRI study for quantitative analysis, without access to the PET images (n=7) (Donati et al. 2014).

Standard reference and histology-imaging matching

Section-based TTSB was performed under general anesthesia by board certified urologists with a minimum of 2 years of experience in fusion-guided biopsies as described previously (Mortezavi et al. 2018). Cores were taken throughout the prostate according to the modifed Barzell zones (20 sectors) with number of cores adapted to the prostate volume (Kanthabalan et al. 2016). All biopsies and prostatectomy specimens were analysed by one of the genito-urinary pathologists, with 9 and 11 years of experience for Gleason score (GS) and International Society of Urological Society (ISUP) grade groups (Epstein et al. 2016). In case of discordant results between PSMA PET/MRI or mpMRI and TTSB results in patients who underwent a clinically indicated prostatectomy, final GS/ISUP grade groups and lesion location from radical prostatectomy (RPE) specimen were analysed for possible explanations of false-positive or negative results, but since RPE was not available in all patients, this information was not used for the primary accuracy calculation with TTSB as the sole reference standard. We however further investigated every quadrant with discrepant results between imaging modalities or imaging and TTSB for the RPE result and calculated a secondary accuracy based on the mixed standard.

Lesions delineated by the more experienced reader from each modality were matched with the TTSB map automatically generated by the fusion software (Fig. 2). For both PSMA PET/MRI and mpMRI, readouts scores 1 and 2 were considered as negative and 3, 4 and 5 as positive for suspicious lesions. Because there are no clear anatomic landmarks to delineate the quadrants, lesions involving the anterior

and posterior ipsilateral quadrants were considered as matching between imaging and histology if the main part of the lesion was delineated in the positive quadrant on histology. However, this concession was not made for lesions crossing the midline, because involvement of both lobes has prognostic value and therefore is relevant information on imaging. Clinically significant PCa (csPCa) was defined as GS≥3+4 (ISUP≥2) (Mottet et al. 2017; Briganti et al. 2018).

Data analysis and statistics

Descriptive statistics and frequencies were calculated in Excel (Excel2016, Microsoft, USA) and presented as median (interquartile range (IQR) Q1, Q3) and mean (±standard deviation (SD)). Gleason score (GS) and quadrant localization of lesions (data concatenated into quadrants anterior right, anterior left, posterior right, posterior left) were compared to the lesions delineated by the two more experienced readers to define the accuracy of PSMA PET/MRI and mpMRI using accuracy tables and was compared using the area under the curve (AUC) from clustered receiver operating characteristic curves (ROC) data with DeLong test. Interreader agreement was calculated per quadrant using Cohen's kappa for dichotomized data (1, 2 = negative and 3, 4, 5 = positive). Intraclass correlation coefficient (ICC) of semiquantitative parameters was calculated per imaging findings (regardless of score on imaging) only for the findings in common for the two readers of each modality. Interreader coefficients were categorized according to Landis and Koch as poor (less than 0.20), fair (0.21–0.40), moderate (0.41–0.60), substantial (0.61–0.80) or almost perfect agreement (0.81–1.00) (Landis and Koch 1977). Percentage of interreader agreement for each PIRADS category or PET score category was calculated dividing the number of quadrants classified as a certain category by both readers by the number of quadrants classified as that category by at least one of the readers. Correlations between semiquantitative parameters and GS were based on the readout of the more experienced readers using Spearman's rank correlation, and GS was included as a continuous parameter for patients with cancer on biopsy, separating GS 7 in 3+4 and 4+3. All statistical computations were performed using R version 4.0.5 (R Foundation for Statistical Computing, Vienna, Austria).

Results

Thirty-nine consecutive patients were included (Fig. 1). Table 1 shows patient

characteristics at study inclusion. Median interval between mpMRI and PSMA PET/MRI was 14 days (IQR 2, 78) and between biopsy and last performed imaging eight days (IQR 6, 17). RPE was available in 23 patients.

Biopsy

Median number of biopsy cores was 43 (IQR 38, 44). TTSB showed csPCa in 29/39 patients (74.3%), in 57/156 quadrants (36.5%). In 11 patients, csPCa was found in only one quadrant, in nine patients in two quadrants, in eight patients in three quadrants, and in one patient all four quadrants were positive for csPCa on TTSB. GS 3+4 (ISUP 2), 4+3 (ISUP 3), 4+4 (ISUP 4) and 4+5 (ISUP 5) were found in 30, 14, 11 and two quadrants, respectively. Among the quadrants without csPCa, GS 3+3 (ISUP 1) was found in 15/99 (15%).

mpMRI and 68Ga-PSMA-11 PET/MRI results

MpMRI was positive (PIRADS v2.1≥3) in 42 quadrants (27%, 42/156). PSMA PET/MRI was positive in 45 quadrants (29%, 45/156). Table 2 shows the quadrant-based accuracy for detection of csPCa for both modalities and Fig. 3 shows readout results in relation to biopsy findings, using the results from the two more experienced readers. Results of all four readers are given in the supplements (Additional file 1: Table S1). MpMRI and PSMA PET/MRI were concordant in 135 quadrants regarding suspicion for csPCa (positive or negative) (86.5%, 135/156). Both were negative in 102 quadrants (65%, 102/156): 90 true-negative (88%, 90/102) and 12 false-negative (12%, 12/102). Both were positive in 33 quadrants (21%, 33/156): 28 true-positive (85%, 28/33) and 5 false-positive (15%, 5/33).

MpMRI and PSMA PET/MRI were discordant in 21 quadrants: only mpMRI was positive in nine (seven true-positive, two false-positive), and only PSMA/PET/MRI was positive in 12 (10 true-positive, two false-positive). Figures 4 and 5 show imaging and histopathological findings of some illustrative cases in which imaging modalities were discordant or there was discordance between images and TTS, respectively. RPE specimen was available for analysis in 18 of these patients. Detailed information about false-positive and false-negative cases as well as RPE results can be found in Tables 3 and 4.

In a per quadrant analysis, performing PSMA PET instead of mpMRI prior to biopsy leads to detection of 10/156 (6.4%) additional quadrants and miss 7/156

(4.5%) quadrants harboring csPCa assessed by TTPB. These seven false-negative quadrants in PSMA were graded after TTPB as GS 3+4=7 (ISUP 2) in five cases, GS 4+3=7 (ISUP 3) in one case and GS 4+4=8 (ISUP 4) in one case.

Semiquantitative results

Correlation between semiquantitative parameters and GS is also shown in Table 5, with significant correlation for both PET parameters (SUVmax and PSMAvol) but no association between GS with size or ADC values on mpMRI.

Interreader agreement

Both modalities yielded a substantial interreader agreement for primary tumour localization per quadrant (Table 2). The main reason of discordance was that the less-experienced readers considered as suspicious lesions that were not suspicious for the more-experiences readers, which occurred in 13 quadrants in mpMRI and 11 quadrants in PSMA PET/MRI. Most of these quadrants (8/13 in mpMRI and 9/11 in PSMA PET/ MRI) were proven negative by TTSB resulting in a lower specificity for the less-experienced readers (Additional file 1: Table S1). The score that held the highest disagreement rates was score 3, with an agreement rate of 13.3% for mpMRI (2/15 quadrants) and no agreement for PSMA PET (0/5 quadrants). MpMRI and PSMA PET/MRI agreement rates for scores 1 and/or 2 were 82% and 85%, respectively, and for scores 4 and/or 5 was 54% and 74%, respectively. Reasons for disagreement on PSMA PET/MRI included physiological uptake in the central zone and uptake close to the urethra that was misinterpreted by the less-experienced reader.

Interreader agreement for semiquantitative parameters was based on 31 lesions on mpMRI (31 common lesions for both readers, R1-M reported additional 10 lesions and R2-M reported 8), and 50 lesions were reported on PSMA PET/MRI by both readers (R1-P reported 5 and R2-P reported 9 additional funding). Lesion size on mpMRI as well as PSMA PET/MRI semiquantitative parameters yielded an almost perfect interreader agreement while for ADC it was only moderate (Table 5).

Secondary analysis of quadrants with discrepant findings between imaging and biopsy

RPE was available in 23 of the 38 quadrants with discrepant findings (false-

negative or false-positive on mpMRI or PSMA PET (Table 3) or on both (Table 4)). For those quadrants without RPE available, TTSB remained the standard reference. Of the 12 quadrants that were false-negative on both imaging modalities, further workup with RPE showed that two had no cancer (biopsy GS 3+4 and 4+3, ISUP 2 and 3). Eight quadrants were confirmed as GS 3+4 (ISUP 2) disease and one quadrant harbored a lesion with GS 4+3 (ISUP 3). Among the five quadrants that were false-positive on PSMA PET/MRI and mpMRI, RPE was available in four, showing GS 3+4 (ISUP 2) or GS 4+3 (ISUP 3) disease in all of them. Among the 21 quadrants with disagreement between mpMRI and PSMA PET/MRI, RPE showed true-positive lesions in 10 quadrants on PSMA PET/MRI and five quadrants on mpMRI. One quadrant negative on biopsy showed GS 4+3 (ISUP 3) cancer on RPE (true-positive on PSMA PET/MRI with PIRADS 1 on mpMRI). Taking the discrepancies between biopsy results and RPE into account, the sensitivity and specificity of reader one for mpMRI would rise to 63.9% and 94.7%, and for PSMA PET/MRI to 72.1% and 96.8%, respectively.

Discussion

Per-quadrant accuracy for tumour localization before biopsy did not differ significantly for mpMRI and PSMA PET/MRI, with sensitivities of around 61% and 67%, respectively, and specificity of ≈ 93% for both methods. Interreader agreement for lesion localization was substantial for both modalities but slightly higher for PSMA PET/MRI compared to mpMRI (0.73 vs 0.65). PSMA PET/MRI semiquantitative parameters (SUVmax and PSMAvol) had an almost perfect interreader agreement as well as lesion size on mpMRI, while for ADC it was only moderate. Furthermore, SUVmax and PSMAvol correlated with biopsy GS, but mpMRI semiquantitative parameters did not. Our findings suggest PSMA PET/MRI could be used to guide biopsy in patients with suspicious prostate cancer, with similar accuracy and reliability in comparison with mpMRI regarding lesion localization, but with a more robust assessment of lesion aggressiveness by semiquantitative parameters.

The relatively lower per-quadrant accuracy for primary tumour localization on PSMA PET/MRI compared to our previously published per-patient accuracy (83.3% vs 88.0%) (Ferraro et al. 2021) is in concordance with other results. Eiber et al. reported 98% tumour detection with PSMA PET/MRI on a patient basis but only 76% of sensitivity for lesion localization in prostate per sextants (Eiber et al. 2016), and

Park et al. reported a sensitivity of around 85% using per-lobe localization (Park et al. 2018). Bodar et al. reported a significant drop in sensitivity and specificity in their cohort from 84.4 to 61.4% and from 97 to 88%, respectively, when using more stringent criteria of tumour localization with PSMA PET/CT using 12 prostate regions (Bodar et al. 2020). This drop in accuracy might also reflect the limitation of TTSB as a reference standard.

Furthermore, the current results also point out that TTSB as a reference standard has limitations. Incorporating the RPE results for all quadrants with discrepant findings was rising the specificity for both imaging modalities to around 95% (mpMRI) and 97% (PSMA PET/MRI). Also, the sensitivity improved for both imaging methods, from around 61 to 64% for mpMRI and from around 67 to 72% for PSMA PET/MRI, respectively. Given that several patients did not have any evidence for significant PCa on imaging or biopsy, despite the initial PIRADS 3 lesions on the clinical read out of the mpMRI, we could not incorporate RPE systematically within this study. However, the observation reflects the limitation of TTSB, which despite being the most accurate way to study the prostate through biopsies still has a substantial disagreement with RPE results (Crawford et al. 2013). Causes of false-positive and false-negative results on PSMA PET/MRI in this cohort were already published and discussed elsewhere (Ferraro et al. 2021).

MpMRI PIRADS version 2 interreader agreement has been extensively assessed in the literature. In a meta-analysis including 4095 patients, Greer et al. (2019) found substantial interreader agreement using score 4 as cutoff but observed fair to moderate agreement using score 3. They also found significant variation associated with reader experience. Similarly, we have observed a low interreader agreement on lesions classified as PIRADS 3, and in our cohort, reader experienced affected specificity more than sensitivity. Furthermore, a high agreement of 82–85% on negative quadrants was already reported by Brembilla et al. (2020), which matches well our result of 82%.

PSMA PET interreader agreement is known to be high for primary tumour detection and agreement for T, N and M range from substantial to almost perfect in the literature (Basha et al. 2019; Fendler et al. 2017; Toriihara et al. 2020). Therefore, we expected it to be high in the pre-biopsy context for primary tumour localization, which is crucial in the biopsy-guidance setting. Our results indeed show substantial agreement for both primary tumour detection and its localization but also draw

attention to some pitfalls on PSMA PET/MRI such as physiological uptake in the central zone (Pizzuto et al. 2018) or uptake close to the urethra, which can potentially mislead readers that lack MRI training despite of awareness of the potential pitfalls.

The full potential of semiquantitative measures on imaging is still under investigation. SUVmax correlation to GS has been shown before (Uprimny et al. 2017) as well as to presence of lymph node metastasis (Ferraro 2019). In fact, SUVmax reflects the tumour PSMA expression (Woythal et al. 2018), which correlates to tumour aggressiveness and has prognostic value (Paschalis et al. 2019; Hupe et al. 2018). In our cohort, both SUVmax and PSMAvol positively correlated with GS on TTSB. While an inverse correlation between mpMRI ADC value and GS can be demonstrated in large meta-analysis (Shaish et al. 2017), ADC more strongly correlates with other cellularity metrics/differences in tumour architecture (Chatterjee et al. 2015). As expected, in our cohort however, neither ADC nor tumour size on mpMRI correlated significantly with GS. Furthermore, ADC had the lowest interreader agreement, suggesting overall that parameters derived from PSMA expression and tumour size are more robust for prediction of GS.

Important considerations must be made about PSMA PET/MRI. It is not an ionizing radiation-free modality, it is not widely available, and no study so far assessed its cost-effectiveness in the pre-biopsy setting of PCa. This study showed that PSMA PET/ MRI can localize the primary tumour with similar accuracy to mpMRI read by a dedicated genitourinary radiologist and it has substantial interreader agreement. However, further studies are needed to determine which patients could benefit from it in clinical routine. Interestingly, in the present readout 11 of 39 patients that had a PIRADS≥3 lesion on clinical read out were considered as not suspicious (PIRADS 1/2) by Reader 1. This probably reflects the higher accuracy of mpMRI read by a dedicated genitourinary radiologist compared to clinical reports, whose positive predictive value can vary widely (Westphalen et al. 2020). Interestingly, this seems to be less problematic on PSMA PET/ MRI, since a nuclear medicine physician without specific MRI training with two years of experience was able to reach a moderate interreader agreement.

Limitations of this study include its retrospective nature, the lack of whole mount prostatectomy specimens as standard of reference and the quadrant-based approach. These limitations were partially mitigated by using TTSB with an extensive number of cores (median 43) and a careful readout by a nuclear physician and a

radiologist together to defiine quadrant status as positive or negative based on matching histopathology and lesions delineated on the imaging readouts. Another drawback is the lack of validation for the 5-point score used for PSMA PET/MRI, which was chosen to allow a direct comparison between the two imaging modalities. Finally, inherent limitations of using score 3 as cutoff for positive quadrants must be acknowledged since its impact in accuracy was already shown for mpMRI (Wadera et al. 2021). However, we believe this is the most reasonable approach for patients imaged in the pre-biopsy setting, in which targeting a false-positive lesion would probably bring less harm than failing to target a csPCa lesion or dismissing from biopsy a patient with csPCa.

Conclusion

PSMA PET/MRI has similar accuracy and reliability to mpMRI regarding primary PCa localization. Semiquantitative parameters from PSMA PET/MRI correlated with tumour grade and were more reliable than the ones from mpMRI. Further studies are needed to determine which patients could benefit from pre-biopsy PSMA PET/MRI in clinical routine.

Declarations

Ethics approval This study was performed in line with the principles of the Declaration of Helsinki. Approval was granted by the Cantonal Ethics Committee of Zurich (Date: 03/23/2017/BASEC Nr: 2017-00016).

Consent to participate Informed consent was obtained from all individual participants included in the study.

Competing interests IAB has received research grants and speaker honorarium from GE Healthcare, research grants from Swiss Life, and speaker honorarium from Bayer Health Care and Astellas Pharma AG. MM received speaker fees from GE Healthcare. The Department of Nuclear Medicine holds an institutional Research Contract with GE Healthcare. NJR has provided consultancy services (advisory board member) to F. Hofmann- La Roche AG. ASB received research grants from the Prof. Dr. Max Cloëtta Foundation, medAlumni UZH, and the Swiss Society of Radiology. All other authors declare no competing interests.

References

Ahdoot M et al (2020) MRI-targeted, systematic, and combined biopsy for prostate cancer diagnosis. N Engl J Med 382(10):917–928

Ahmed HU et al (2017) Diagnostic accuracy of multi-parametric MRI and TRUS biopsy in prostate cancer (PROMIS): a paired validating confirmatory study. Lancet 389(10071):815–822

American Joint Committee on Cancer, Amin MB (2017) AJCC cancer staging manual. Springer, New York

Basha MAA et al (2019) (68)Ga-PSMA-11 PET/CT in newly diagnosed prostate cancer: diagnostic sensitivity and interobserver agreement. Abdom Radiol (NY) 44(7):2545–2556

Bodar YJL et al (2020) Detection of prostate cancer with (18)F-DCFPyL PET/CT compared to final histopathology of radical prostatectomy specimens: is PSMA-targeted biopsy feasible? The DeTeCT trial. World J Urol 39:2439–2446

Brembilla G et al (2020) Interreader variability in prostate MRI reporting using prostate imaging reporting and data system version 2.1. Eur Radiol 30(6):3383–3392

Briganti A et al (2018) Active surveillance for low-risk prostate cancer: The European Association of Urology Position in 2018. Eur Urol 74(3):357–368

Chatterjee A et al (2015) Changes in epithelium, stroma, and lumen space correlate more strongly with gleason pattern and are stronger predictors of prostate ADC changes than cellularity metrics. Radiology 277(3):751–762

Crawford ED et al (2013) Clinical-pathologic correlation between transperineal mapping biopsies of the prostate and three-dimensional reconstruction of prostatectomy specimens. Prostate 73(7):778–787

de Rooij M et al (2016) Accuracy of magnetic resonance imaging for local staging of prostate cancer: a diagnostic meta-analysis. Eur Urol 70(2):233–245

Donati OF et al (2014) Difusion-weighted MR imaging of upper abdominal organs: field strength and intervendor variability of apparent diffusion coefficient. Radiology 270(2):454–463

Eiber M et al (2016) Simultaneous (68)Ga-PSMA HBED-CC PET/MRI improves the localization of primary prostate cancer. Eur Urol 70(5):829–836

Elkhoury FF et al (2019) Comparison of targeted vs systematic prostate biopsy in men who are biopsy naive: the prospective assessment of image registration in the diagnosis of prostate cancer (PAIREDCAP) study. JAMA Surg 154(9):811–818

Epstein JI et al (2016) The 2014 International Society of Urological Pathology (ISUP)

consensus conference on gleason grading of prostatic carcinoma: definition of grading patterns and proposal for a new grading system. Am J Surg Pathol 40(2):244–252

Fendler WP et al (2017) (68)Ga-PSMA-11 PET/CT Interobserver Agreement for Prostate Cancer Assessments: an international multicenter prospective study. J Nucl Med 58(10):1617–1623

Ferraro DA et al (2019) Impact of (68)Ga-PSMA-11 PET staging on clinical decision-making in patients with intermediate or high-risk prostate cancer. Eur J Nucl Med Mol Imaging 47:652–664

Ferraro DA et al (2021) Diagnostic performance of (68)Ga-PSMA-11 PET/MRI-guided biopsy in patients with suspected prostate cancer: a prospective single-center study. Eur J Nucl Med Mol Imaging 48:3315–3324

Ferraro DA et al (2019) (68)Ga-PSMA-11 PET has the potential to improve patient selection for extended pelvic lymph node dissection in intermediate to high-risk prostate cancer. Eur J Nucl Med Mol Imaging

Futterer JJ et al (2015) Can clinically significant prostate cancer be detected with multiparametric magnetic resonance imaging? A systematic review of the literature. Eur Urol 68(6):1045–1053

Greer MD et al (2019) Interreader variability of prostate imaging reporting and data system version 2 in detecting and assessing prostate cancer lesions at prostate MRI. AJR Am J Roentgenol. https://doi.org/10.2214/AJR.18.20536

Grubmuller B et al (2018) PSMA ligand PET/MRI for primary prostate cancer: staging performance and clinical impact. Clin Cancer Res 24(24):6300–6307

Han S et al (2018) Impact of (68)Ga-PSMA PET on the management of patients with prostate cancer: a systematic review and meta-analysis. Eur Urol 74:179–190

Hofman MS et al (2020) Prostate-specific membrane antigen PET-CT in patients with high-risk prostate cancer before curative-intent surgery or radiotherapy (proPSMA): a prospective, randomised, multi-centre study. Lancet 395:1208–1216

Hupe MC et al (2018) Expression of prostate-specific membrane antigen (PSMA) on biopsies is an independent risk stratifier of prostate cancer patients at time of initial diagnosis. Front Oncol 8:623

Kanthabalan A et al (2016) Transperineal magnetic resonance imaging-targeted biopsy versus transperineal template prostate mapping biopsy in the detection of localised radio-recurrent prostate cancer. Clin Oncol (r Coll Radiol) 28(9):568–576

Kasivisvanathan V et al (2018) MRI-targeted or standard biopsy for prostate-cancer diagnosis. N Engl J Med 378(19):1767–1777

Landis JR, Koch GG (1977) The measurement of observer agreement for categorical data. Biometrics 33(1):159–174

Li M et al (2019) Comparison of PET/MRI with multiparametric MRI in diagnosis of primary prostate cancer: a meta-analysis. Eur J Radiol 113:225–231

Loeb S et al (2013) Systematic review of complications of prostate biopsy. Eur Urol 64(6):876–892

Mortezavi A et al (2018) Diagnostic accuracy of multiparametric magnetic resonance imaging and fusion guided targeted biopsy evaluated by transperineal template saturation prostate biopsy for the detection and characterization of prostate cancer. J Urol 200(2):309–318

Mottet N et al (2017) EAU-ESTRO-SIOG guidelines on prostate cancer. Part 1: Screening, diagnosis, and local treatment with curative intent. Eur Urol 71(4):618–629

Muehlematter UJ et al (2019) Diagnostic accuracy of multiparametric MRI versus (68)Ga-PSMA-11 PET/MRI for extracapsular extension and seminal vesicle invasion in patients with prostate cancer. Radiology 293(2):350–358

Park SY et al (2018) Gallium 68 PSMA-11 PET/MR imaging in patients with intermediate- or high-risk prostate cancer. Radiology 288(2):495–505

Park KJ et al (2020) Interreader agreement with prostate imaging reporting and data system version 2 for prostate cancer detection: a systematic review and meta-analysis. J Urol 204(4):661–670

Paschalis A et al (2019) Prostate-specific membrane antigen heterogeneity and DNA repair defects in prostate cancer. Eur Urol 76:469–478

Pizzuto DA et al (2018) The central zone has increased (68)Ga-PSMA-11 uptake: “Mickey Mouse ears” can be hot on (68)
Ga-PSMA-11 PET. Eur J Nucl Med Mol Imaging 45(8):1335–1343

Roach PJ et al (2018) The Impact of (68)Ga-PSMA PET/CT on management intent in prostate cancer: results of an australian prospective multicenter study. J Nucl Med 59(1):82–88

Shaish H, Kang SK, Rosenkrantz AB (2017) The utility of quantitative ADC values for differentiating high-risk from low-risk prostate cancer: a systematic review and meta-

analysis. Abdom Radiol (NY) 42(1):260–270
Toriihara A et al (2020) Comparison of 3 interpretation criteria for (68)Ga-PSMA11 PET based on inter- and intrareader agreement. J Nucl Med 61(4):533–539
Turkbey B et al (2019) Prostate imaging reporting and data system version 2.1: 2019 update of prostate imaging reporting and data system version 2. Eur Urol 76(3):340–351

Uprimny C et al (2017) (68)Ga-PSMA-11 PET/CT in primary staging of prostate cancer: PSA and Gleason score predict the intensity of tracer accumulation in the primary tumour. Eur J Nucl Med Mol Imaging 44(6):941–949

Wadera A et al (2021) Impact of PI-RADS Category 3 lesions on the diagnostic accuracy of MRI for detecting prostate cancer and the prevalence of prostate cancer within each PI-RADS category: a systematic review and meta-analysis. Br J Radiol 94(1118):20191050
Westphalen AC et al (2020) Variability of the positive predictive value of PI-RADS for prostate MRI across 26 centers: experience of the society of abdominal radiology prostate cancer disease-focused panel. Radiology 296(1):76–84
Woythal N et al (2018) Immunohistochemical validation of PSMA expression measured by (68)Ga-PSMA PET/CT in primary prostate cancer. J Nucl Med 59(2):238–243

Tables

Table 1 Patient characteristics at study inclusion (n=39)

Characteristics	Value
Age (years)	
Mean ± SD	64 ± 6
Median (IQR)	65 (59–68)
PSA at time of PET scan (ng/ml)	
Mean ± SD	9.9 ± 7
Median (IQR)	7.1 (6.3–10.4)
PIRADS* 2.0 *n* (%)	
3	5 (13%)
4	24 (61%)
5	10 (26%)

* Refers to mpMRI clinical report used for inclusion in the study

Table 2 Per-quadrant accuracy and interreader agreement results for PSMA PET/MRI and mpMRI for detection of csPCa

	PSMA PET/MRI	mpMRI	*p* value
AUC (95% CI)	0.80 (0.73, 0.86)	0.77 (0.71, 0.83)	0.56
Sensitivity	66.7%	61.4%	
Specificity	92.9%	92.9%	
PPV	84.4%	83.3%	
NPV	82.9%	80.7%	
Accuracy	83.3%	81.4%	
Cohen's Kappa coefficient* (95% CI)	0.73 (0.61–0.84)	0.65 (0.52–0.79)	

AUC, area under the receiving operator characteristics curve; CI, confidence interval; csPCa, clinically significant prostate cancer; NPV, negative predictive value; PPV, positive predictive value

*Calculated considering readout scores 1 and 2 as negative and 3, 4 and 5 as positive

Table 3 Imaging and histopathological fndings of quadrants with disagreement between PSMA PET/MRI and mpMRI (n=21*)

	Quad	mpMRI PIRADS	PSMA PET/MRI score	Biopsy ISUP	Final diagnosis
Pat. 1	4	2	4	2	No RPE. PSA dropped after HIFU
Pat. 8	1	1	4	1	ISUP 2
Pat. 11	1/2	1/1	4/4	2/3	ISUP 3
Pat. 11	3	2	4	3	ISUP 3
Pat. 22	4	1	5	3	No follow up or RPE
Pat. 24	2	1	4	No cancer	ISUP 3
Pat. 30	1/4	1/1	4/4	2/4	ISUP 2/ISUP 4
Pat. 32	4	1	4	2	ISUP 3
Pat. 35	2	1	3	2	ISUP 2
Pat. 42	1	1	4	2	ISUP 2
Pat. 6	3	5	1	No cancer	No follow up or RPE
Pat. 10	1	5	1	3	ISUP 3
Pat. 17	3	3	1	No cancer	No cancer
Pat. 19	4	4	2	2	ISUP 3
Pat. 26	2	5	1	4	ISUP 2
Pat. 33	3	4	1	2	ISUP 2
Pat. 39	1/2	5/5	1/1	2/2	No RPE. IHC of biopsy cores showed PSMA-negative tumour
Pat. 42	3	3	1	2	ISUP 2 (infiltrative pattern)

HIFU, high intensity focused ultrasound; IHC, immunohistochemistry staining; Pat., patient; Quad, quadrant; RPE, radical prostatectomy

* PSMA PET positive in 12 and mpMRI in 9

Table 4 Imaging and histopathological fndings of the quadrants in which both imaging modalities. (PSMA PET/MRI and mpMRI) disagree with template biopsy results (n=17 quadrants)

	Quad	Imaging	mpMRI PIRADS	PSMA PET/MRI score	Biopsy ISUP	Final diagnosis
Pat. 4	3	FN	1	1	2	No follow up or RPE
Pat. 7	1	FN	1	1	3 (1 mm)	No cancer
Pat. 16	1/4	FN	1/1	1/2	3/2	ISUP 2
Pat. 17	4	FN	1	1	2	ISUP 2
Pat. 24	3	FN	1	1	2 (2 mm)	No cancer
Pat. 26	1	FN	1	1	4	ISUP 2
Pat. 31	4	FN	1	1	2	ISUP 2
Pat. 33	1	FN	1	1	2	ISUP 3 (infiltrative pattern)
Pat. 34	2	FN	1	1	2 (2 mm)	ISUP 2 (1 mm)
Pat. 40	2	FN	1	1	4	ISUP 2
Pat. 41	4	FN	2	1	2	ISUP 2
Pat. 8	4	FP	4	4	1	ISUP 2
Pat. 23	4	FP	3	3	1 (several cores, 7 mm)	No follow up or RPE
Pat. 34	1	FP	4	4	No cancer	ISUP 3
Pat. 35	3	FP	3	4	No cancer	ISUP 3
Pat. 38	1	FP	5	4	No cancer	ISUP 2 (8 mm, foamy differentiation)

FN, false-negative; FP, false-positive; Pat., patient; Quad, quadrant; RPE, radical prostatectomy

Table 5 Semiquantitative parameters

	Median (IQR)	Mean (± SD)	ICC R1 × R2	Correlation with GS
SUV_{max}	6.8 (4.7, 10.5)	10.2 (± 12.3)	0.99 (0.99, 0.99)	$\rho = 0.474$ ($p = 0.002$)
$PSMA_{vol}$	0.8 (0.4, 0.6)	1.8 (± 2.1)	0.90 (0.83, 0.94)	$\rho = 0.468$ ($p = 0.003$)
ADC	832.5 (688.8, 966.3)	836.3 (± 263.9)	0.54 (0.04, 0.78)	$\rho = -0.182$ ($p = 0.26$)
Size*	1.3 (1, 1.6)	1.4 (± 0.6)	0.90 (0.8, 0.95)	$\rho = 0.220$ ($p = 0.16$)

Median, mean and correlation with GS based on results from the more experienced reader

GS, Gleason score; IQR, interquartile rage (Q1, Q3); ICC, intraclass correlation coefficient; R1, reader 1; R2, reader 2; SD, standard deviation

* On mpMRI

Figures

Fig. 1 Patient selection. After signing the informed consent, three patients refused PSMA PET/MRI and other four patients gave up participation before the biopsy. mpMRI images from three patients were not available for review

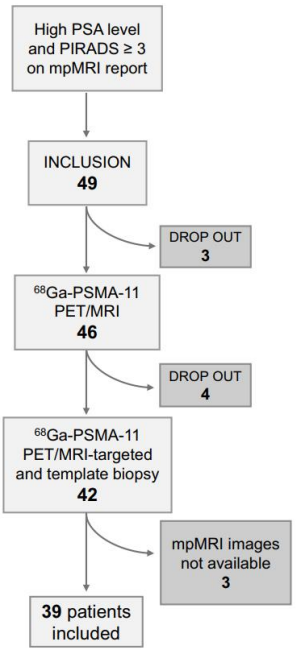

Fig. 2 Example of the method used for lesion localization. **A** Readout of PSMA PET/MRI by one of the readers with the prostate gland divided in 4 quadrants (Q1: anterior right; Q2: anterior left; Q3: posterior left and Q4: posterior right). The reader delineated three areas of 68Ga-PSMA-11 uptake and labeled area 1 as suspicious for malignancy and areas 2 and 3 as benign/physiological. **B** 68Ga-PSMA-11 PET/MRI images of this patient show physiological bilateral uptake in the central zone (arrows) and a suspicious area with intense uptake in the posterior peripheral zone on the left (**D**). **C** histopathological map automatically generated by the biopsy fusion software with numbered biopsy cores, red spots represent the localization of needles with Gleason score≥3+4, confrming the suspicious lesion on Q3 and showing another lesion on Q1 not depicted on PSMA PET/MRI. For the analysis , Q1 was considered false-negative, Q2 true-negative, Q3 true-positive and Q4 false-negative (lesion crossing the midline not depicted by imaging)

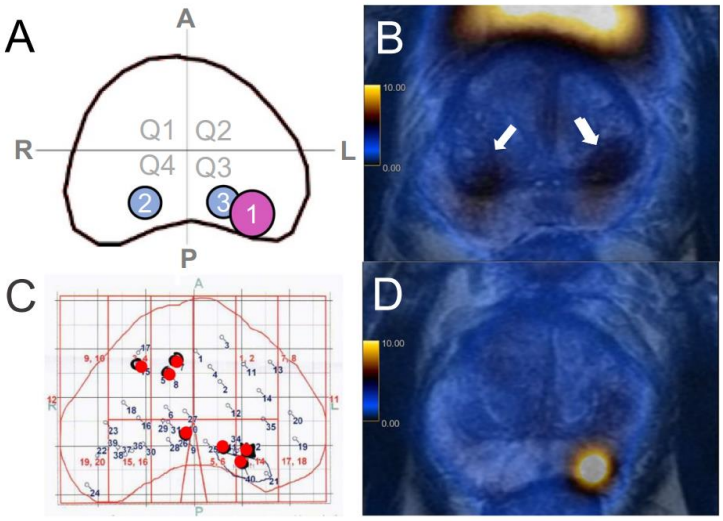

Fig. 3 Imaging fndings in relation to biopsy results. Quadrant-based (n=156) biopsy results in relation to PIRADS on mpMRI and to an adaptation of the same scale for focal uptake on PSMA PET/MRI (1=no focal uptake; 2=benign; 3=undetermined; 4=suspicious for malignancy≤1.5 cm; 5=suspicious for malignancy>1.5 cm). csPCa=clinically signifcant cancer (red, GS≥3+4); ciPCa=clinically insignifcant cancer (blue, GS 3+3)

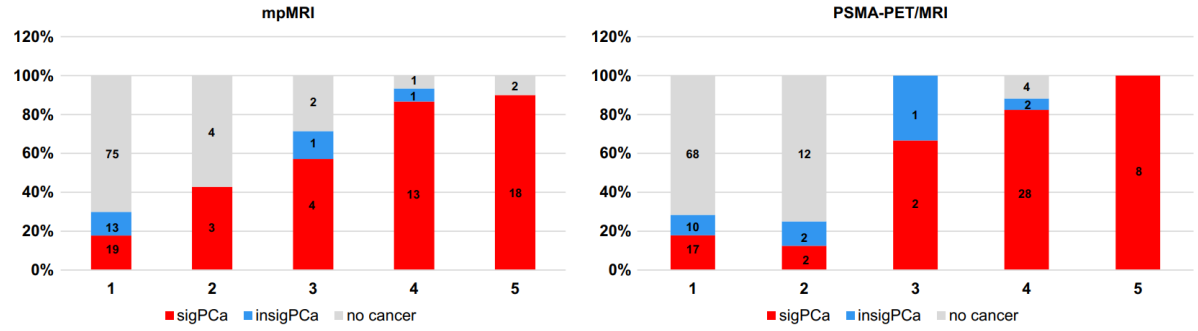

Fig. 4 Imaging and histopathological fndings of cases with discordance between PSMA PET/MRI and mpMRI fndings. Each line corresponds to one patient. From left to right: mpMRI readout, DWI, T2-w, PSMA PET/MRI readout, fusion PSMA PET/MRI and template biopsy map. Readouts:.lesions in red were classifed by the readers as suspicious while the ones in green were classifed as non-suspicious. Template biopsy maps: red dots correspond to GS≥3+4 biopsy cores and blue dots to GS 3+3. **A** The lesion in the left posterior quadrant was depicted on both mpMRI and PSMA PET, corresponding to csPCa on template biopsy, but the two lesions in the right quadrants were only seen on PSMA PET (arrow in the anterior one). **B**

PSMA PET and mpMRI were concordant regarding the lesions in the anterior right and posterior left quadrants but the apex lesion crossing the midline to the posterior right quadrant was only seen on PSMA PET (arrow). **C** The lesion in the right posterior quadrant was seen on mpMRI but not on PSMA PET because physiological uptake in the central zones impaired the visual analysis

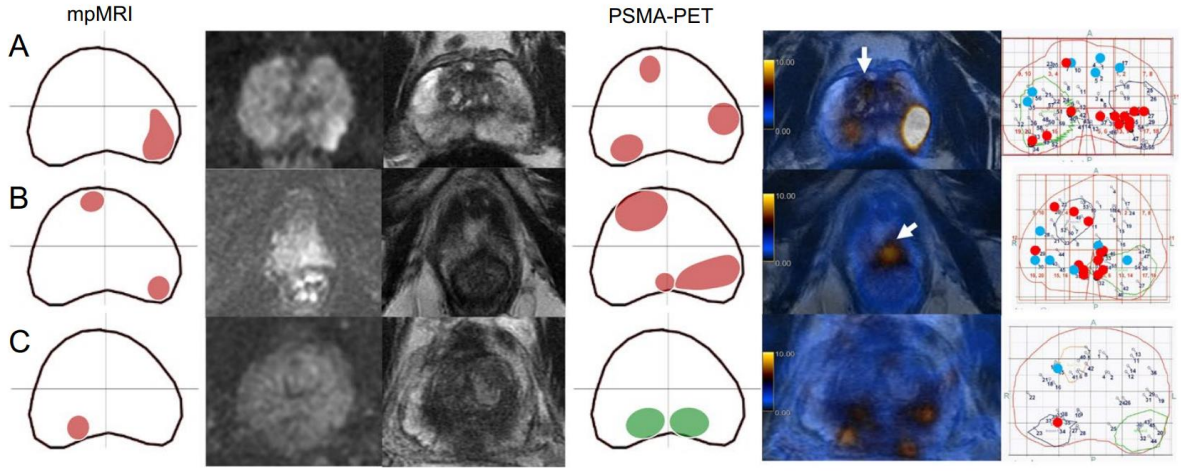

Fig. 5 Imaging and histopathological fndings of cases in which imaging fndings of both mpMRI and PSMA PET were false-positive or false-negative using template biopsy as reference standard. Each line corresponds to one patient. From left to right: mpMRI readout, DWI, T2-w, PSMA PET/MRI readout, fusion PSMA PET/MRI and template biopsy map. **A** Both imaging modalities depicted the lesion in the posterior right quadrant (arrows) but missed the lesion in the anterior right one (Pat. 7). **B** Both imaging modalities depicted the lesion in the posterior right quadrant (not shown) but missed the left one and PSMA PET was also false-positive for the anterior left quadrant (arrow). **C** Imaging was false-positive in the anterior right quadrant, on mpMRI the lesion seems to cross the midline while in PSMA PET the uptake suggests a second lesion (arrow)

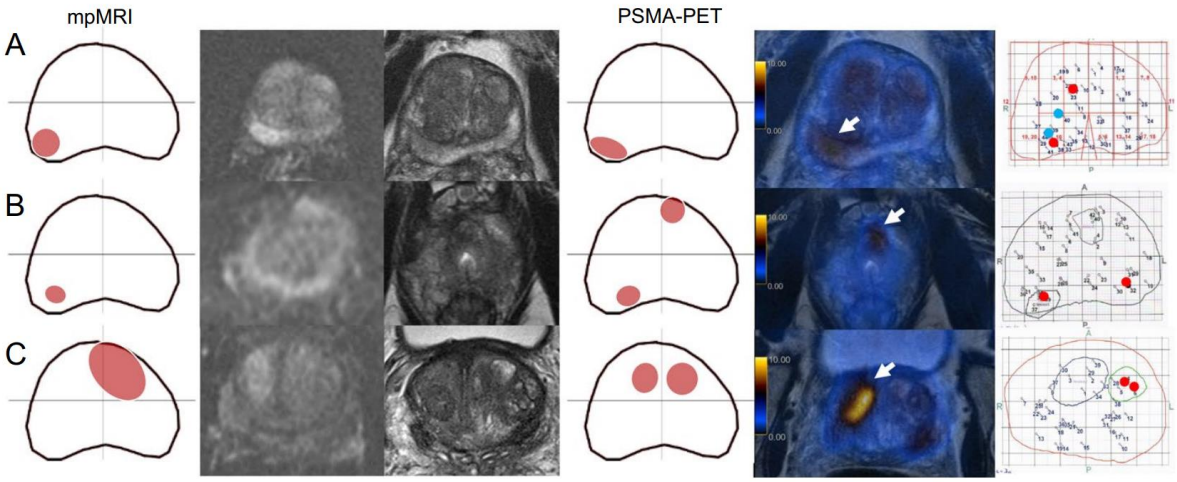

Supplementary Material Readout sheet layout, Table S1 and mpMRI protocol.

^{68}Ga-PSMA-11 PET/MRI and mpMRI readout sheets

Patient study identification code XXX

PET/MRI
Reader 1

Lesion	"PSMA-RADS"	SUVmax	PSMAvol
1			
2			
3			
4			

Patient study identification code XXX

mpMRI
Reader 1

Lesion	PIRADS	ADC	Size
1			
2			
3			
4			

Table S1 Per-reader results

	PSMA-PET/MRI R1	PSMA-PET/MRI R2	MpMRI R1	MpMRI R2
Sensitivity	66.7%	61.4%	61.4%	57.9%
Specificity	92.9%	85.9%	92.9%	86.9%
PPV	84.4%	72.9%	83.3%	71.7%
NPV	82.9%	78.7%	80.7%	78.2%
Accuracy	83.3%	76.9%	81.4%	76.3%

R1 were the more experienced ones.

Multiparametric MRI protocol

At our institution, the typical multiparametric MRI protocol consisted of T2-weighted fast spin-echo images covering the prostate gland and the seminal vesicles, which were obtained in three planes (transverse, sagittal, and coronal). Diffusion-weighted imaging was performed in the transverse plane with identical orientation as the T2-weighted images. The apparent diffusion coefficient parametric maps were calculated by using three *b* values (0, 50, and 1000 sec/mm^2 or 100, 600, and 1000 sec/mm^2). A high–*b*-value image (1400 sec/mm^2) was calculated. Dynamic contrast material– enhanced MRI was performed to yield transverse sections with a temporal resolution of less than 8 seconds. Gadoterate meglumine (Dotarem; Guerbet, Darmstadt, Germany) was used as a contrast agent in a dose of 0.1 mmol per kilogram of body weight. The typical MRI protocol included T2-weighted images in three planes, diffusion-weighted imaging, and dynamic contrast-enhanced imaging.

4 ANÁLISE CRÍTICA E PERSPECTIVAS

Em relação ao principal achado dos estudos, o ^{68}Ga-PSMA-11 PET/RM apresenta alta acurácia na detecção de câncer de próstata clinicamente significante, sem diferença significativa em relação à RMmp para localização de lesões primárias nos pacientes com suspeita de neoplasia de próstata. Apesar da elevada acurácia, a biópsia guiada por ^{68}Ga-PSMA-11 PET/RM não permite dispensar biópsia sistemática.

Nesse contexto, considerando que a RMmp faz parte da investigação estabelecida do câncer de próstata e que cerca de 6% dos adenocarcinomas de próstata não expressam o PSMA, a investigação de pacientes com suspeita de neoplasia de próstata seria usualmente iniciada pela RMmp e seguida pelo PET-PSMA, com potencial de ser particularmente útil em casos de RMmp duvidosa ou alta suspeita clínica com RMmp negativa. O PET-PSMA e a RMmp podem, teoricamente, ser realizados simultaneamente em um único equipamento de PET/RM, similar ao empregado neste projeto, com pequenos ajustes de protocolo de aquisição. A vantagem de realizar os métodos em único tempo deve ser considerada à luz da baixa disponibilidade e alto custo dos equipamentos de PET/RM. Outra opção, provavelmente mais exequível clinicamente, seria a realização do exame em dois tempos, iniciando-se por uma RMmp e, num segundo momento, o estudo PET. O mais provável, frente a disponibilidade de equipamentos e custo do exame, seria a realização do estudo PET em equipamento tomografia por emissão de pósitrons/tomografia computadorizada (PET/CT), com a possibilidade de avaliação locorregional e, também, a investigação de metástases em casos de maior risco. Estudo publicado posteriormente a este trabalho demonstrou ser possível o uso de PET/CT com PSMA para guiar biópsias de próstata, confirmando a correta amostragem da lesão de interesse por mensuração imediata da atividade radioativa do tecido retirado por espectroscopia gama (Ferraro et al., 2022).

Idealmente o método de referência para avaliação de acurácia do exame de imagem seria a análise da peça cirúrgica de prostatectomia, o que não seria possível pela ausência de indicação clínica de prostatectomia em todos os pacientes desta coorte. Dessa forma, mesmo com a realização de biópsia com alto número de amostras, existem limitações inerentes ao procedimento. Os estudos apresentados evidenciaram casos em que o PET/RM detecta lesão suspeita, inclusive confirmada na peça cirúrgica, mas com biópsia negativa.

Também ocorreram casos com biópsia guiada negativa e biópsia sistemática em campo adjacente positiva (dados não publicados), sugerindo erro na localização da biópsia. Este erro é provavelmente resultante da somatória de pequenos erros ou desvios inerentes a cada componente da cadeia de procedimentos, que parte da aquisição dos métodos de imagem até a conclusão da biópsia. A lesão suspeita localizada na imagem é inicialmente identificada visualmente, havendo uma boa correlação interobservador no presente estudo, e, a seguir, transposta para a US com auxílio do software de fusão (Biopsee ®), o qual depende da correta delineação da próstata na RM e no US. O procedimento de biópsia também depende da experiência e habilidade do profissional responsável, no presente estudo sempre realizada pelo mesmo urologista, com extensa experiência no procedimento e no uso do software. O *core* da biópsia é de pequena extensão, e pequenos desvios nas fases precedentes podem levar ao erro de amostragem. Outro fator a ser considerado é a possível deformidade da próstata devido a manipulação durante o próprio procedimento, decorrentes de edema ou sangramento a cada biópsia (mediana de 43 biópsias por paciente neste estudo). Considerando que a morfologia e localização das lesões à RM já foram fusionadas à US no início do procedimento, eventuais distorções do parênquima ao longo do procedimento não serão corrigidas e irão impactar as biópsias obtidas ao final mais do que no início do procedimento. Para reduzir este impacto da localização precisa do sítio de biópsia, neste estudo foi empregada a correlação da RMmp e ^{68}Ga-PSMA-11 PET com os quadrantes e não por lesão específica. Frente ao exposto, uma proposta prática a ser considerada na biópsia guiada seria aumentar as amostras por lesão suspeita, incluindo outras áreas na periferia ou adjacentes à lesão suspeita, além de manter a biópsia sistemática com 12 amostras.

Outro ponto significativo a ser considerado é o valor de predição negativa pela associação do ^{68}Ga-PSMA-11 PET e RMmp demonstrado nos quadrantes com ambos os métodos negativos. Caso comprovado, outra possibilidade de aplicação dos métodos seria a não realização de biópsia imediata em pacientes sem outros critérios de gravidade e que poderiam realizar seguimento clínico-laboratorial. Em publicação posterior a este trabalho foi demonstrada sensibilidade próxima a 97% para detecção de tumor clinicamente significante pela associação de ^{68}Ga-PSMA-11 PET e RMmp (Emmett et al., 2021). Desta

forma, uma possível aplicação do ^{68}Ga-PSMA-11 PET em associação com a RMmp seria evitar a biópsia imediata nos pacientes com resultados negativos em ambos. Esta conduta precisaria ser mais bem avaliada, inclusive diferenciando características clínico-laboratoriais dos pacientes (exemplo: a elevação de PSA é menos específica que alterações do toque retal). Evitar a biópsia poderia reduzir complicações como sangramento (hematúria, hematospermia e sangramento retal), sintomas de trato urinário baixo incluindo retenção urinária, disfunção erétil, infecção e dor, além dos custos diretos e indiretos associados.

5 CONCLUSÕES

1. A acurácia do ^{68}Ga-PSMA-11 PET/RM para guiar biópsia da próstata usando o resultado da biópsia de saturação como padrão-ouro é de 90%, com sensibilidade de 96% e especificidade de 81%.
2. O ^{68}Ga-PSMA-11 PET/RM apresentou acurácia semelhante à da RMmp na localização do tumor primário de próstata e, a despeito de terem resultados concordantes para a maioria das lesões, os dois métodos apresentam complementariedade na detecção de tumores perdidos por um dos métodos.
3. A maioria dos casos falso-positivos ao ^{68}Ga-PSMA-11 PET/RM trata-se de tumores clinicamente insignificantes, destacando-se que essa é uma definição variável na literatura, e tumores sem expressão de PSMA são potenciais falso-negativos.
4. ^{68}Ga-PSMA-11 PET/RM e RMmp apresentam concordância interobservador substancial.
5. Os parâmetros semiquantitativos do ^{68}Ga-PSMA-11 PET (SUVmax e PSMAvol) apresentaram correlação com o grau do tumor primário de próstata, ao contrário dos parâmetros da RMmp (diâmetro tumoral e ADC), que não apresentaram correlação.

REFERÊNCIAS*

* De acordo com Estilo Vancouver.

Abdollah F, Novara G, Briganti A, Scattoni V, Raber M, Roscigno M, Suardi N, Gallina A, Artibani W, Ficarra V, Cestari A, Guazzoni G, Rigatti P, Montorsi F. Trans-rectal versus trans-perineal saturation rebiopsy of the prostate: is there a difference in cancer detection rate? Urology. 2011 Apr;77(4):921-5.

Ahdoot M, Wilbur AR, Reese SE, Lebastchi AH, Mehralivand S, Gomella PT, Bloom J, Gurram S, Siddiqui M, Pinsky P, Parnes H, Linehan WM, Merino M, Choyke PL, Shih JH, Turkbey B, Wood BJ, Pinto PA. MRI-Targeted, Systematic, and Combined Biopsy for Prostate Cancer Diagnosis. N Engl J Med. 2020 Mar 5;382(10):917-928.

Ahmed HU, El-Shater Bosaily A, Brown LC, Gabe R, Kaplan R, Parmar MK, Collaco-Moraes Y, Ward K, Hindley RG, Freeman A, Kirkham AP, Oldroyd R, Parker C, Emberton M; PROMIS study group. Diagnostic accuracy of multi-parametric MRI and TRUS biopsy in prostate cancer (PROMIS): a paired validating confirmatory study. Lancet. 2017 Feb 25;389(10071):815-822.

Ahmed HU, Hu Y, Carter T, Arumainayagam N, Lecornet E, Freeman A, Hawkes D, Barratt DC, Emberton M. Characterizing clinically significant prostate cancer using template prostate mapping biopsy. J Urol. 2011 Aug;186(2):458-64.

Andreoiu M, Cheng L. Multifocal prostate cancer: biologic, prognostic, and therapeutic implications. Hum Pathol. 2010 Jun;41(6):781-93

Arora R, Koch MO, Eble JN, Ulbright TM, Li L, Cheng L. Heterogeneity of Gleason grade in multifocal adenocarcinoma of the prostate. Cancer. 2004 Jun 1;100(11):2362-6.

Bauman G, Martin P, Thiessen JD, Taylor R, Moussa M, Gaed M, Rachinsky I, Kassam Z, Chin J, Pautler S, Lee TY, Valliant JF, Ward A. [18F]-DCFPyL Positron Emission Tomography/Magnetic Resonance Imaging for Localization of Dominant Intraprostatic Foci: First Experience. Eur Urol Focus. 2018 Sep;4(5):702-706.

Borghesi M, Ahmed H, Nam R, Schaeffer E, Schiavina R, Taneja S, Weidner W, Loeb S. Complications After Systematic, Random, and Image-guided Prostate Biopsy. Eur Urol. 2017 Mar;71(3):353-365.

Bravaccini S, Puccetti M, Bocchini M, Ravaioli S, Celli M, Scarpi E, De Giorgi U, Tumedei MM, Raulli G, Cardinale L, Paganelli G. PSMA expression: a potential ally for the pathologist in prostate cancer diagnosis. Sci Rep. 2018 Mar 9;8(1):4254.

Byrd DR, Brookland RK, Washington MK, Gershenwald JE, Compton CC, Hess KR, Sullivan DC. AJCC cancer staging manual. 8th. ed. New York: Springer, 2017.

Catalano OA, Rosen BR, Sahani DV, Hahn PF, Guimaraes AR, Vangel MG, Nicolai E, Soricelli A, Salvatore M. Clinical impact of PET/MR imaging in patients with cancer undergoing same-day PET/CT: initial experience in 134 patients--a hypothesis-generating exploratory study. Radiology. 2013 Dec;269(3):857-69.

Cornford P, van den Bergh RCN, Briers E, Van den Broeck T, Cumberbatch MG, De Santis M, Fanti S, Fossati N, Gandaglia G, Gillessen S, Grivas N, Grummet J, Henry AM, der Kwast THV, Lam TB, Lardas M, Liew M, Mason MD, Moris L, Oprea-Lager DE, der Poel HGV, Rouvière O, Schoots IG, Tilki D, Wiegel T, Willemse PM, Mottet N. EAU-EANM-ESTRO-ESUR-SIOG Guidelines on Prostate Cancer. Part II-2020 Update: Treatment of Relapsing and Metastatic Prostate Cancer. Eur Urol. 2021 Feb;79(2):263-282.

Crawford ED, Wilson SS, Torkko KC, Hirano D, Stewart JS, Brammell C, Wilson RS, Kawata N, Sullivan H, Lucia MS, Werahera PN. Clinical staging of prostate cancer: a computer-simulated study of transperineal prostate biopsy. BJU Int. 2005 Nov;96(7):999-1004.

Eiber M, Fendler WP, Rowe SP, Calais J, Hofman MS, Maurer T, Schwarzenboeck SM, Kratowchil C, Herrmann K, Giesel FL. Prostate-Specific Membrane Antigen Ligands for Imaging and Therapy. J Nucl Med. 2017;58(Suppl 2):67S-76S.

Eiber M, Weirich G, Holzapfel K, Souvatzoglou M, Haller B, Rauscher I, Beer AJ, Wester HJ, Gschwend J, Schwaiger M, Maurer T. Simultaneous 68Ga-PSMA HBED-CC PET/MRI Improves the Localization of Primary Prostate Cancer. Eur Urol. 2016 Nov;70(5):829-836.

Eichler K, Hempel S, Wilby J, Myers L, Bachmann LM, Kleijnen J. Diagnostic value of systematic biopsy methods in the investigation of prostate cancer: a systematic review. J Urol. 2006 May;175(5):1605-12.

Emmett L, Buteau J, Papa N, Moon D, Thompson J, Roberts MJ, Rasiah K, Pattison DA, Yaxley J, Thomas P, Hutton AC, Agrawal S, Amin A, Blazevski A, Chalasani V, Ho B, Nguyen A, Liu V, Lee J, Sheehan-Dare G, Kooner R, Coughlin G, Chan L, Cusick T, Namdarian B, Kapoor J, Alghazo O, Woo HH, Lawrentschuk N, Murphy D, Hofman MS, Stricker P. The Additive Diagnostic Value of Prostate-specific Membrane Antigen Positron Emission Tomography Computed Tomography to Multiparametric Magnetic Resonance Imaging Triage in the Diagnosis of Prostate Cancer (PRIMARY): A Prospective Multicentre Study. Eur Urol. 2021 Dec;80(6):682-689.

Epstein JI, Egevad L, Amin MB, Delahunt B, Srigley JR, Humphrey PA; Grading Committee. The 2014 International Society of Urological Pathology (ISUP) Consensus Conference on Gleason Grading of Prostatic Carcinoma: Definition of Grading Patterns and Proposal for a New Grading System. Am J Surg Pathol. 2016 Feb;40(2):244-52.

Evangelista L, Zattoni F, Cassarino G, Artioli P, Cecchin D, Dal Moro F, Zucchetta P. PET/MRI in prostate cancer: a systematic review and meta-analysis. Eur J Nucl Med Mol Imaging. 2021;48(3):859-873.

Ferraro DA, Laudicella R, Zeimpekis K, Mebert I, Müller J, Maurer A, Grünig H, Donati O, Sapienza MT, Rueschoff JH, Rupp N, Eberli D, Burger IA. Hot needles can confirm accurate lesion sampling intraoperatively using [18F]PSMA-1007 PET/CT-guided biopsy in patients with suspected prostate cancer. Eur J Nucl Med Mol Imaging. 2022 Apr;49(5):1721-1730.

Fütterer JJ, Briganti A, De Visschere P, Emberton M, Giannarini G, Kirkham A, Taneja SS, Thoeny H, Villeirs G, Villers A. Can Clinically Significant Prostate Cancer Be Detected with Multiparametric Magnetic Resonance Imaging? A Systematic Review of the Literature. Eur Urol. 2015 Dec;68(6):1045-53.

Giesel FL, Hadaschik B, Cardinale J, Radtke J, Vinsensia M, Lehnert W, Kesch C, Tolstov Y, Singer S, Grabe N, Duensing S, Schäfer M, Neels OC, Mier W, Haberkorn U, Kopka K, Kratochwil C. F-18 labelled PSMA-1007: biodistribution, radiation dosimetry and histopathological validation of tumor lesions in prostate cancer patients. Eur J Nucl Med Mol Imaging. 2017;44(4):678-688.

Goldberg R. Prostate biopsy options [internet]. 2023 [acesso em 13 jan. 2023]. Disponível em: https://partnersprostate.com/prostate-biopsy/.

Grummet J. How to Biopsy: Transperineal Versus Transrectal, Saturation Versus Targeted, What's the Evidence? Urol Clin North Am. 2017 Nov;44(4):525-534.

Han S, Woo S, Kim YJ, Suh CH. Impact of 68Ga-PSMA PET on the Management of Patients with Prostate Cancer: A Systematic Review and Meta-analysis. Eur Urol. 2018 Aug;74(2):179-190.

Hara R, Jo Y, Fujii T, Kondo N, Yokoyoma T, Miyaji Y, Nagai A. Optimal approach for prostate cancer detection as initial biopsy: prospective randomized study comparing transperineal versus transrectal systematic 12-core biopsy. Urology. 2008 Feb;71(2):191-5.

Hofman MS, Lawrentschuk N, Francis RJ, Tang C, Vela I, Thomas P, Rutherford N, Martin JM, Frydenberg M, Shakher R, Wong LM, Taubman K, Ting Lee S, Hsiao E, Roach P, Nottage M, Kirkwood I, Hayne D, Link E, Marusic P, Matera A, Herschtal A, Iravani A, Hicks RJ, Williams S, Murphy DG; proPSMA Study Group Collaborators. Prostate-specific membrane antigen PET-CT in patients with high-risk prostate cancer before curative-intent surgery or radiotherapy (proPSMA): a prospective, randomised, multicentre study. Lancet. 2020 Apr 11;395(10231):1208-1216.

Iczkowski KA, van Leenders GJLH, van der Kwast TH. The 2019 International Society of Urological Pathology (ISUP) Consensus Conference on Grading of Prostatic Carcinoma. Am J Surg Pathol. 2021 Jul 1;45(7):1007.

Instituto Nacional de Câncer (INCA). Estatísticas de câncer: ações de Vigilância do Câncer, componente estratégico para o planejamento eficiente e efetivo dos programas de prevenção e controle de câncer no país [internet]. 2022 [acesso em: 29 ago. 2023]. Disponível em: https://www.gov.br/inca/pt-br/assuntos/cancer/numeros/.

Jiang X, Zhu S, Feng G, Zhang Z, Li C, Li H, Wang C, Xu Y. Is an initial saturation prostate biopsy scheme better than an extended scheme for detection of prostate cancer? A systematic review and meta-analysis. Eur Urol. 2013 Jun;63(6):1031-9.

Johnson DC, Raman SS, Mirak SA, Kwan L, Bajgiran AM, Hsu W, Maehara CK, Ahuja P, Faiena I, Pooli A, Salmasi A, Sisk A, Felker ER, Lu DSK, Reiter RE. Detection of Individual Prostate Cancer Foci via Multiparametric Magnetic Resonance Imaging. Eur Urol. 2019 May;75(5):712-720.

Lardas M, Liew M, van den Bergh RC, De Santis M, Bellmunt J, Van den Broeck T, Cornford P, Cumberbatch MG, Fossati N, Gross T, Henry AM, Bolla M, Briers E, Joniau S, Lam TB, Mason MD, Mottet N, van der Poel HG, Rouvière O, Schoots IG, Wiegel T, Willemse PM, Yuan CY, Bourke L. Quality of Life Outcomes after Primary Treatment for Clinically Localised Prostate Cancer: A Systematic Review. Eur Urol. 2017 Dec;72(6):869-885.

Minner S, Wittmer C, Graefen M, Salomon G, Steuber T, Haese A, Huland H, Bokemeyer C, Yekebas E, Dierlamm J, Balabanov S, Kilic E, Wilczak W, Simon R, Sauter G, Schlomm T. High level PSMA expression is associated with early PSA recurrence in surgically treated prostate cancer. Prostate. 2011 Feb 15;71(3):281-8.

Moses KA, Sprenkle PC, Bahler C, Box G, Carlsson SV, Catalona WJ, Dahl DM, Dall'Era M, Davis JW, Drake BF, Epstein JI, Etzioni RB, Farrington TA, Garraway IP, Jarrard D, Kauffman E, Kaye D, Kibel AS, LaGrange CA, Maroni P, Ponsky L, Reys B, Salami SS, Sanchez A, Seibert TM, Shaneyfelt TM, Smaldone MC, Sonn G, Tyson MD, Vapiwala N, Wake R, Washington S, Yu A, Yuh B, Berardi RA, Freedman-Cass DA. NCCN Guidelines® Insights: Prostate Cancer Early Detection, Version 1.2023. J Natl Compr Canc Netw. 2023 Mar;21(3):236-246.

Mottet N, Bellmunt J, Bolla M, Briers E, Cumberbatch MG, De Santis M, Fossati N, Gross T, Henry AM, Joniau S, Lam TB, Mason MD, Matveev VB, Moldovan PC, van den Bergh RCN, Van den Broeck T, van der Poel HG, van der Kwast TH, Rouvière O, Schoots IG, Wiegel T, Cornford P. EAU-ESTRO-SIOG Guidelines on Prostate Cancer. Part 1: Screening, Diagnosis, and Local Treatment with Curative Intent. Eur Urol. 2017 Apr;71(4):618-629.

Onur R, Littrup PJ, Pontes JE, Bianco FJ Jr. Contemporary impact of transrectal ultrasound lesions for prostate cancer detection. J Urol. 2004 Aug;172(2):512-4.

Pepe P, Aragona F. Morbidity after transperineal prostate biopsy in 3000 patients undergoing 12 vs 18 vs more than 24 needle cores. Urology. 2013 Jun;81(6):1142-6.

Perera M, Papa N, Roberts M, Williams M, Udovicich C, Vela I, Christidis D, Bolton D, Hofman MS, Lawrentschuk N, Murphy DG. Gallium-68 Prostate-specific Membrane Antigen Positron Emission Tomography in Advanced Prostate Cancer-Updated Diagnostic Utility, Sensitivity, Specificity, and Distribution of Prostate-specific Membrane Antigen-avid Lesions: A Systematic Review and Meta-analysis. Eur Urol. 2020 Apr;77(4):403-417.

Robbins SL, Kumar V, Cotran RS. Robbins and Cotran Pathologic Basis of Disease. 8th ed. New York: Saunders/Elsevier; 2010.

Roberts MJ, Bennett HY, Harris PN, Holmes M, Grummet J, Naber K, Wagenlehner FME. Prostate Biopsy-related Infection: A Systematic Review of Risk Factors, Prevention Strategies, and Management Approaches. Urology. 2017;104:11-21.

Rouvière O, Puech P, Renard-Penna R, Claudon M, Roy C, Mège-Lechevallier F, Decaussin-Petrucci M, Dubreuil-Chambardel M, Magaud L, Remontet L, Ruffion A, Colombel M, Crouzet S, Schott AM, Lemaitre L, Rabilloud M, Grenier N; MRI-FIRST Investigators. Use of prostate systematic and targeted biopsy on the basis of multiparametric MRI in biopsy-naive patients (MRI-FIRST): a prospective, multicentre, paired diagnostic study. Lancet Oncol. 2019 Jan;20(1):100-109.

Scattoni V, Roscigno M, Raber M, Dehò F, Maga T, Zanoni M, Riva M, Sangalli M, Nava L, Mazzoccoli B, Freschi M, Guazzoni G, Rigatti P, Montorsi F. Initial extended transrectal prostate biopsy--are more prostate cancers detected with 18 cores than with 12 cores? J Urol. 2008 Apr;179(4):1327-31; discussion 1331.

Singh PB, Anele C, Dalton E, Barbouti O, Stevens D, Gurung P, Arya M, Jameson C, Freeman A, Emberton M, Ahmed HU. Prostate cancer tumour features on template prostate-mapping biopsies: implications for focal therapy. Eur Urol. 2014 Jul;66(1):12-9.

Smeenge M, Barentsz J, Cosgrove D, de la Rosette J, de Reijke T, Eggener S, Frauscher F, Kovacs G, Matin SF, Mischi M, Pinto P, Rastinehad A, Rouviere O, Salomon G, Polascik T, Walz J, Wijkstra H, Marberger M. Role of transrectal ultrasonography (TRUS) in focal therapy of prostate cancer: report from a Consensus Panel. BJU Int. 2012 Oct;110(7):942-8.

Takenaka A, Hara R, Ishimura T, Fujii T, Jo Y, Nagai A, Fujisawa M. A prospective randomized comparison of diagnostic efficacy between transperineal and transrectal 12-core prostate biopsy. Prostate Cancer Prostatic Dis. 2008;11(2):134-8.

Tu X, Zhang C, Liu Z, Shen G, Wu X, Nie L, Chang T, Xu H, Bao Y, Yang L, Wei Q. The Role of 68Ga-PSMA Positron Emission Tomography/Computerized Tomography for Preoperative Lymph Node Staging in Intermediate/High Risk Patients With Prostate Cancer: A Diagnostic Meta-Analysis. Front Oncol. 2020 Aug 18;10:1365.

Turkbey B, Rosenkrantz AB, Haider MA, Padhani AR, Villeirs G, Macura KJ, Tempany CM, Choyke PL, Cornud F, Margolis DJ, Thoeny HC, Verma S, Barentsz J, Weinreb JC. Prostate Imaging Reporting and Data System Version 2.1: 2019 Update of Prostate Imaging Reporting and Data System Version 2. Eur Urol. 2019 Sep;76(3):340-351.

Xiang J, Yan H, Li J, Wang X, Chen H, Zheng X. Transperineal versus transrectal prostate biopsy in the diagnosis of prostate cancer: a systematic review and meta-analysis. World J Surg Oncol. 2019;17(1):31.

Zogal P, Sakas G, Rösch W, Baltas D. BiopSee® - transperineal stereotactic navigated prostate biopsy. J Contemp Brachytherapy. 2011 Jun;3(2):91-95.

ANEXOS

Anexo A - Aprovação Comissão de Ética Cantonal de Zurique

Kanton Zürich
Kantonale Ethikkommission

Prof. Dr. med. Peter Meier-Abt
Präsident

Dr. med. Peter Kleist
Geschäftsführer
Stampfenbachstrasse 121
Postfach
8090 Zürich
Telefon +41 43 259 79 70
Fax +41 43 259 79 72
admin.kek@kek.zh.ch
www.kek.zh.ch

Einschreiben
UniversitätsSpital Zürich
Klinik für Nuklearmedizin
PD Dr. med. Irene Burger
Rämistrasse 100
8091 Zürich

23. März 2017/ktr
Beschlussmitteilung der Kantonalen Ethikkommission Zürich

Gesuch BASEC-Nr. 2017-00016
Single-center study investigating the diagnostic performance of biopsy guidance using the [68Ga]PSMA PET/MR in patients with elevated PSA eligible for prostate biopsy in comparison to multiparametric MRI.

Gesuchsteller PD Dr. med. Irene Burger, UniversitätsSpital Zürich

Zentren PD Dr. med. Irene Burger, UniversitätsSpital Zürich

I. Verfahren

☐ ordentliches Verfahren ☐ vereinfachtes Verfahren ☒ präsidiales Verfahren

II. Entscheid

☒ **Die Bewilligung wird erteilt**

Bedeutet: Das Vorhaben gemäss bewilligtem Forschungsplan kann gestartet und im Rahmen der anwendbaren rechtlichen Bestimmungen durchgeführt werden.

Bewilligungen für **klinische Versuche der Kategorie B und C** stehen unter dem **Vorbehalt**, dass

1. allfällig durch die zuständige eidgenössische Zulassungsbehörde (Swissmedic/BAG) festgestellte Mängel keine Änderungen der von der Ethikkommission evaluierten Unterlagen erfordern, und dass
2. die Bewilligung der eidgenössischen Zulassungsbehörde (Swissmedic/BAG) vorliegt.

☐ **Die Bewilligung wird mit Auflagen erteilt**

Bedeutet: Das Vorhaben gemäss bewilligtem Forschungsplan:

kann gestartet und im Rahmen der anwendbaren rechtlichen Bestimmungen durchgeführt werden.

Die Auflagen sind innert angemessener Frist zu erfüllen. Die revidierten Dokumente werden nach Einreichung im präsidialen Verfahren geprüft.

Folgende Auflagen müssen erfüllt werden:

Kontaktperson:

☐ **Gegenwärtig kann die Bewilligung noch nicht erteilt werden**

Bedeutet: Das Vorhaben kann **noch nicht** gestartet werden. Die nachfolgenden Bedingungen sind zu erfüllen. Die revidierten Dokumente werden nach Einreichung von der Ethikkommission geprüft.

Folgende Bedingungen müssen für alle Zentren erfüllt werden:

Kontaktperson:

☐ **Die Bewilligung wird nicht erteilt**

Bedeutet: Das Vorhaben kann in der vorliegenden Form nicht durchgeführt werden. Eine Neueinreichung ist möglich.

☐ **Auf das Gesuch wird nicht eingetreten**

Bedeutet: Die Ethikkommission ist für die Beurteilung rechtlich nicht zuständig (entweder ist eine andere Stelle für die Bewilligung zuständig, oder das Vorhaben kann ohne Bewilligung durchgeführt werden). Oder: Das Gesuch ist nicht vollständig.

☐ **Das Verfahren wird infolge Gegenstandslosigkeit abgeschrieben**

Bedeutet: Das Verfahren wird wegen Rückzugs des Gesuchs oder anderen Gründen gegenstandslos.

☐ **Das Verfahren wird sistiert**

☐ **Die Bewilligung wird entzogen**

III. Einteilung

☒ **Das Vorhaben gilt als klinischer Versuch gemäss KlinV**

☒ Kategorie ☒ A ☐ B ☐ C

☒ mit Arzneimitteln

☐ mit Medizinprodukten

☐ mit Transplantatprodukten

☐ der Gentherapie

☐ mit gentechnisch veränderten oder pathogenen Organismen

☐ der Transplantation

☐ anderer klinischer Versuch gemäss 4. Kapitel KlinV

☐ Umkategorisierung gemäss Art. 71 Abs. 3 KlinV, Kategorie ☐A ☐B ☐C

☐ mit Strahlenquellen

☐ **Das Vorhaben gilt als Forschungsprojekt gemäss HFV**

☐ Forschung mit Personen, Kategorie ☐A ☐B

☐ Umkategorisierung gemäss Art. 48 Abs. 2 HFV, Risiko-Kategorie ☐A ☐B

☐ mit Strahlenquellen

☐ Weiterverwendung biologischen Materials und/oder gesundheitsbezogener Personendaten

☐ Forschung mit verstorbenen Personen

☐ Forschung an Embryonen und Föten einschliesslich Totgeburten

☐ **Weiterverwendung ohne vorbestehende Einwilligung (Art. 34 HFG, Art. 37-40 HFV)**

a. Verwendungszweck

b. Bezeichnung des biologischen Materials/Personendaten

c. zur Weitergabe berechtigter Personenkreis

d. zur Entgegennahme berechtigter Personenkreis

☐ **Multizentrisches Forschungsprojekt**

☐BE ☐NZ ☐GE ☐OS ☐ TI ☐VD ☐ZH

IV. Begründung

Die Ethikkommission stützt ihre Begründung auf die Unterlagen, wie sie aufgeführt sind:

- ☒ in der submission summary vom 17.03.2017
- ☐ in der /den Stellungnahme/n der Kantonalen Ethikkommission/en:
- ☒ im Beschluss der Kantonalen Ethikkommission Zürich vom 08.02.2017
- ☐ sowie auf
- ☐ Wir bitten Sie, die geänderten Unterlagen im BASEC hochzuladen.

V. Kosten

Die Gebühren wurden bereits in Rechnung gestellt.

VI. Rechtsmittelbelehrung

Gegen diesen Beschluss kann innert 30 Tagen, von der Mitteilung an gerechnet, beim Regierungsrat des Kantons Zürich schriftlich Rekurs eingereicht werden. Die Rekursschrift muss einen Antrag und dessen Begründung enthalten. Der angefochtene Entscheid ist beizulegen oder genau zu bezeichnen. Die angerufenen Beweismittel sind genau zu bezeichnen und soweit möglich beizulegen.

VII. Mitteilung an den Gesuchsteller

und in Kopie an:

- ☐ **Sponsor**
- ☒ **Swissmedic**
- ☐ **BAG**
- ☐ **beteiligte, lokale EKs (multizentrische Studien)**
- ☐ **Behörden:**
- ☐ **andere:**

Kantonale Ethikkommission
5/8

VIII. Zusammensetzung der am Entscheid beteiligten Kommission

					am Beschluss beteiligt		
					ja	nein	
	Name, Vorname	Berufliche Stellung / Titel	m	f		abwesend	In Ausstand
Vorsitz	Meier-Abt Peter	Prof. Dr. med.	☒	☐	☒	☐	☐
Mitglieder	Baumann-Hölzle Ruth	Dr. theol.	☐	☒	☐	☐	☐
	Betschart Cornelia	Dr. med.	☐	☒	☐	☐	☐
	Bloch E. Konrad	Prof. Dr. med.	☒	☐	☐	☐	☐
	Geschwindner Heike	PhD MNSc Pflegewissenschaft	☐	☒	☐	☐	☐
	Gussmann-Bader Marianne	Rechtsanwältin, lic. iur.	☐	☒	☐	☐	☐
	Haug Achim	Prof. Dr.med.	☒	☐	☐	☐	☐
	Hess Christian	Dr. med.	☒	☐	☐	☐	☐
	Jetter Alexander	PD Dr. med.	☒	☐	☐	☐	☐
	Jokeit Hennric*	Prof. Dr. rer. nat. Dipl.-Psych.	☒	☐	☐	☐	☐
	Kapossy Katrin	Fürsprecherin	☐	☒	☐	☐	☐
	Keller-Senn Anita	Pflegefachfrau MScN	☐	☒	☐	☐	☐
	Künig Gabriella	PD Dr. med.	☐	☒	☐	☐	☐
	Lütolf Urs M.	Prof. em. Dr. med.	☒	☐	☐	☐	☐
	Metzger Urs	Prof. Dr. med.	☒	☐	☐	☐	☐
	Nadal David	Prof. Dr. med.	☒	☐	☐	☐	☐
	Ramel Urs	Dr. med. dent.	☒	☒	☐	☐	☐
	Siegrist Michael	Prof. Dr. phil.	☒	☐	☐	☐	☐
für Biometrie zuständiges Mitglied*	Stocker Reto	Prof. Dr. med.	☒	☐	☐	☐	☐
	Ziltener Erika	Lic. phil. I, Patientenstelle	☐	☒	☐	☐	☐

Peter Meier-Abt

Peter Kleist

Bemerkungen

Registrierungspflicht

Der Sponsor muss – falls es sich um einen klinischen Versuch handelt – diesen in einem WHO-Primärregister oder im Register der Nationalen Medizinbibliothek der USA (clinicaltrials.gov) erfassen und anschliessend diese Nummer im BASEC-Portal eingeben. Die Übertragung der erforderlichen Daten in das Swiss National Clinical Trials Portal (SNCTP) kann nach Bewilligung der Ethikkommission und Zustimmung des Gesuchstellers automatisch erfolgen. Die Informationen über den klinischen Versuch sind in beiden Registern öffentlich zugänglich. Zusätzlich veröffentlicht swissethics wenige Informationen wie Titel, Projekttyp oder Leit-Ethikkommission aller durch die kantonalen Ethikkommissionen bewilligten Gesuche auf swissethics.ch (ausser Phase-I-Studien).

Die Kantonale Ethikkommission Zürich bestätigt, dass sie nach ICH-GCP arbeitet.

Vorgehen zur Einreichung revidierter Dokumente

- Revidierte Unterlagen sind der Ethikkommission über BASEC zuzustellen.
- Die Änderungen sind in den revidierten Dokumenten zu markieren.
- Die revidierten Dokumente sind auch weiteren involvierten Zulassungsbehörden zuzustellen, sofern sie von diesen für die Bewilligung benötigt werden.

Meldungen und Berichterstattung an die Ethikkommission siehe Anhang 1 und Anhang 2

Anhang 1
Meldungen und Berichterstattung an die Ethikkommission ab 1. Januar 2014 für klinische Versuche (KlinV)

Meldung von Sicherheits- und Schutzmassnahmen
siehe Art. 37 KlinV:
Meldung an die EK innerhalb von 7 Tagen
Versuche mit Medizinprodukten: innerhalb von 2 Tagen

Abschluss, Abbruch oder Unterbruch des klinischen Versuchs
siehe Art. 38 KlinV:
Abschlussmeldung an die EK innerhalb von 90 Tagen
Abbruch- oder Unterbruchmeldung an die EK innerhalb von 15 Tagen
Schlussbericht an die EK: innerhalb 1 Jahres nach Abschluss/Abbruch

Schwerwiegende unerwünschte Ereignisse (Serious Adverse Events, SAE) bei klinischen Versuchen mit Arzneimitteln
Siehe Art. 40 KlinV:
Falls gemäss Protokoll nicht anders vorgesehen SAE mit Todesfolge innerhalb von 7 Tagen (an lokale EK nur lokale Ereignisse, an Leit-EK alle Ereignisse in der CH).

Verdacht auf eine unerwartete schwerwiegende Arzneimittelwirkung (Suspected Unexpected Serious Adverse Reaction, SUSAR)
Siehe Art. 41 KlinV:
SUSAR mit Todesfolge innerhalb von 7 Tagen, sonstige SUSARs innerhalb von 15 Tagen (an lokale EK nur lokale Ereignisse, an Leit-EK alle Ereignisse in der CH).

Schwerwiegende unerwünschte Ereignisse (Serious Adverse Events, SAE) bei klinischen Versuchen mit Medizinprodukten
Siehe Art. 42 KlinV:
Bei Versuchen der Kategorie C SAE bei Verdacht auf Zusammenhang mit Prüfprodukt oder erfolgtem Eingriff innerhalb von 7 Tagen (an lokale EK nur lokale Ereignisse, an Leit-EK alle Ereignisse in der CH).

Schwerwiegende unerwünschte Ereignisse (Serious Adverse Events, SAE) mit möglichem Zusammenhang zu untersuchter Intervention bei übrigen klinischen Versuchen
Siehe Art. 63 KlinV:
Meldung an EK innerhalb von 15 Tagen.

Berichterstattung über die Sicherheit der teilnehmenden Personen
Siehe Art. 43 KlinV:
1 mal jährlich Auflistung der Ereignisse weltweit (Annual Safety Report)

Mit dem jährlichen Sicherheitsbericht sind der EK auch alle Änderungen zu melden, die nicht bewilligungspflichtig sind (d.h. alle Änderungen, die gemäss Art. 29 KlinV nicht als wesentliche gelten).

Anhang 2
Meldungen und Berichterstattung an die Ethikkommission ab 1. Januar 2014 für Forschungsprojekte mit Ausnahme der klinischen Versuche (HFV)

Forschung mit Personen, die mit Massnahmen zur Entnahme biologischen Materials oder zur Erhebung gesundheitsbezogener Personendaten verbunden
Sicherheits- und Schutzmassnahmen siehe Art. 20 HFV
Meldung an die EK innerhalb von 7 Tagen

Schwerwiegende Ereignisse siehe Art. 21 HFV
Meldung innerhalb von 7 Tagen (an lokale EK nur lokale Ereignisse, an Leit-EK alle Ereignisse in der CH) und Unterbruch des Forschungsprojektes.

Abschluss und Abbruch des Forschungsprojekts siehe Art. 22 HFV
Meldung an die EK innerhalb von 90 Tagen

Weiterverwendung biologischen Materials und gesundheitsbezogener Personendaten für die Forschung
Siehe Art. 36 HFV:
Wechsel Projektleitung: Meldung an die EK: vorgängig

Abschluss und Abbruch des Forschungsprojekts
Meldung an die EK innerhalb von 90 Tagen

Weiterverwendung biologischen Materials und gesundheitsbezogener Personendaten für die Forschung bei fehlender Einwilligung und Information nach Artikel 34 HFG
Siehe Art. 40 HFV:
Änderungen der in der Bewilligung genannten Angaben
Meldung an die EK (vorgängig)

Abschluss oder Abbruch des Forschungsprojekts
Meldung an die EK innerhalb von 90 Tagen

Forschung an verstorbenen Personen (Art. 43 HFV)
Siehe Art. 43 HFV:
Wechsel der Projektleitung: Meldung an die EK (vorgängig)

Bei Forschungsprojekten mit verstorbenen Personen, die künstlich beatmet werden
Wesentliche Änderungen des Forschungsplans
Meldung an die EK (vorgängig)

Abschluss oder Abbruch des Forschungsprojekts
Meldung an die EK innerhalb von 90 Tagen

Kanton Zürich
Kantonale Ethikkommission

Prof. Dr. med. Peter Meier-Abt
Präsident

Dr. med. Peter Kleist
Geschäftsführer
Stampfenbachstrasse 121
Postfach
8090 Zürich
Telefon +41 43 259 79 70
Fax +41 43 259 79 72
admin.kek@kek.zh.ch
www.kek.zh.ch

UniversitätsSpital Zürich
Klinik für Nuklearmedizin
PD Dr. med. Irene A. Burger
Rämistrasse 100
8091 Zürich

07. Februar 2020 / mom

Verfügung der Kantonalen Ethikkommission Zürich

Wesentliche Änderung	Amendment 5
Eingereicht am	30. Januar 2020
BASEC-Nr.	2017-00016
Projekttitel	Single-center study investigating the diagnostic performance of biopsy guidance using the [68Ga]PSMA PET/MR in patients with elevated PSA eligible for prostate biopsy in comparison to multiparametric MRI.
Zentrum	PD Dr. med. Irene A. Burger, Klinik für Nuklearmedizin, USZ

Entscheid

Die Bewilligung wird erteilt.
Allfällige weitere Bewilligungspflichten sind zu beachten.

Entscheidverfahren

☐ vereinfachtes Verfahren ☒ Präsidialentscheid

Die Ethikkommission bestätigt, dass sie nach ICH-GCP arbeitet.

Gebühren

Betrag: CHF 300.- Tarifcode: 3.3.2
Gemäss der geltenden Gebührenordnung von swissethics.

Rechtsmittelbelehrung
Gegen diesen Beschluss kann innert 30 Tagen, von der Mitteilung an gerechnet, beim Regierungsrat des Kantons Zürich schriftlich Rekurs eingereicht werden. Die Rekursschrift muss einen Antrag und dessen Begründung enthalten. Der angefochtene Entscheid ist beizulegen oder genau zu bezeichnen. Die angerufenen Beweismittel sind genau zu bezeichnen und soweit möglich beizulegen.

Kopie an

- ☐ Sponsor
- ☐ Swissmedic
- ☐ Bundesamt für Gesundheit
- ☐ beteiligte Ethikkommission
- ☐ andere:

Prof. Dr. med. Peter Meier-Abt
Präsident

Dr. med. Peter Kleist
Geschäftsführer

Anhang: - Liste der Dokumente

Anexo B - Aprovação CEP Faculdade de Medicina da Universidade de São Paulo

USP - FACULDADE DE MEDICINA DA UNIVERSIDADE DE SÃO PAULO - FMUSP

Plataforma Brasil

PARECER CONSUBSTANCIADO DO CEP

DADOS DO PROJETO DE PESQUISA

Título da Pesquisa: DESEMPENHO DO 68Ga-PSMA-11 PET/RM EM COMPARAÇÃO COM A RESSONÂNCIA MAGNÉTICA MULTIPARAMÉTRICA NA BIÓPSIA DE PRÓSTATA GUIADA EM PACIENTES COM PSA ELEVADO

Pesquisador: Marcelo Tatit Sapienza

Área Temática:

Versão: 1

CAAE: 25929919.2.0000.0065

Instituição Proponente: Faculdade de Medicina da Universidade de São Paulo

Patrocinador Principal: Financiamento Próprio

DADOS DO PARECER

Número do Parecer: 3.807.518

Apresentação do Projeto:

Trata-se de um estudo para avaliar a performance do PET/RM com antígeno de membrana específico da próstata (PSMA) na detecção e localização do câncer primário da próstata clinicalmente significativo para finalidade de guiar biópsia, usando o escore de Gleason (GS) da amostra como padrão-ouro.

Objetivo da Pesquisa:

O objetivo principal do estudo é avaliar a performance do PET/RM com PSMA em detectar e localizar câncer primário da próstata clinicalmente significativo para guiar biópsia, usando o GS da amostra como padrão-ouro. Num segundo momento, a performance do PET/RM com PSMA para guiar biópsia de próstata será comparada com a da RM sozinha. Primariamente será determinada a taxa de detecção de câncer de próstata do PET/RM com PSMA com base nos resultados histopatológicos, por paciente e por segmento prostático. Em segundo lugar, será determinada a proporção de lesões detectadas pela RM sozinha, pelo PET com PSMA sozinho e pelo 68Ga-PSMA-11 PET/RM.

Avaliação dos Riscos e Benefícios:

Esse estudo apresenta riscos mínimos associados à execução da biópsia prostática

Endereço: DOUTOR ARNALDO 251 21º andar sala 36
Bairro: PACAEMBU **CEP:** 01.246-903
UF: SP **Município:** SAO PAULO
Telefone: (11)3893-4401 **E-mail:** cep.fm@usp.br

USP - FACULDADE DE MEDICINA DA UNIVERSIDADE DE SÃO PAULO - FMUSP

Plataforma Brasil

Continuação do Parecer: 3.807.518

Comentários e Considerações sobre a Pesquisa:

Esse estudo foi aprovado pelo Comitê De Ética Competente do Hospital da Universidade de Zürich (BASEC Nr: 2017-00016, documento em anexo) e será realizado de acordo com os princípios enunciados na versão atual da Declaração de Helsinki, as diretrizes de boa prática clinica do International Council on Harmonization (www.ich.org) e requerimentos das autoridades Suíças competentes. O protocolo e o termo de consentimento livre e esclarecido bem como outros documentos específicos a respeito do estudo foram submetidos e o estudo não foi iniciado até o momento da sua aprovação pelo Comitê de Ética.

Considerações sobre os Termos de apresentação obrigatória:

Os termos estão adequados à legislação vigente

Conclusões ou Pendências e Lista de Inadequações:

Aprovo o estudo e submeto esse parecer ao colegiado

Considerações Finais a critério do CEP:

Este parecer foi elaborado baseado nos documentos abaixo relacionados:

Tipo Documento	Arquivo	Postagem	Autor	Situação
Informações Básicas do Projeto	PB_INFORMAÇÕES_BÁSICAS_DO_PROJETO_1451436.pdf	19/11/2019 07:13:45		Aceito
Outros	declaracao_cooperacao_deptos_ingles.pdf	19/11/2019 07:12:06	DANIELA ANDRADE FERRARO	Aceito
Outros	APROVACAO_DEPARTAMENTO.pdf	19/11/2019 07:11:31	DANIELA ANDRADE FERRARO	Aceito
Outros	FORMULARIO_CEP.pdf	19/11/2019 07:11:16	DANIELA ANDRADE FERRARO	Aceito
Folha de Rosto	FOLHA_DE_ROSTO_PB_ASSINATURA.pdf	19/11/2019 06:50:13	DANIELA ANDRADE FERRARO	Aceito
TCLE / Termos de Assentimento / Justificativa de Ausência	traducaoTCLE_Suica.pdf	21/10/2019 16:53:35	Marcelo Tatit Sapienza	Aceito
Projeto Detalhado / Brochura Investigador	BG_project_Portuguese.docx	11/10/2019 19:18:55	DANIELA ANDRADE FERRARO	Aceito
Outros	decisao_comissao_etica_alemao.pdf	11/10/2019 19:17:20	DANIELA ANDRADE FERRARO	Aceito
Outros	Decisao_Comissao_Cantonal_de_Etica_de_Zurich_portugues.pdf	11/10/2019 19:16:46	DANIELA ANDRADE FERRARO	Aceito

Endereço: DOUTOR ARNALDO 251 21º andar sala 36
Bairro: PACAEMBU **CEP:** 01.246-903
UF: SP **Município:** SAO PAULO
Telefone: (11)3893-4401 **E-mail:** cep.fm@usp.br

USP - FACULDADE DE MEDICINA DA UNIVERSIDADE DE SÃO PAULO - FMUSP

Continuação do Parecer: 3.807.518

Situação do Parecer:
Aprovado

Necessita Apreciação da CONEP:
Não

SAO PAULO, 23 de Janeiro de 2020

Assinado por:
Maria Aparecida Azevedo Koike Folgueira
(Coordenador(a))

Endereço: DOUTOR ARNALDO 251 21º andar sala 36
Bairro: PACAEMBU **CEP:** 01.246-903
UF: SP **Município:** SAO PAULO
Telefone: (11)3893-4401 **E-mail:** cep.fm@usp.br

Publicação 1

European Journal of Nuclear Medicine and Molecular Imaging (2021) 48:3315–3324
https://doi.org/10.1007/s00259-021-05261-y

ORIGINAL ARTICLE

Diagnostic performance of ^{68}Ga-PSMA-11 PET/MRI-guided biopsy in patients with suspected prostate cancer: a prospective single-center study

Daniela A. Ferraro[1,2] · Anton S. Becker[3,4] · Benedikt Kranzbühler[5] · Iliana Mebert[1,5] · Anka Baltensperger[1,5] · Konstantinos G. Zeimpekis[1] · Hannes Grünig[1] · Michael Messerli[1] · Niels J. Rupp[6] · Jan H. Rueschoff[6] · Ashkan Mortezavi[5] · Olivio F. Donati[3] · Marcelo T. Sapienza[2] · Daniel Eberli[5] · Irene A. Burger[1,7,8]

Received: 27 December 2020 / Accepted: 11 February 2021 / Published online: 23 February 2021
© The Author(s) 2021

Abstract

Purpose Ultrasound-guided biopsy (US biopsy) with 10–12 cores has a suboptimal sensitivity for clinically significant prostate cancer (sigPCa). If US biopsy is negative, magnetic resonance imaging (MRI)–guided biopsy is recommended, despite a low specificity for lesions with score 3–5 on Prostate Imaging Reporting and Data System (PIRADS). Screening and biopsy guidance using an imaging modality with high accuracy could reduce the number of unnecessary biopsies, reducing side effects. The aim of this study was to assess the performance of positron emission tomography/MRI with ^{68}Ga-labeled prostate-specific membrane antigen (PSMA-PET/MRI) to detect and localize primary sigPCa (ISUP grade group 3 and/or cancer core length ≥ 6 mm) and guide biopsy.

Methods Prospective, open-label, single-center, non-randomized, diagnostic accuracy study including patients with suspected PCa by elevation of prostate-specific antigen (PSA) level and a suspicious lesion (PIRADS ≥3) on multiparametric MRI (mpMRI). Forty-two patients underwent PSMA-PET/MRI followed by both PSMA-PET/MRI-guided and section-based saturation template biopsy between May 2017 and February 2019. Primary outcome was the accuracy of PSMA-PET/MRI for biopsy guidance using section-based saturation template biopsy as the reference standard.

Results SigPCa was found in 62% of the patients. Patient-based sensitivity, specificity, negative and positive predictive value, and accuracy for sigPCa were 96%, 81%, 93%, 89%, and 90%, respectively. One patient had PSMA-negative sigPCa. Eight of nine false-positive lesions corresponded to cancer on prostatectomy and one in six false-negative lesions was negative on prostatectomy.

Conclusion PSMA-PET/MRI has a high accuracy for detecting sigPCa and is a promising tool to select patients with suspicion of PCa for biopsy.

Trial registration This trial was retrospectively registered under the name "Positron Emission Tomography/Magnetic Resonance Imaging (PET/MRI) Guided Biopsy in Men with Elevated PSA," (NCT03187990) on 06/15/2017 (https://clinicaltrials.gov/ct2/show/NCT03187990).

Daniel Eberli and Irene A. Burger contributed equally to this work.

This article is part of the Topical Collection on Oncology - Genitourinary

✉ Irene A. Burger
irene.burger@usz.ch

[1] Department of Nuclear Medicine, University Hospital Zurich, University of Zurich, Zurich, Switzerland

[2] Department of Radiology and Oncology, Faculdade de Medicina FMUSP, Universidade de Sao Paulo, Sao Paulo, Brazil

[3] Institute of Interventional and Diagnostic Radiology, University Hospital Zurich, University of Zurich, Zurich, Switzerland

[4] Department of Radiology, Memorial Sloan Kettering Cancer Center, New York City, NY, USA

[5] Department of Urology, University Hospital Zürich, University of Zurich, Zurich, Switzerland

[6] Department of Pathology and Molecular Pathology, University Hospital Zurich, University of Zurich, Zurich, Switzerland

[7] Department of Nuclear Medicine, Kantonsspital Baden, Baden, Switzerland

[8] Department of Nuclear Medicine, University Hospital Zürich, Rämistrasse 100, 8091 Zürich, Switzerland

Keywords Imaging-guided biopsy · PET/MR · Prostate biopsy · PSMA-PET accuracy · Targeted biopsy · Template biopsy

Introduction

Assessment of histological tumor grade on biopsy is needed for diagnosis and risk classification of prostate cancer (PCa). The updated European Association of Urology (EAU) guideline recommends ultrasound-guided systematic prostate biopsy (US biopsy) in patients with suspicion of PCa [1, 2]. Magnetic resonance imaging (MRI)–guided biopsy is considered for cases in which no cancer was detected [2]. The PROMIS trial revealed sensitivity of only 48% for their primary definition of clinically significant cancer (sigPCa) using 10–12 cores US biopsy and suggested that, instead, multiparametric MRI (mpMRI) should be used to reduce the number of unnecessary biopsies. However, if all lesions with a score ≥ 3 on Prostate Imaging Reporting and Data System (PIRADS) are targeted, the specificity of mpMRI is only 41% [3]. Several other studies also showed superior detection rates of sigPCa in MRI-guided biopsy compared to US biopsy [4–7]. Nevertheless, false-negative results or histological upgrade after surgery are found in 21% of patients [8–10]. The most reliable method to reduce undersampling and false-negative results is transperineal saturation biopsy (template biopsy) with samples taken from all 20 Barzell zones, leading to organ coverage of approximately 95% [10]. Screening and imaging-guided biopsy could potentially reduce side effects of saturation prostate biopsies [11], but recent studies suggest that a template-based systematic approach should not be omitted despite mpMRI [6, 12].

Positron emission tomography (PET)/MRI targeting prostate-specific membrane antigen (PSMA) could be an ideal technique to improve the accuracy of imaging-guided biopsies, combining the high sensitivity and specificity of PSMA-PET for PCa with the high anatomical contrast and spatial resolution of MRI [13–15]. Despite promising results in PSMA-PET/computed tomography (CT) for biopsy targeting [16], with an accuracy of 80.6% for sigPCa [17], the diagnostic accuracy of PSMA-PET/MRI-guided biopsy has not yet been prospectively assessed. Therefore, the aim of this study is to assess the performance of ^{68}Ga-PSMA-11 PET/MRI (PSMA-PET/MRI) to detect and localize primary sigPCa for accurate prostate biopsy guidance.

Patients and methods

Study design

The study was designed as an open-label, single-center, non-randomized, prospective diagnostic accuracy study including patients with suspected PCa. Patients without biopsy-proven sigPCa but suspicion of cancer due to persistently elevated prostate-specific antigen (PSA) (PSA > 2.5 ng/ml if age 30–50 years and PSA > 4 ng/ml if age 50–80 years) and at least one suspicious lesion on mpMRI clinical report (PIRADS ≥3) were included. All patients underwent PSMA-PET/MRI followed by both PSMA-PET/MRI-guided and section-based saturation template biopsy of the prostate between May 2017 and February 2019. Exclusion criteria were age < 30 and > 80, previous biopsy within 8 weeks prior to imaging, previous pelvic irradiation, prostatectomy, transurethral resection of the prostate (TURP) or androgen deprivation hormonal therapy (ADT), and any contra-indication to MRI or prostate biopsy as well active urinary tract infection or indwelling catheter. PSMA-PET/MRI and biopsy were performed with an interval of up to 30 weeks from mpMRI (median 2.7 weeks, IQR 0.4–12). Figure 1 illustrates patient selection. This study was approved by the institutional review board (BASEC Nr. 2017-00016), was carried out in accordance with the Declaration of Helsinki, and is registered in the international trial registry ClinicalTrials.gov (NCT03187990).

^{68}Ga-PSMA-11 PET/MRI imaging acquisition and analysis

All patients underwent a pelvic PET/MRI on a hybrid scanner (SIGNA PET/MR, GE Healthcare, Waukesha, WI, USA)

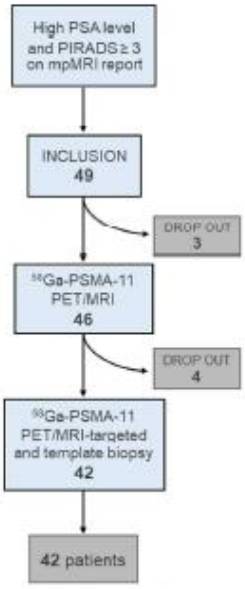

Fig. 1 Patient selection and inclusion in the study

60 min after injection of 85 MBq of ^{68}Ga-PSMA-11. A 15-min frame over the prostate was recorded, allowing reducing the dose since patients without confirmed cancer were included. For biopsy targeting, suspected lesions were delineated on PSMA-PET/MRI by a double-board-certified nuclear medicine physician and radiologist, specialist in pelvic imaging, with 10 and 5 years of experience (IAB,MM), with a maximum of three target lesions. Imaging protocol and analysis are given in the supplements (Online Resource 1).

Biopsy

Biopsies were performed under general anesthesia by specialized urologists with US-MRI software fusion (BiopSee®). Axial fused PSMA-PET/MRI images in DICOM format were uploaded to BiopSee® instead of T2w MRI sequences. Standard transperineal template biopsy with number of cores adapted to prostate volume as well as PSMA-PET/MRI-targeted biopsy was performed with a maximum of three cores per target lesion (Online Resource 2). Patients with no suspicious uptake on PSMA-PET/MRI or with discordant lesions between PSMA-PET/MRI and mpMRI underwent template biopsy and the urologist was free to target any suspicious lesion on mpMRI.

Clinically significant cancer definition

SigPCa was defined as International Society of Urological Pathology (ISUP) grade group 3 and/or cancer core length ≥ 6 mm [18]. Conversely, clinically insignificant cancer (insigPCa) was defined as ISUP 1 or 2 lesions with cancer core length < 6 mm. Biopsies with the latter characteristics were classified as negative for further analysis. Results based on other definition of sigPCa (ISUP ≥2) are in Table S3 (Online Resource 1).

Reference standard

Results of PSMA-PET/MRI-targeted biopsies were compared to template biopsies regarding presence of sigPCa on histopathology. All patients classified as having a false-positive or false-negative ^{68}Ga-PSMA-11 PET/MRI result had the biopsy samples, or radical prostatectomy (RPE) specimens if available, reevaluated on histopathology for possible explanations including PSMA immunohistochemistry (IHC). Biopsies and RPE specimens were evaluated by two board-certified genitourinary pathologists (NR, JR) with 8–10 years of experience.

Data analysis

Study results were analyzed using descriptive statistics and frequency tables in Excel (Excel2016, Microsoft, USA). Accuracy was assessed on 2 × 2 contingency tables on patient and lesion basis. For lesion-based analysis, the number of lesions was defined as number of PSMA-positive lesions added to number of PSMA-negative lesions with sigPCa found on biopsy. For patient-based analysis in patients with more than one lesion and different classifications (for example, one true-positive and one false-negative lesion), we considered whether PSMA-PET/MRI correctly staged the patient regarding the presence or absence of sigPCa according to Table S1 (Online Resource 1). We also assessed patient-based accuracy for PET/MRI-targeted cores.

Results

General

Forty-nine patients met the inclusion criteria and were included between May 2017 and January 2020. Seven patients withdrew participation before the PSMA-PET/MRI scan or the biopsy was performed; therefore, data from 42 patients were analyzed (descriptive characteristics in Table 1). Median interval between PSMA-PET/MRI and biopsy was 12 days (interquartile range (IQR) 6–18).

Biopsy

Based on template and targeted biopsy, 26 of 42 (62%) patients had sigPCa. While there was no malignancy in seven of 42 patients (17%), in the remaining nine patients (21.4%), cancer detected on biopsy did not meet the criteria of sigPCa. Fifteen cases of sigPCa were detected by both template and targeted biopsies (58%, 15/26), nine only by template (35%) and two only by targeted (8%). Two cases of insigPca were detected by both biopsy methods (22%, 2/9), six only by template (67%) and one only by targeted. Table 2 and Fig. 2 show the distribution of sigPCa, insigPCa, and no disease, in correlation to PIRADS, ISUP, and PSMA-PET/

Table 1 Characteristics of the patients at inclusion in the study ($n = 42$)

Characteristics	Value
Age at scan (years)	
Mean±SD	64±6
Median (IQR)	65 (59–68)
PSA at time of PET scan (ng/ml)	
Mean±SD	10±7.4
Median (IQR)	8 (7–11)
PIRADS (*n*)	
3	7 (16.7%)
4	24 (57.1%)
5	11 (26.2%)

SD = standard deviation; IQR = interquartile range

Table 2 Distribution of patients with sigPCa and insigPCa, based on biopsy, according to ISUP grade groups. Clinically significant prostate cancer defined as ISUP grade ≥ 3 and/or cancer core length ≥ 6 mm. Seven patients had no cancer on biopsy

	sigPCa	insigPCa
ISUP		
1	1 (4%)	3 (33%)
2	6 (23%)	6 (67%)
3	9 (34%)	–
4	8 (31%)	–
5	2 (8%)	–
Total	26	9

sigPCa = clinically significant prostate cancer; insigPCa = clinically insignificant prostate cancer

MRI result. Eighteen patients had one lesion, seven patients had two, and one patient had three lesions, resulting in 35 sigPCa lesions in total. The median number of positive cores per patient was three (IQR 2–6). The median number of samples taken per patient was 43 (IQR 36–44). Eight patients (19%, 8/42) had biopsy procedure complications, none life-threatening. Six patients presented to the emergency department for acute urinary retention, one patient had postinterventional bleeding with need of catheter irrigation, and one patient with anesthesia complications was admitted for observation and released the day after.

^{68}Ga-PSMA-11 PET/MRI

Table 3 shows sensitivity, specificity, positive predictive value (PPV), negative predictive value (NPV), and accuracy of PSMA-PET/MRI per patient and per lesion. PSMA-PET/MRI was positive in 28 patients (66.7%, 28/42), of which 25 had sigPCa on biopsy (89%, 25/28) and negative in 14 patients (33.3%, 14/42), of which only one had sigPCa (7%, 1/14)

Table 3 Performance of PSMA-PET/MRI for biopsy guidance, given patient-based for PSMA-PET/MRI imaging findings and PET-targeted cores, and lesion-based

	Patient-based	Patient-based targeted cores	Lesion-based
Sensitivity	96% (25/26)	65% (17/26)	83% (29/35)
Specificity	81% (13/16)	81% (13/16)	–
PPV	89% (25/28)	61% (17/28)	76% (29/38)
NPV	93% (13/14)	93% (13/14)	–
Accuracy	90% (38/42)	71% (30/42)	–

PPV = positive predictive value; NPV = negative predictive value. For the targeted core analysis, values were calculated as if patients with a negative PSMA-PET/MRI were not submitted to biopsy and patients with a positive PSMA-PET/MRI underwent only PSMA-PET/MRI-targeted biopsy. Lesion-based specificity and NPV were not calculated since patients with negative PSMA-PET/MRI and no significant cancer on biopsy have, per definition, no lesion

(Figs. 2b and 3a). Nineteen patients had one PSMA-positive lesion, eight patients had two lesions, and one patient had three lesions, resulting in 38 PSMA-positive lesions. One patient had a lesion without PSMA uptake but clear PIRADS 5 features on MRI, confirmed as sigPCa by MRI-targeted biopsy and classified as negative PSMA-PET/MRI for further analysis. Figure 3b shows PSMA-PET/MRI results in relation to PIRADS.

The accuracy of PSMA-targeted cores was lower compared to PSMA-PET/MRI imaging findings. In eight cases with PSMA uptake in the sigPCa lesion, the three target needles were negative, but additional adjacent template needles confirmed sigPCa.

Per lesion, 44 lesions were detected in 29 patients (38 on PSMA-PET/MRI and 35 on biopsy, with 29 concordant lesions). Six sigPCa lesions and 24 insigPCa lesions were not detected by PSMA-PET/MRI.

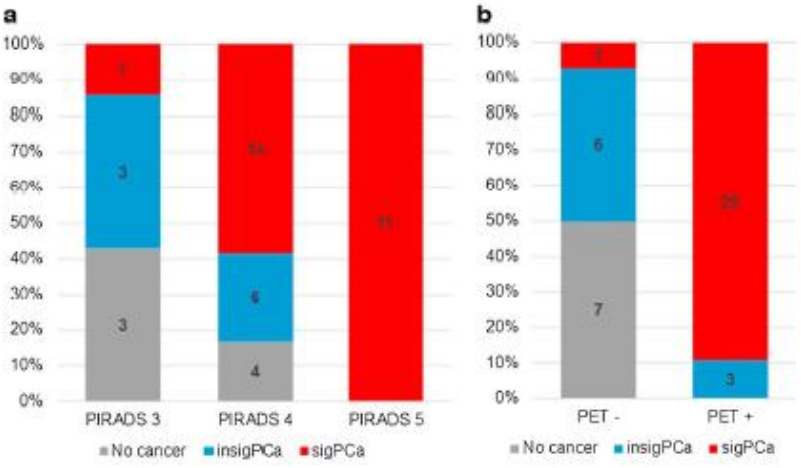

Fig. 2 Distribution of patients with clinically significant prostate cancer (sigPCa), clinically insignificant prostate cancer (insigPCa), and no evidence of disease on biopsy in correlation to PIRADS classification on multiparametric resonance magnetic imaging (**a**) and ^{68}Ga-PSMA-11 PET/MRI result (**b**)

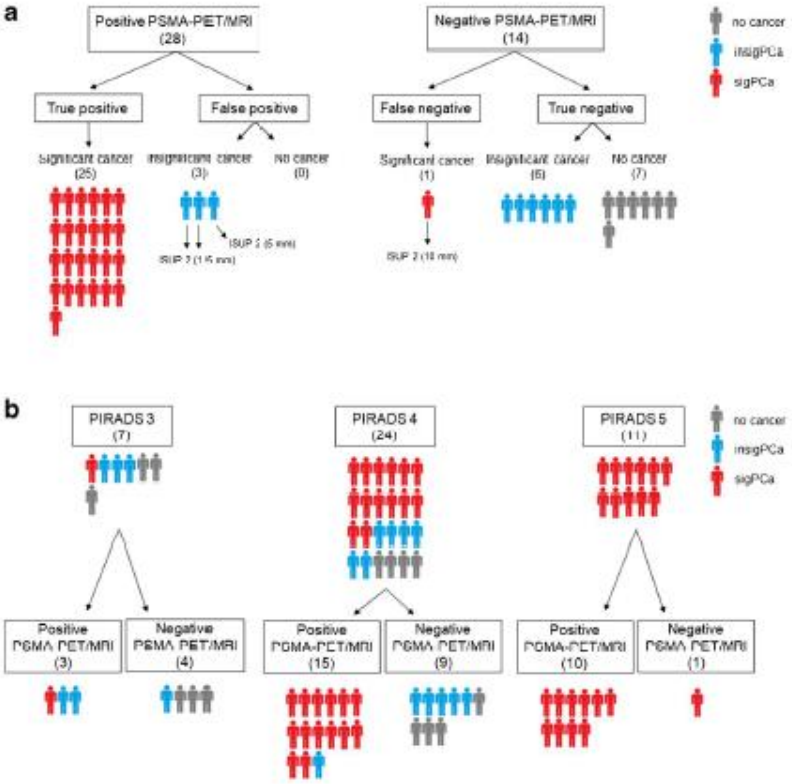

Fig. 3 Distribution of patients with clinically significant prostate cancer (sigPCa), clinically insignificant prostate cancer (insigPCa), and no evidence of disease on biopsy according to ^{68}Ga-PSMA-11 PET/MRI results (**a**) and according to ^{68}Ga-PSMA-11 PET/MRI results in correlation to PIRADS classification on multiparametric resonance magnetic imaging (**b**). The single false-negative case and the three false-positive cases shown in part "**a**" are shown in part "**b**" under PIRADS 5/negative PSMA-PET/MRI and PIRADS 3/positive PSMA-PET/MRI (two cases) and 4/positive PSMA-PET/MRI (one case), respectively

False-positive PSMA-PET/MRI

Three patients had a false-positive PSMA-PET/MRI, but insigPCa on biopsy in at least one of the PSMA uptake areas (ISUP grade group 2 with cancer length of 1.5–5 mm). Relevant cancer was confirmed on RPE specimen in all three cases (Fig. 4).

Per lesion, nine lesions were false-positive (Online Resource 3). In all patients, RPE was available and showed cancer in eight lesions (Table 4). In the case without cancer, additional pathology workup showed clear PSMA overexpression on IHC, but no benign or malignant alterations. Interval between biopsy and RPE in these patients ranged from 1 to 3.8 months.

False-negative PSMA-PET/MRI

^{68}Ga-PSMA-11 PET/MRI was false-negative in one patient with sigPCa, who had two positive cores with ISUP grade group 2 and lengths of 9 and 10 mm. Despite no PSMA uptake, the lesion was easily appreciated on T2- and diffusion-weighted sequences of the MRI component (Fig. 5).

Per lesion, six were false-negatives (Online Resource 4). In four lesions, ISUP grade was low or tumor volume small (up to 3 mm) on biopsy. In one case, there was no cancer on RPE in the corresponding location of the positive biopsy core (Table 4). One lesion with positive cores of ISUP grade group 4 (6 mm) was downgraded to ISUP grade 2 on RPE and in one lesion (ISUP 2, 10 mm) biopsy cores stained for PSMA on IHC showed a PSMA-negative tumor (Fig. 5). The interval between biopsy and RPE in these patients ranged from 1.4 to 3.7 months.

Discussion

PSMA-PET/MRI showed a patient-based accuracy of 90% for detecting sigPCa in our cohort, with a sensitivity of 96% and specificity of 81%. This is higher than the mpMRI accuracy reported in most studies using template biopsy as reference standard [19], including the PROMIS trial, which reported sensitivity and specificity of 93% and 41%, respectively [3]. Our improved specificity was mainly due to PSMA-PET mitigating false-positive mpMRI PIRADS 3 and 4 lesions harboring no sigPCa (Fig. 3b). The PROMIS authors conclude

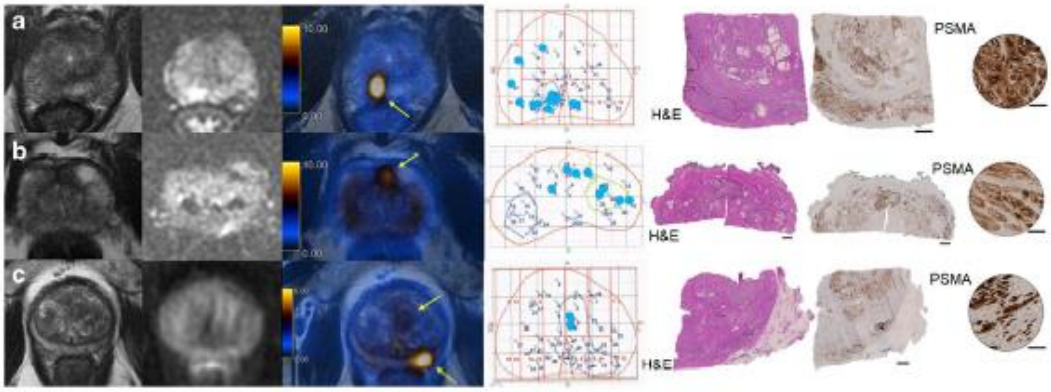

Fig. 4 All three patients with a false-positive PSMA-PET/MRI. From left to right, prostatic MRI sequences T2-weighted and diffusion-weighted images (*b* value 1000), fused PET/MRI, representative pathology map with biopsy results, and radical prostatectomy (RPE) specimen with tumor outlined on hematoxylin and eosin staining (H&E) and PSMA-IHC (overview and magnification). Bars represent 2.5 mm in the H&E and PSMA-IHC images and 100 μm in the PSMA-IHC magnified images. Blue dots in the pathology map correspond to location of needles with clinically insignificant cancer diagnosed. **a** 67-year-old patient, with a PSA of 7.3 ng/ml and a PIRADS 4 lesion on mpMRI. PSMA-PET/MRI shows one targeted lesion (arrow) in the posterior right peripheral zone, where biopsy found ISUP grade group 2 tumor with up to 1.5-mm length. RPE specimen shows a PSMA-positive ISUP grade group 3 tumor in the PSMA uptake area. **b** 65-year-old patient, with a PSA of 7.18 ng/ml and a PIRADS 3 lesion on mpMRI. PSMA-PET/MRI shows one targeted lesion (arrow) in the anterior zone, where biopsy found ISUP grade group 2 tumor with up to 1.5-mm length. RPE specimen shows a PSMA-positive ISUP grade group 2 tumor in the PSMA uptake area. **c** 65-year-old patient, with a PSA of 48.5 ng/ml and a PIRADS 3 lesion on mpMRI. PSMA-PET/MRI shows two targeted lesions (arrows) in the transition zone corresponding on biopsy to ISUP grade group 2 tumor up to 5 mm length, and in the posterior left peripheral zone, where biopsy was negative. RPE specimen shows a PSMA-positive ISUP grade group 3 tumor in the PSMA uptake area of the posterior left peripheral zone

that screening by mpMRI prior to biopsy could reduce the number of unnecessary biopsies. Our study suggests PSMA-PET/MRI could further improve on mpMRI patient selection.

In our cohort, 16 patients (38%) without sigPCa underwent biopsy based on equivocal or suspicious lesions on mpMRI (PIRADS 3 to 5). Omitting biopsy in patients with negative PSMA-PET/MRI would have spared 13 (13/16, 81%), without missing any patient with sigPCa. Only one patient had a false-negative PSMA-PET result; however, his ISUP 2 tumor would not have been missed due to clear PIRADS 5 features on MRI. The tumor was PSMA-negative on IHC, which is in accordance with the reported rate of around 5% of PSMA-negative tumors in the literature [20]. For the three patients with false-positive PSMA-PET/MR results, insigPCa was present on template biopsy, and cancer with Gleason 4 pattern was confirmed on RPE in each case.

Interestingly, despite PET findings confirmed by biopsy in 90% of the cases, the accuracy of 71% with a sensitivity of 65% for PET-targeted biopsy shows that some of the sigPCa lesions seen on PET are actually missed by the three targeted cores. This was already reported by van der Leest et al. [9] in a study comparing transrectal US-guided biopsy versus MRI-guided biopsy. They found that positive TRUS cores were obtained from the mpMRI lesion area or its neighboring and suggested that four additional perilesional cores greatly improved sigPCa detection with MRI-guided biopsy. They concluded that the majority of sigPCa missed by targeted biopsy was probably due to sampling errors related to spatial heterogeneity of the tumor [9].

False-negative and false-positive lesions in our study were often lesions with borderline characteristics regarding clinical significance. The lower PSMA expression in Gleason pattern 3 compared to 4 has been demonstrated on IHC [20–22] and our results probably reflect it: most false-negative lesions corresponded to low-grade groups (ISUP 1 and 2) or small volume tumors and, in only one case, a significant PSMA-negative tumor. Omitting template biopsy in our cohort would leave undetected six sigPCa, but also 24 lesions with insigPCa, mitigating overdiagnosis. On the other hand, eight of nine false-positive lesions based on biopsy were insigPCa, with only one showing no cancer on RPE specimen. This case was previously published as a case report with extensive histopathology workup excluding inflammation, pre-cancerous lesions, or other malignancies [23]. Therefore, template and targeted biopsies were false-negative for significant disease for eight lesions.

The definition of sigPCa is not standardized among centers; therefore, we chose the definition used in the PROMIS trial [3] to allow a direct comparison of our results. We recognize that other definitions can be found in the literature and that more recent guidelines of the EAU suggest considering any ISUP grade group 2 biopsy as sigPCa [1, 2]. Incorporating

Table 4 Findings on PET (SUV_{max}), biopsy, and radical prostatectomy (RPE) specimen of the false-positive and false-negative lesions on PSMA-PET/MRI. PSMA-PET/MRI image of each lesion can be seen in the correspondent supplementary figure (Online Resources 3 for Fig. S2 and 4 for Fig. S3) showed in the first column

	Fig.	SUV_{max}	Biopsy			RPE specimen	
False-positive lesions*			Finding	ISUP	Length (mm)	Finding	ISUP
Pat. 03	S2 a	7.9	ASAP	–	–	PSMA overexpression	–
Pat. 24	S2 b	5.3	Inflammation	–	–	Cancer	3
Pat. 30	S2 c	5.4	insigPCa	2	1.0	Cancer	2
Pat. 32	S2 d	12.9	insigPCa	2	2.0	Cancer	2
Pat. 33	S2 e	9.4	insigPCa	2	1.5	Cancer	3
Pat. 35	S2 f	4.4	insigPCa	2	5.0	Cancer	2
Pat. 35	S2 g	5.7	None	–	–	Cancer	3
Pat. 38	S2 h	10.1	None	–	–	Cancer	2
Pat. 42	S2 i	8	insigPCa	2	1.5	Cancer	2
False-negative lesions*							
Pat. 05	S3 a	–	sigPCa	1	6.0	Not available	–
Pat. 07	S3 b	–	sigPCa	3	1.0	No cancer	–
Pat. 16	S3 c	–	sigPCa	3	3.0	Cancer	3
Pat. 26	S3 d	–	sigPCa	4	6.0	Cancer	2
Pat. 32	S3 e	–	sigPCa	2	6.0	Cancer	2
Pat. 39	S3 f	–	sigPCa PSMA-negative	2	10.0	Not available	–

*Based on biopsy findings

ASAP = atypical small acinar proliferation; insigPCa = clinically insignificant prostate cancer; sigPCa = clinically significant prostate cancer; SUVmax = maximum standardized uptake value

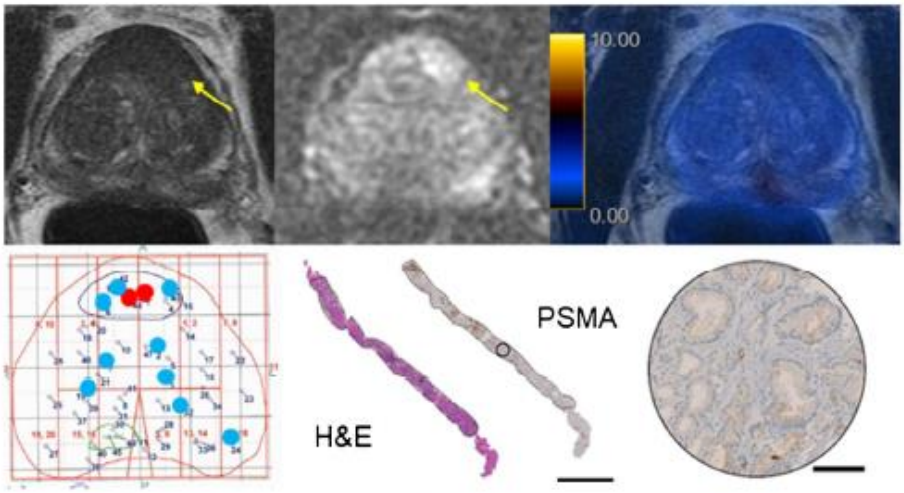

Fig. 5 The only patient with a false-negative PSMA-PET/MRI in our cohort. A 62-year-old patient with a PSA of 11.38 ng/ml. Top images from left to right are prostate MRI sequences T2-weighted and diffusion-weighted images and fused PET/MRI showing a PIRADS 5 lesion in the anterior transition zone (arrows) with no PSMA uptake. Bottom left image shows the representative pathology map with biopsy results including two cores with clinically significant cancer in the lesion area (red dots, ISUP grade group 2 tumor with length up to 10 mm) and many cores with clinically insignificant cancer (blue dots). Remaining bottom images show one of the biopsy cores with clinically significant cancer. The tumor is outlined in hematoxylin and eosin staining (H&E) and PSMA-IHC (overview and magnification), showing a virtually PSMA-negative tumor. Bars represent 2.5 mm in the H&E and PSMA-IHC images and 100 µm in the PSMA-IHC magnified image

this cutoff, we would have had only one false-positive PET in our cohort on per-patient analysis, but four false-negative PET scans. Therefore, we also give the results using this other definition of sigPCa in Tables S2 and S3 (Online Resource 1).

There is sparse literature on PSMA-PET/CT-guided biopsy. Recently, PSMA-PET/CT was compared, for biopsy purposes, to micro-ultrasound, a novel imaging technique with promising results when added to mpMRI [24]. PSMA-PET/CT yielded an accuracy of 83% versus 61% of micro-ultrasound [25]. No study so far compared PSMA-PET/CT to PET/MRI for biopsy guidance. In our limited experience (anecdotal data not included in present study), delineating the prostate and PSMA-positive lesions on non-contrast-enhanced CT using US-fusion-software is feasible but cumbersome. In a study with 31 patients, sensitivity and specificity for sigPCa of PSMA-PET/CT-guided biopsy was 100% and 68% [17]. The higher sensitivity and lower specificity compared to our study may be explained by the approach to biopsy the prostate area with highest PSMA uptake if no suspicious lesion was reported. This probably led to false-positives, which could be ruled out by MRI but not by CT, such as activity in the central zone [26]. Another study found a region-based sensitivity of PET/CT for sigPCa of 61%, lower than our lesion-based sensitivity (83%). However, patients did not undergo mpMRI so no insights on PET/CT limitations compared to PET/MRI could be drawn [27]. A prospective study showed higher detection rate of sigPCa for PET/CT compared to 12-core TRUS biopsy; however, biopsies were performed within the CT scanner, and again mpMRI was not performed routinely [28]. In a study with 97 patients that compared PSMA-PET/CT with mpMRI, PSMA-PET/CT identified 25% of patients with Gleason 7 tumors missed by mpMRI [29]. Due to their inclusion criteria, around half of the patients that were biopsied had contra-indications to mpMRI or PIRADS 1 or 2; what makes it difficult to compare their results to ours but rather offers nice complementary data. Interestingly, these results are similar to the results found by the same group in a smaller cohort using 11C-Choline PET/CT, with 26% of patients with Gleason 7 tumors detected by PET in patients with negative or contra-indication to mpMRI [30]. Advantages of PET/MRI over PET/CT are that surgeons are already used to delineate prostate and target lesions based on MRI and that they can target lesions by both PSMA-PET and MRI in case of discordance. That a combination of these both methods could further improve the sensitivity for detecting PCa was already shown by Eiber et al. [13]. While PET/MRI profits from the higher soft tissue contrast, studies performing head-to-head comparisons are needed to investigate whether this offsets the higher general availability and lower cost of PET/CT. Moreover, post hoc image fusion of MRI and PSMA-PET (from PET/CT) may be a viable option for centers without a dedicated PET/MRI device.

Despite the good coverage of template biopsy, absence of RPE specimen as reference standard in some cases is a limitation of this study. Given that RPE specimen were not available for all patients, we opted to use RPE results only to investigate false-positive or false-negative lesions on PSMA-PET/MRI. Another limitation is pre-selection of patients based on mpMRI results. The aim of this proof-of-mechanism study was to assess whether PSMA-PET/MR could add value to mpMRI. Given that the probability of sigPCa in patients with PIRADS 1–2 is very low, we opted to exclude those patients in a first step. However, this limits the conclusion about the accuracy of PET scans in an mpMRI naïve population.

Conclusions

PSMA-PET/MRI has a high accuracy for detecting sigPCa and is a promising tool to select patients for biopsy as well as to guide it, with the potential to substantially reduce unnecessary biopsies compared to mpMRI and might even improve the detection of sigPCa in comparison to systematic template biopsies.

Supplementary Information The online version contains supplementary material available at https://doi.org/10.1007/s00259-021-05261-y.

Acknowledgements We acknowledge the technicians Marlena Hofbauer and Josephine Trinckauf and their team for the excellent work on high quality PET images. DAF thanks the USZ ICT team for making it possible for her to do part of this work remotely.

Data and materials availability The datasets generated during and/or analyzed during the current study are available from the corresponding author on reasonable request.

Author contribution Conceptualization: Irene A. Burger, Daniel Eberli. Methodology: Olivio F. Donati, Daniel Eberli, Irene A. Burger. Formal analysis: Daniela A. Ferraro, Anton S. Becker. Investigation: Daniela A. Ferraro, Benedikt Kranzbühler, Konstantinos G. Zeimpekis, Hannes Grünig, Michael Messerli, Ashkan Mortezavi. Data curation: Daniela A. Ferraro, Irene A. Burger. Analysis and interpretation of data: Daniela A. Ferraro, Anton S. Becker, Niels J. Rupp, Jan H. Rueschoff, Olivio F. Donati. Manuscript drafting: Daniela A. Ferraro, Irene A. Burger. Manuscript review and editing: all authors. Visualization: Daniela A. Ferraro, Anton S. Becker, Irene A. Burger. Project administration: Iliana Mebert, Anka Baltensperger; Supervision: Marcelo T. Sapienza, Daniel Eberli, Irene A. Burger.

Funding Open Access funding provided by Universität Zürich. The authors thank the Sick legat and the Iten-Kohaut foundation for their financial support. This study was financed in part by the Coordenação de Aperfeiçoamento de Pessoal de Nível Superior-Brasil (CAPES)-Finance Code 001. This research was funded in part through the National Institutes of Health/National Cancer Institute (NIH/NCI) Cancer Center Support Grant P30 CA008748.

Declarations

Ethics approval This study was performed in line with the principles of the Declaration of Helsinki. Approval was granted by the Cantonal Ethics Committee of Zurich (Date: 03/23/2017/ BASEC Nr: 2017-00016).

Consent to participate Informed consent was obtained from all individual participants included in the study.

Conflict of interest I. A. B. has received research grants and speaker honorarium from GE Healthcare, research grants from Swiss Life, and speaker honorarium from Bayer Health Care and Astellas Pharma AG. M. M. received speaker fees from GE Healthcare. The Department of Nuclear Medicine holds an institutional Research Contract with GE Healthcare. N. J. R. has provided consultancy services (advisory board member) to F. Hoffmann- La Roche AG. A. S. B. received research grants from the Prof. Dr. Max Cloëtta Foundation, medAlumni UZH, and the Swiss Society of Radiology. All other authors declare no competing interests.

Open Access This article is licensed under a Creative Commons Attribution 4.0 International License, which permits use, sharing, adaptation, distribution and reproduction in any medium or format, as long as you give appropriate credit to the original author(s) and the source, provide a link to the Creative Commons licence, and indicate if changes were made. The images or other third party material in this article are included in the article's Creative Commons licence, unless indicated otherwise in a credit line to the material. If material is not included in the article's Creative Commons licence and your intended use is not permitted by statutory regulation or exceeds the permitted use, you will need to obtain permission directly from the copyright holder. To view a copy of this licence, visit http://creativecommons.org/licenses/by/4.0/.

References

1. Cornford P, Bellmunt J, Bolla M, Briers E, De Santis M, Gross T, et al. EAU ESTRO SIOG guidelines on prostate cancer. Part II: treatment of relapsing, metastatic, and castration-resistant prostate cancer. Eur Urol. 2017;71:630–42. https://doi.org/10.1016/j.eururo.2016.08.002.
2. Mottet N, Bellmunt J, Bolla M, Briers E, Cumberbatch MG, De Santis M, et al. EAU-ESTRO-SIOG guidelines on prostate cancer. Part 1: screening, diagnosis, and local treatment with curative intent. Eur Urol. 2017;71:618–29. https://doi.org/10.1016/j.eururo.2016.08.003.
3. Ahmed HU, El-Shater Bosaily A, Brown LC, Gabe R, Kaplan R, Parmar MK, et al. Diagnostic accuracy of multi-parametric MRI and TRUS biopsy in prostate cancer (PROMIS): a paired validating confirmatory study. Lancet. 2017;389:815–22. https://doi.org/10.1016/S0140-6736(16)32401-1.
4. Schoots IG, Roobol MJ, Nieboer D, Bangma CH, Steyerberg EW, Hunink MG. Magnetic resonance imaging-targeted biopsy may enhance the diagnostic accuracy of significant prostate cancer detection compared to standard transrectal ultrasound-guided biopsy: a systematic review and meta-analysis. Eur Urol. 2015;68:438–50. https://doi.org/10.1016/j.eururo.2014.11.037.
5. Valerio M, Donaldson I, Emberton M, Ehdaie B, Hadaschik BA, Marks LS, et al. Detection of clinically significant prostate cancer using magnetic resonance imaging-ultrasound fusion targeted biopsy: a systematic review. Eur Urol. 2015;68:8–19. https://doi.org/10.1016/j.eururo.2014.10.026.
6. Abdoot M, Wilbur AR, Reese SE, Lebastchi AH, Mehralivand S, Gomella PT, et al. MRI-targeted, systematic, and combined biopsy for prostate cancer diagnosis. N Engl J Med. 2020;382:917–28. https://doi.org/10.1056/NEJMoa1910038.
7. Kasivisvanathan V, Rannikko AS, Borghi M, Panebianco V, Mynderse LA, Vaarala MH, et al. MRI-targeted or standard biopsy for prostate-cancer diagnosis. N Engl J Med. 2018;378:1767–77. https://doi.org/10.1056/NEJMoa1801993.
8. Kasivisvanathan V, Dufour R, Moore CM, Ahmed HU, Abd-Alazeez M, Charman SC, et al. Transperineal magnetic resonance image targeted prostate biopsy versus transperineal template prostate biopsy in the detection of clinically significant prostate cancer. J Urol. 2013;189:860–6. https://doi.org/10.1016/j.juro.2012.10.009.
9. van der Leest M, Cornel E, Israel B, Hendriks R, Padhani AR, Hoogenboom M, et al. Head-to-head comparison of transrectal ultrasound-guided prostate biopsy versus multiparametric prostate resonance imaging with subsequent magnetic resonance-guided biopsy in biopsy-naive men with elevated prostate-specific antigen: a large prospective multicenter clinical study. Eur Urol. 2019;75:570–8. https://doi.org/10.1016/j.eururo.2018.11.023.
10. Mortezavi A, Marzendorfer O, Donati OF, Rizzi G, Rupp NJ, Wettstein MS, et al. Diagnostic accuracy of multiparametric magnetic resonance imaging and fusion guided targeted biopsy evaluated by Transperineal template saturation prostate biopsy for the detection and characterization of prostate cancer. J Urol. 2018;200:309–18. https://doi.org/10.1016/j.juro.2018.02.067.
11. Loeb S, Vellekoop A, Ahmed HU, Catto J, Emberton M, Nam R, et al. Systematic review of complications of prostate biopsy. Eur Urol. 2013;64:876–92. https://doi.org/10.1016/j.eururo.2013.05.049.
12. Rouviere O, Puech P, Renard-Penna R, Claudon M, Roy C, Mege-Lechevallier F, et al. Use of prostate systematic and targeted biopsy on the basis of multiparametric MRI in biopsy-naive patients (MRI-FIRST): a prospective, multicentre, paired diagnostic study. Lancet Oncol. 2019;20:100–9. https://doi.org/10.1016/S1470-2045(18)30569-2.
13. Eiber M, Weirich G, Holzapfel K, Souvatzoglou M, Haller B, Rauscher I, et al. Simultaneous (68)Ga-PSMA HBED-CC PET/MRI improves the localization of primary prostate cancer. Eur Urol. 2016;70:829–36. https://doi.org/10.1016/j.eururo.2015.12.053.
14. Donato P, Morton A, Yaxley J, Ranasinghe S, Teloken PE, Kyle S, et al. (68)Ga-PSMA PET/CT better characterises localised prostate cancer after MRI and transperineal prostate biopsy: Is (68)Ga-PSMA PET/CT guided biopsy the future? Eur J Nucl Med Mol Imaging. 2020. https://doi.org/10.1007/s00259-019-04620-0.
15. Berger I, Annabattula C, Lewis J, Shetty DV, Kam J, Maclean F, et al. (68)Ga-PSMA PET/CT vs. mpMRI for locoregional prostate cancer staging: correlation with final histopathology. Prostate Cancer Prostatic Dis. 2018;21:204–11. https://doi.org/10.1038/s41391-018-0048-7.
16. Lopci E, Saita A, Lazzeri M, Lughezzani G, Colombo P, Buffi NM, et al. (68)Ga-PSMA positron emission tomography/computerized tomography for primary diagnosis of prostate cancer in men with contraindications to or negative multiparametric magnetic resonance imaging: a prospective observational study. J Urol. 2018;200:95–103. https://doi.org/10.1016/j.juro.2018.01.079.
17. Liu C, Liu T, Zhang Z, Zhang N, Du P, Yang Y, et al. PSMA PET/CT and standard plus PET/CT-ultrasound fusion targeted prostate biopsy can diagnose clinically significant prostate cancer in men with previous negative biopsies. J Nucl Med. 2020. https://doi.org/10.2967/jnumed.119.235333.
18. Ahmed HU, Hu Y, Carter T, Arumainayagam N, Lecornet E, Freeman A, et al. Characterizing clinically significant prostate cancer using template prostate mapping biopsy. J Urol. 2011;186:458–64. https://doi.org/10.1016/j.juro.2011.03.147.
19. Kasivisvanathan V, Stabile A, Neves JB, Giganti F, Valerio M, Shanmugabavan Y, et al. Magnetic resonance imaging-targeted biopsy versus systematic biopsy in the detection of prostate cancer: a systematic review and meta-analysis. Eur Urol. 2019;76:284–303. https://doi.org/10.1016/j.eururo.2019.04.043.
20. Minner S, Wittmer C, Graefen M, Salomon G, Steuber T, Haese A, et al. High level PSMA expression is associated with early PSA

recurrence in surgically treated prostate cancer. Prostate. 2011;71:281–8. https://doi.org/10.1002/pros.21241.
21. Bravaccini S, Puccetti M, Bocchini M, Ravaioli S, Celli M, Scarpi E, et al. PSMA expression: a potential ally for the pathologist in prostate cancer diagnosis. Sci Rep. 2018;8:4254. https://doi.org/10.1038/s41598-018-22594-1.
22. Hupe MC, Philippi C, Roth D, Kumpers C, Ribbat-Idel J, Becker F, et al. Expression of prostate-specific membrane antigen (PSMA) on biopsies is an independent risk stratifier of prostate cancer patients at time of initial diagnosis. Front Oncol. 2018;8:ARTN 623. https://doi.org/10.3389/fonc.2018.00623.
23. Ferraro DA, Rupp NJ, Donati OF, Messerli M, Eberli D, Burger IA. 68Ga-PSMA-11 PET/MR can be false positive in normal prostatic tissue. Clin Nucl Med. 2019;44:e291–3.
24. Wiemer L, Hollenbach M, Heckmann R, Kittner B, Plage H, Reimann M, et al. Evolution of targeted prostate biopsy by adding micro-ultrasound to the magnetic resonance imaging pathway. Eur Urol Focus. 2020. https://doi.org/10.1016/j.euf.2020.06.022.
25. Lopci E, Lughezzani G, Castello A, Colombo P, Casale P, Saita A, et al. PSMA-PET and micro-ultrasound potential in the diagnostic pathway of prostate cancer. Clin Transl Oncol. 2021;23:172–8. https://doi.org/10.1007/s12094-020-02384-w.
26. Pizzuto DA, Muller J, Muhlematter U, Rupp NJ, Topfer A, Mortezavi A, et al. The central zone has increased (68)Ga-PSMA-11 uptake: "Mickey Mouse ears" can be hot on (68)Ga-PSMA-11 PET. Eur J Nucl Med Mol Imaging. 2018;45:1335–43. https://doi.org/10.1007/s00259-018-3979-2.
27. Bodar YJL, Jansen BHE, van der Voorn JP, Zwezerijnen GJC, Meijer D, Nieuwenhuijzen JA, et al. Detection of prostate cancer with (18)F-DCFPyL PET/CT compared to final histopathology of radical prostatectomy specimens: is PSMA-targeted biopsy feasible? The DeTeCT trial. World J Urol. 2020. https://doi.org/10.1007/s00345-020-03490-8.
28. Zhang LL, Li WC, Xu Z, Jiang N, Zang SM, Xu LW, et al. (68)Ga-PSMA PET/CT targeted biopsy for the diagnosis of clinically significant prostate cancer compared with transrectal ultrasound guided biopsy: a prospective randomized single-centre study. Eur J Nucl Med Mol Imaging. 2020. https://doi.org/10.1007/s00259-020-04863-2.
29. Lopci E, Lughezzani G, Castello A, Saita A, Colombo P, Hurle R, et al. Prospective evaluation of (68)Ga-labeled prostate-specific membrane antigen ligand positron emission tomography/computed tomography in primary prostate cancer diagnosis. Eur Urol Focus. 2020. https://doi.org/10.1016/j.euf.2020.03.004.
30. Lazzeri M, Lopci E, Lughezzani G, Colombo P, Casale P, Hurle R, et al. Targeted 11C-choline PET-CT/TRUS software fusion-guided prostate biopsy in men with persistently elevated PSA and negative mpMRI after previous negative biopsy. Eur J Hybrid Imaging. 2017;1:9. https://doi.org/10.1186/s41824-017-0011-1.

Publisher's note Springer Nature remains neutral with regard to jurisdictional claims in published maps and institutional affiliations.

Publicação 2

Ferraro et al.
European Journal of Hybrid Imaging (2022) 6:14
https://doi.org/10.1186/s41824-022-00135-4

European Journal of Hybrid Imaging

ORIGINAL ARTICLE Open Access

^{68}Ga-PSMA-11 PET/MRI versus multiparametric MRI in men referred for prostate biopsy: primary tumour localization and interreader agreement

Daniela A. Ferraro[1,2,3†], Andreas M. Hötker[4†], Anton S. Becker[4,5], Iliana Mebert[1,6], Riccardo Laudicella[1,7], Anka Baltensperger[1,6], Niels J. Rupp[8], Jan H. Rueschoff[8], Julian Müller[1], Ashkan Mortezavi[6,9], Marcelo T. Sapienza[2], Daniel Eberli[6], Olivio F. Donati[4†] and Irene A. Burger[1,3,10*†]

*Correspondence: irene.burger@usz.ch
†Daniela A. Ferraro and Andreas M. Hötker equally contributed to this work
†Olivio F. Donati and Irene A. Burger equally contributed to this work
[1] Department of Nuclear Medicine, University Hospital Zürich, University of Zurich, Rämistrasse 100, 8091 Zurich, Switzerland
Full list of author information is available at the end of the article

Abstract

Background: Magnetic resonance imaging (MRI) is recommended by the European Urology Association guidelines as the standard modality for imaging-guided biopsy. Recently positron emission tomography with prostate specific membrane antigen (PSMA PET) has shown promising results as a tool for this purpose. The aim of this study was to compare the accuracy of positron emission tomography with prostate-specific membrane antigen/magnetic resonance imaging (PET/MRI) using the gallium-labeled prostate-specific membrane antigen (^{68}Ga-PSMA-11) and multiparametric MRI (mpMRI) for pre-biopsy tumour localization and interreader agreement for visual and semiquantitative analysis. Semiquantitative parameters included apparent diffusion coefficient (ADC) and maximum lesion diameter for mpMRI and standardized uptake value (SUV_{max}) and PSMA-positive volume ($PSMA_{vol}$) for PSMA PET/MRI.

Results: Sensitivity and specificity were 61.4% and 92.9% for mpMRI and 66.7% and 92.9% for PSMA PET/MRI for reader one, respectively. RPE was available in 23 patients and 41 of 47 quadrants with discrepant findings. Based on RPE results, the specificity for both imaging modalities increased to 98% and 99%, and the sensitivity improved to 63.9% and 72.1% for mpMRI and PSMA PET/MRI, respectively. Both modalities yielded a substantial interreader agreement for primary tumour localization (mpMRI kappa = 0.65 (0.52–0.79), PSMA PET/MRI kappa = 0.73 (0.61–0.84)). ICC for SUV_{max}, $PSMA_{vol}$ and lesion diameter were almost perfect (≥ 0.90) while for ADC it was only moderate (ICC = 0.54 (0.04–0.78)). ADC and lesion diameter did not correlate significantly with Gleason score ($\rho = 0.26$ and $\rho = 0.16$) while SUV_{max} and $PSMA_{vol}$ did ($\rho = -0.474$ and $\rho = -0.463$).

Conclusions: PSMA PET/MRI has similar accuracy and reliability to mpMRI regarding primary prostate cancer (PCa) localization. In our cohort, semiquantitative parameters from PSMA PET/MRI correlated with tumour grade and were more reliable than the ones from mpMRI.

Springer Open

© The Author(s) 2022. **Open Access** This article is licensed under a Creative Commons Attribution 4.0 International License, which permits use, sharing, adaptation, distribution and reproduction in any medium or format, as long as you give appropriate credit to the original author(s) and the source, provide a link to the Creative Commons licence, and indicate if changes were made. The images or other third party material in this article are included in the article's Creative Commons licence, unless indicated otherwise in a credit line to the material. If material is not included in the article's Creative Commons licence and your intended use is not permitted by statutory regulation or exceeds the permitted use, you will need to obtain permission directly from the copyright holder. To view a copy of this licence, visit http://creativecommons.org/licenses/by/4.0/.

Keywords: Biopsy guidance, PSMA PET, mpMRI, Targeted biopsy, Primary staging, Interreader agreement, Template biopsy, PET/MRI, SUV_{max}, ADC

Introduction

Precise diagnosis and risk assessment are of major importance for treatment planning of prostate cancer (PCa) (American Joint Committee on Cancer and Amin 2017). Tumour diagnosis is based on prostate biopsy (American Joint Committee on Cancer and Amin 2017; Mottet, et al. 2017). While systematic 12-core ultrasound-guided biopsy lacks accuracy, saturation biopsy (SB) has a high number of cores with increased side effects (Loeb et al. 2013). Therefore, MRI-guided biopsy has been adopted by many centers in addition to systematic biopsy (Kasivisvanathan et al. 2018; Ahdoot et al. 2020; Ahmed et al. 2017; Elkhoury et al. 2019). Magnetic resonance imaging (MRI) is recommended by the European Urology Association guidelines as the standard modality for imaging-guided biopsy (Mottet, et al. 2017) with reported sensitivity and specificity ranging between 58–96% and 23–87%, respectively [Futterer et al. 2015). Furthermore, accurate and robust lesion localization needs good interreader agreement and implementation and continuous improvement of the PI-RADS scoring system has significantly improved MRI rates over time, achieving substantial agreement (Park et al. 2020).

Recently, positron emission tomography with prostate-specific membrane antigen (PSMA PET) has gained importance in the setting of PCa initial staging, especially because of its known high sensitivity and specificity for metastasis (Hofman et al. 2020). Lately, there is an increasing use of the method in treatment-naive patients. It was shown that staging PSMA PET has a general impact on management in about 21–29% of patients (Han et al. 2018; Ferraro et al. 2019; Grubmuller et al. 2018; Roach et al. 2018). Furthermore, studies have shown that the combination of PET and MRI in PSMA PET/MRI may have additional value for local assessment when compared to multiparametric MRI (mpMRI) alone, including 98% sensitivity for tumour detection without missing important information such as extraprostatic extension (Muehlematter et al. 2019; Eiber et al. 2016). Primary tumour localization with PSMA PET/MRI was assessed retrospectively in patients with biopsy-proven intermediate to high-risk PCa, showing it outperforms mpMRI (Grubmuller et al. 2018; Eiber et al. 2016; Park et al. 2018; Li et al. 2019). In the pre-biopsy setting, a recent prospective trial at our institution found PSMA PET/MRI to be negative in all seven patients with false-positive findings on mpMRI (Ferraro et al. 2021). The aim of this study was to perform a head-to-head comparison between mpMRI and PSMA PET/MR for pre-biopsy tumour localization accuracy and interreader agreement for visual and semiquantitative analysis using transperineal template saturation biopsy (TTSB) as reference standard.

Patients and methods

Study design

This is a retrospective analysis of data collected within a prospective trial (trial identification number blinded for review). The original trial aimed to assess PSMA PET/MRI diagnostic accuracy for biopsy targeting. The aim of this study is to compare PSMA PET/MRI with ^{68}Ga-PSMA-11 and mpMRI with respect to accuracy for primary

prostate cancer detection and localization and interreader agreement, using histopathology from TTSB as reference standard. Patients with elevated PSA and at least one suspicious lesion on mpMRI (PIRADS v.2 ≥ 3) were included in the trial and underwent PSMA PET/MRI. For this analysis , only patients with available mpMRI classified as adequate by our radiologist were selected. Thirty-nine of the 42 previously published patients were included, and three patients were excluded because of mpMRI imaging not available for a second readout (15). Images were anonymized and read by four specialists at our institution. Figure 1 illustrates patient selection.

^{68}Ga-PSMA-11 PET/MRI protocol

All patients underwent a pelvic PET/MRI on a dedicated hybrid scanner (SIGNA PET/MR, GE Healthcare, Waukesha, WI, USA) 60 min after injection of 85 MBq PSMA. Detailed protocol has been published previously (Ferraro et al. 2021). In brief, the PET/MR protocol included specific sequences covering the pelvis: a high-resolution T1-weighted 3D-FSPGR sequence, T2-weighted fast recovery fast spin-echo sequence in three planes and diffusion-weighted images. A 15-min frame over the prostate was recorded, allowing reducing the dose since patients without confirmed cancer were

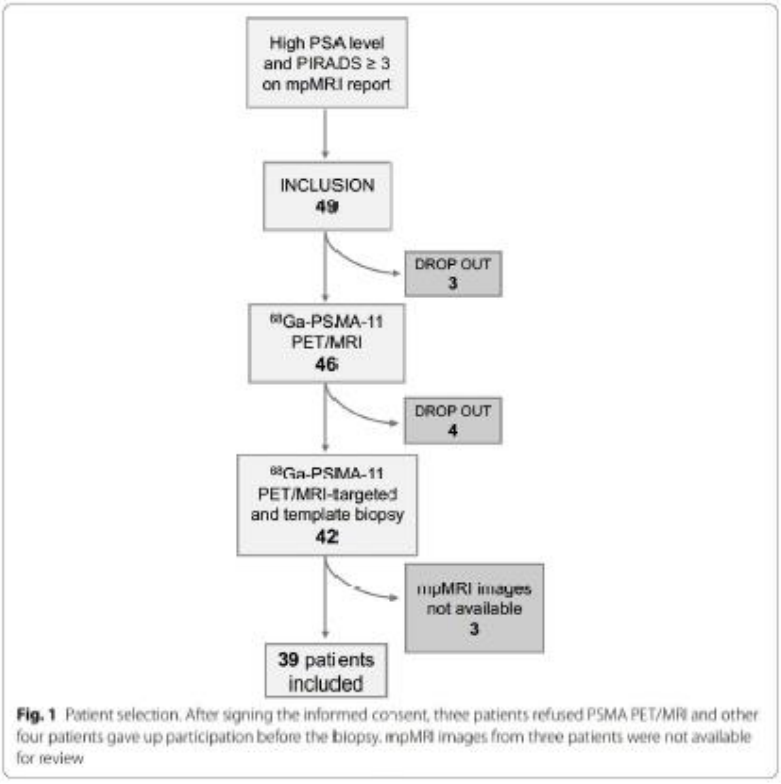

Fig. 1 Patient selection. After signing the informed consent, three patients refused PSMA PET/MRI and other four patients gave up participation before the biopsy. mpMRI images from three patients were not available for review

included. To reduce PSMA activity in the bladder, furosemide was injected intravenously 30 min prior to the ^{68}Ga-PSMA-11 injection.

mpMRI

mpMRI acquisition protocol at our institution was already published elsewhere (Muehlematter et al. 2019). The typical protocol included diffusion-weighted imaging, T2-weighted fast spin-echo in three planes and dynamic contrast-enhanced imaging and was in accordance with current guidelines (PI-RADS v2.1). Detailed information of the mpMRI protocol is given in the supplements.

Imaging analysis

Two readers for each modality (R1-M and R2-M for mpMRI and R1-P and R2-P for PSMA PET/MRI) analysed anonymized images, blinded for the results of the biopsy or for the other imaging modality as well as for clinical data. A double board-certified nuclear medicine physician and radiologist with 10 years of experience (R1-P) and a nuclear medicine physician with 2 years of experience (R2-P) analysed the PSMA PET/MRI images (PET and T2 sequence), and two expert radiologists (Rooij et al. 2016) with 10 (R1-M) and 8 (R2-M) years of experience in interpretation of mpMRI of the prostate analysed the mpMRI images. Imaging findings were delineated by the readers using a transaxial prostate map and classified according to PIRADS v2.1 (Turkbey et al. 2019) for mpMRI and according to an adaptation of the same scale for focal uptake on

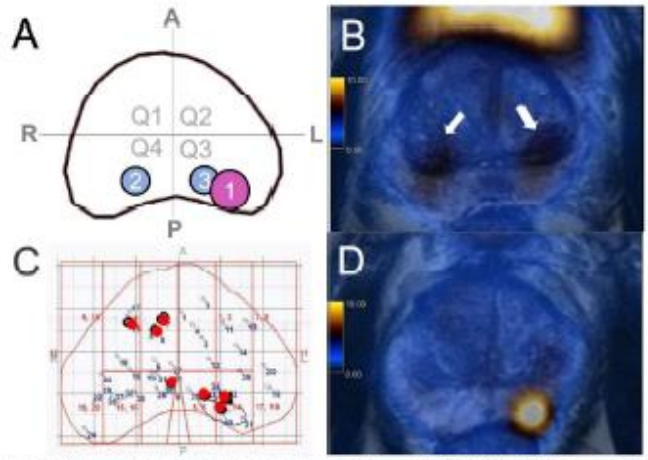

Fig. 2 Example of the method used for lesion localization. **A** Readout of PSMA PET/MRI by one of the readers with the prostate gland divided in 4 quadrants (Q1: anterior right; Q2: anterior left; Q3: posterior left and Q4: posterior right). The reader delineated three areas of ^{68}Ga-PSMA-11 uptake and labeled area 1 as suspicious for malignancy and areas 2 and 3 as benign/physiological. **B** ^{68}Ga-PSMA-11 PET/MRI images of this patient show physiological bilateral uptake in the central zone (arrows) and a suspicious area with intense uptake in the posterior peripheral zone on the left (**D**). **C** histopathological map automatically generated by the biopsy fusion software with numbered biopsy cores, red spots represent the localization of needles with Gleason score ≥ 3 + 4, confirming the suspicious lesion on Q3 and showing another lesion on Q1 not depicted on PSMA PET/MRI. For the analysis , Q1 was considered false-negative, Q2 true-negative, Q3 true-positive and Q4 false-negative (lesion crossing the midline not depicted by imaging)

^{68}Ga-PSMA-11 PET/MRI (1 = no focal uptake; 2 = benign; 3 = undetermined; 4 = suspicious for malignancy ≤ 1.5 cm; 5 = suspicious for malignancy > 1.5 cm) as illustrated in Fig. 2. Readers also recorded quantitative parameters for suspected lesions: maximum standardized uptake value (SUV_{max}) and PSMA-positive volume ($PSMA_{vol}$) from PSMA PET/MRI and from mpMRI diffusion restriction were assessed measuring the mean apparent diffusion coefficient (ADC_{mean} in 10^{-3} mm^2/s) and lesion size (maximum diameter) from mpMRI. In the case of artifacts on diffusion-weighted imaging (DWI) from the mpMRI that would affect ADC measurement, mpMRI readers were allowed to use the ADC data set from the PSMA PET/MRI study for quantitative analysis, without access to the PET images ($n = 7$) (Donati et al. 2014).

Standard reference and histology-imaging matching

Section-based TTSB was performed under general anesthesia by board certified urologists with a minimum of 2 years of experience in fusion-guided biopsies as described previously (Mortezavi et al. 2018). Cores were taken throughout the prostate according to the modified Barzell zones (20 sectors) with number of cores adapted to the prostate volume (Kanthabalan et al. 2016). All biopsies and prostatectomy specimens were analysed by one of the genito-urinary pathologists, with 9 and 11 years of experience for Gleason score (GS) and International Society of Urological Society (ISUP) grade groups (Epstein et al. 2016). In case of discordant results between PSMA PET/MRI or mpMRI and TTSB results in patients who underwent a clinically indicated prostatectomy, final GS/ISUP grade groups and lesion location from radical prostatectomy (RPE) specimen were analysed for possible explanations of false-positive or negative results, but since RPE was not available in all patients, this information was not used for the primary accuracy calculation with TTSB as the sole reference standard. We however further investigated every quadrant with discrepant results between imaging modalities or imaging and TTSB for the RPE result and calculated a secondary accuracy based on the mixed standard.

Lesions delineated by the more experienced reader from each modality were matched with the TTSB map automatically generated by the fusion software (Fig. 3). For both PSMA PET/MRI and mpMRI, readouts scores 1 and 2 were considered as negative and 3, 4 and 5 as positive for suspicious lesions. Because there are no clear anatomic landmarks to delineate the quadrants, lesions involving the anterior and posterior ipsilateral quadrants were considered as matching between imaging an histology if the main part of the lesion was delineated in the positive quadrant on histology. However, this concession was not made for lesions crossing the midline, because involvement of both lobes has prognostic value and therefore is relevant information on imaging. Clinically significant PCa (csPCa) was defined as GS ≥ 3 + 4 (ISUP ≥ 2) (Mottet et al. 2017; Briganti et al. 2018).

Data analysis and statistics

Descriptive statistics and frequencies were calculated in Excel (Excel2016, Microsoft, USA) and presented as median (interquartile range (IQR) Q1, Q3) and mean (± standard deviation (SD)). Gleason score (GS) and quadrant localization of lesions (data concatenated into quadrants anterior right, anterior left, posterior right, posterior left) were

compared to the lesions delineated by the two more experienced readers to define the accuracy of PSMA PET/MRI and mpMRI using accuracy tables and was compared using the area under the curve (AUC) from clustered receiver operating characteristic curves (ROC) data with DeLong test. Interreader agreement was calculated per quadrant using Cohen's kappa for dichotomized data (1, 2 = negative and 3, 4, 5 = positive). Intraclass correlation coefficient (ICC) of semiquantitative parameters was calculated per imaging finding (regardless of score on imaging) only for the findings in common for the two readers of each modality. Interreader coefficients were categorized according to Landis and Koch as poor (less than 0.20), fair (0.21–0.40), moderate (0.41–0.60), substantial (0.61–0.80) or almost perfect agreement (0.81–1.00) (Landis and Koch 1977). Percentage of interreader agreement for each PIRADS category or PET score category was calculated dividing the number of quadrants classified as a certain category by both readers by the number of quadrants classified as that category by at least one of the readers. Correlations between semiquantitative parameters and GS were based on the readout of the more experienced readers using Spearman's rank correlation, and GS was included as a continuous parameter for patients with cancer on biopsy, separating GS 7 in 3 + 4 and 4 + 3. All statistical computations were performed using R version 4.0.5 (R Foundation for Statistical Computing, Vienna, Austria).

Results

Thirty-nine consecutive patients were included (Fig. 1). Table 1 shows patient characteristics at study inclusion. Median interval between mpMRI and PSMA PET/MRI was 14 days (IQR 2, 78) and between biopsy and last performed imaging eight days (IQR 6, 17). RPE was available in 23 patients.

Biopsy

Median number of biopsy cores was 43 (IQR 38, 44). TTSB showed csPCa in 29/39 patients (74.3%), in 57/156 quadrants (36.5%). In 11 patients, csPCa was found in only one quadrant, in nine patients in two quadrants, in eight patients in three quadrants, and in one patient all four quadrants were positive for csPCa on TTSB. GS 3 + 4 (ISUP 2), 4 + 3 (ISUP 3), 4 + 4 (ISUP 4) and 4 + 5 (ISUP 5) were found in 30, 14, 11 and two

Table 1 Patient characteristics at study inclusion (n = 39)

Characteristics	Value
Age (years)	
Mean ± SD	64 ± 6
Median (IQR)	65 (59–68)
PSA at time of PET scan (ng/ml)	
Mean ± SD	9.9 ± 7
Median (IQR)	7.1 (6.3–10.4)
PIRADS* 2.0 n (%)	
3	5 (13%)
4	24 (61%)
5	10 (26%)

* Refers to mpMRI clinical report used for inclusion in the study

Table 2 Per-quadrant accuracy and interreader agreement results for PSMA PET/MRI and mpMRI for detection of csPCa

	PSMA PET/MRI	mpMRI	*p* value
AUC (95% CI)	0.80 (0.73, 0.86)	0.77 (0.71, 0.83)	0.56
Sensitivity	66.7%	61.4%	
Specificity	92.9%	92.9%	
PPV	84.4%	83.3%	
NPV	82.9%	80.7%	
Accuracy	83.3%	81.4%	
Cohen's Kappa coefficient* (95% CI)	0.73 (0.61–0.84)	0.65 (0.52–0.79)	

AUC, area under the receiving operator characteristics curve; CI, confidence interval; csPCa, clinically significant prostate cancer; NPV, negative predictive value; PPV, positive predictive value

*Calculated considering readout scores 1 and 2 as negative and 3, 4 and 5 as positive

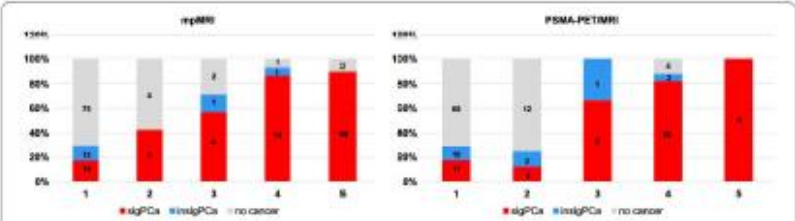

Fig. 3 Imaging findings in relation to biopsy results. Quadrant-based (n = 156) biopsy results in relation to PIRADS on mpMRI and to an adaptation of the same scale for focal uptake on PSMA PET/MRI (1 = no focal uptake; 2 = benign; 3 = undetermined; 4 = suspicious for malignancy ≤ 1.5 cm; 5 = suspicious for malignancy > 1.5 cm). csPCa = clinically significant cancer (red, GS ≥ 3 + 4); ciPCa = clinically insignificant cancer (blue, GS 3 + 3)

quadrants, respectively. Among the quadrants without csPCa, GS 3 + 3 (ISUP 1) was found in 15/99 (15%).

mpMRI and ^{68}Ga-PSMA-11 PET/MRI results

MpMRI was positive (PIRADS v2.1 ≥ 3) in 42 quadrants (27%, 42/156). PSMA PET/MRI was positive in 45 quadrants (29%, 45/156). Table 2 shows the quadrant-based accuracy for detection of csPCa for both modalities and Fig. 3 shows readout results in relation to biopsy findings, using the results from the two more experienced readers. Results of all four readers are given in the supplements (Additional file 1: Table S1).

MpMRI and PSMA PET/MRI were concordant in 135 quadrants regarding suspicion for csPCa (positive or negative) (86.5%, 135/156). Both were negative in 102 quadrants (65%, 102/156): 90 true-negative (88%, 90/102) and 12 false-negative (12%, 12/102). Both were positive in 33 quadrants (21%, 33/156): 28 true-positive (85%, 28/33) and 5 false-positive (15%, 5/33). MpMRI and PSMA PET/MRI were discordant in 21 quadrants: only mpMRI was positive in nine (seven true-positive, two false-positive), and only PSMA/PET/MRI was positive in 12 (10 true-positive, two false-positive). Figures 4 and 5 show imaging and histopathological findings of some illustrative cases in which imaging modalities were discordant or there was discordance between images and TTSB,

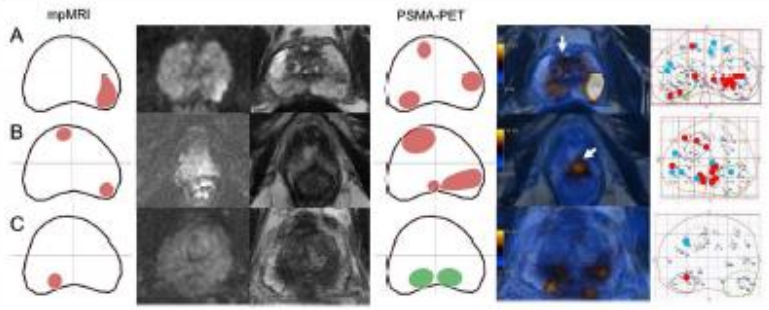

Fig. 4 Imaging and histopathological findings of cases with discordance between PSMA PET/MRI and mpMRI findings. Each line corresponds to one patient. From left to right: mpMRI readout, DWI, T2-w, PSMA PET/MRI readout, fusion PSMA PET/MRI and template biopsy map. Readouts: lesions in red were classified by the readers as suspicious while the ones in green were classified as non-suspicious. Template biopsy maps: red dots correspond to GS ≥ 3 + 4 biopsy cores and blue dots to GS 3 + 3. **A** The lesion in the left posterior quadrant was depicted on both mpMRI and PSMA PET, corresponding to csPCa on template biopsy, but the two lesions in the right quadrants were only seen on PSMA PET (arrow in the anterior one). **B** PSMA PET and mpMRI were concordant regarding the lesions in the anterior right and posterior left quadrants but the apex lesion crossing the midline to the posterior right quadrant was only seen on PSMA PET (arrow). **C** The lesion in the right posterior quadrant was seen on mpMRI but not on PSMA PET because physiological uptake in the central zones impaired the visual analysis

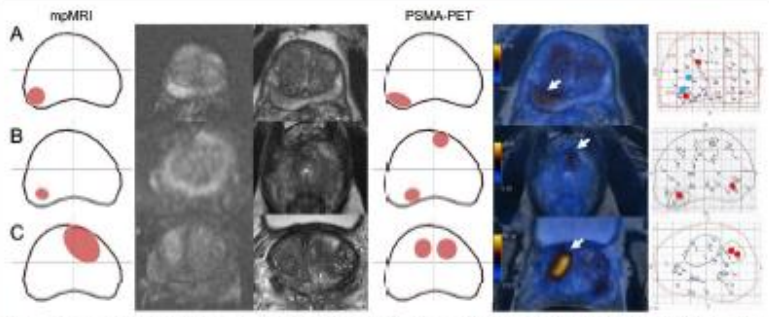

Fig. 5 Imaging and histopathological findings of cases in which imaging findings of both mpMRI and PSMA PET were false-positive or false-negative using template biopsy as reference standard. Each line corresponds to one patient. From left to right: mpMRI readout, DWI, T2-w, PSMA PET/MRI readout, fusion PSMA PET/MRI and template biopsy map. **A** Both imaging modalities depicted the lesion in the posterior right quadrant (arrows) but missed the lesion in the anterior right one (Pat. 7). **B** Both imaging modalities depicted the lesion in the posterior right quadrant (not shown) but missed the left one and PSMA PET was also false-positive for the anterior left quadrant (arrow). **C** Imaging was false-positive in the anterior right quadrant, on mpMRI the lesion seems to cross the midline while in PSMA PET the uptake suggests a second lesion (arrow)

respectively. RPE specimen was available for analysis in 18 of these patients. Detailed information about false-positive and false-negative cases as well as RPE results can be found in Tables 3 and 4.

In a per quadrant analysis, performing PSMA PET instead of mpMRI prior to biopsy leads to detection of 10/156 (6.4%) additional quadrants and miss 7/156 (4.5%) quadrants harboring csPCa assessed by TTPB. These seven false-negative quadrants in

Table 3 Imaging and histopathological findings of quadrants with disagreement between PSMA PET/MRI and mpMRI ($n = 21$*)

	Quad	mpMRI PIRADS	PSMA PET/MRI score	Biopsy ISUP	Final diagnosis
Pat. 1	4	2	4	2	No RPE. PSA dropped after HIFU
Pat. 8	1	1	4	1	ISUP 2
Pat. 11	1/2	1/1	4/4	2/3	ISUP 3
Pat. 11	3	2	4	3	ISUP 3
Pat. 22	4	1	5	3	No follow up or RPE
Pat. 24	2	1	4	No cancer	ISUP 3
Pat. 30	1/4	1/1	4/4	2/4	ISUP 2/ISUP 4
Pat. 32	4	1	4	2	ISUP 3
Pat. 35	2	1	3	2	ISUP 2
Pat. 42	1	1	4	2	ISUP 2
Pat. 6	3	5	1	No cancer	No follow up or RPE
Pat. 10	1	5	1	3	ISUP 3
Pat. 17	3	3	1	No cancer	No cancer
Pat. 19	4	4	2	2	ISUP 3
Pat. 26	2	5	1	4	ISUP 2
Pat. 33	3	4	1	2	ISUP 2
Pat. 39	1/2	5/5	1/1	2/2	No RPE. IHC of biopsy cores showed PSMA-negative tumour
Pat. 42	3	3	1	2	ISUP 2 (infiltrative pattern)

HIFU, high intensity focused ultrasound; IHC, immunohistochemistry staining; Pat., patient; Quad, quadrant; RPE, radical prostatectomy

* PSMA PET positive in 12 and mpMRI in 9

Table 4 Imaging and histopathological findings of the quadrants in which both imaging modalities (PSMA PET/MRI and mpMRI) disagree with template biopsy results ($n = 17$ quadrants)

	Quad	Imaging	mpMRI PIRADS	PSMA PET/MRI score	Biopsy ISUP	Final diagnosis
Pat. 4	3	FN	1	1	2	No follow up or RPE
Pat. 7	1	FN	1	1	3 (1 mm)	No cancer
Pat. 16	1/4	FN	1/1	1/2	3/2	ISUP 2
Pat. 17	4	FN	1	1	2	ISUP 2
Pat. 24	3	FN	1	1	2 (2 mm)	No cancer
Pat. 26	1	FN	1	1	4	ISUP 2
Pat. 31	4	FN	1	1	2	ISUP 2
Pat. 33	1	FN	1	1	2	ISUP 3 (infiltrative pattern)
Pat. 34	2	FN	1	1	2 (2 mm)	ISUP 2 (1 mm)
Pat. 40	2	FN	1	1	4	ISUP 2
Pat. 41	4	FN	2	1	2	ISUP 2
Pat. 8	4	FP	4	4	1	ISUP 2
Pat. 23	4	FP	3	3	1 (several cores, 7 mm)	No follow up or RPE
Pat. 34	1	FP	4	4	No cancer	ISUP 3
Pat. 35	3	FP	3	4	No cancer	ISUP 3
Pat. 38	1	FP	5	4	No cancer	ISUP 2 (8 mm, foamy differentiation)

FN, false-negative; FP, false-positive; Pat., patient; Quad, quadrant; RPE, radical prostatectomy

PSMA were graded after TTPB as GS 3+4=7 (ISUP 2) in five cases, GS 4+3=7 (ISUP 3) in one case and GS 4+4=8 (ISUP 4) in one case.

Semiquantitative results

Correlation between semiquantitative parameters and GS is also shown in Table 5, with significant correlation for both PET parameters (SUV_{max} and $PSMA_{vol}$) but no association between GS with size or ADC values on mpMRI.

Interreader agreement

Both modalities yielded a substantial interreader agreement for primary tumour localization per quadrant (Table 2). The main reason of discordance was that the less-experienced readers considered as suspicious lesions that were not suspicious for the more-experiences readers, which occurred in 13 quadrants in mpMRI and 11 quadrants in PSMA PET/MRI. Most of these quadrants (8/13 in mpMRI and 9/11 in PSMA PET/MRI) were proven negative by TTSB resulting in a lower specificity for the less-experienced readers (Additional file 1: Table S1). The score that held the highest disagreement rates was score 3, with an agreement rate of 13.3% for mpMRI (2/15 quadrants) and no agreement for PSMA PET (0/5 quadrants). MpMRI and PSMA PET/MRI agreement rates for scores 1 and/or 2 were 82% and 85%, respectively, and for scores 4 and/or 5 was 54% and 74%, respectively. Reasons for disagreement on PSMA PET/MRI included physiological uptake in the central zone and uptake close to the urethra that was misinterpreted by the less-experienced reader.

Interreader agreement for semiquantitative parameters was based on 31 lesions on mpMRI (31 common lesions for both readers, R1-M reported additional 10 lesions and R2-M reported 8), and 50 lesions were reported on PSMA PET/MRI by both readers (R1-P reported 5 and R2-P reported 9 additional findings). Lesion size on mpMRI as well as PSMA PET/MRI semiquantitative parameters yielded an almost perfect interreader agreement while for ADC it was only moderate (Table 5).

Secondary analysis of quadrants with discrepant finding between imaging and biopsy

RPE was available in 23 of the 38 quadrants with discrepant findings (false-negative or false-positive on mpMRI or PSMA PET (Table 3) or on both (Table 4)). For those quadrants without RPE available, TTSB remained the standard reference. Of the 12 quadrants that were false-negative on both imaging modalities, further workup with RPE showed

Table 5 Semiquantitative parameters

	Median (IQR)	Mean (± SD)	ICC R1 × R2	Correlation with GS
SUV_{max}	6.8 (4.7, 10.5)	10.2 (± 12.8)	0.99 (0.99, 0.99)	ρ=0.474 (p=0.002)
$PSMA_{vol}$	0.8 (0.4, 0.6)	1.8 (± 2.1)	0.90 (0.83, 0.94)	ρ=0.468 (p=0.003)
ADC	832.5 (688.8, 966.3)	836.3 (± 263.9)	0.54 (0.04, 0.78)	ρ=−0.182 (p=0.26)
Size*	1.3 (1, 1.6)	1.4 (± 0.6)	0.90 (0.8, 0.95)	ρ=0.220 (p=0.16)

Median, mean and correlation with GS based on results from the more experienced reader

GS, Gleason score; IQR, interquartile rage (Q1, Q3); ICC, intraclass correlation coefficient; R1, reader 1; R2, reader 2; SD, standard deviation

* On mpMRI

that two had no cancer (biopsy GS 3+4 and 4+3, ISUP 2 and 3). Eight quadrants were confirmed as GS 3+4 (ISUP 2) disease and one quadrant harbored a lesion with GS 4+3 (ISUP 3). Among the five quadrants that were false-positive on PSMA PET/MRI and mpMRI, RPE was available in four, showing GS 3+4 (ISUP 2) or GS 4+3 (ISUP 3) disease in all of them. Among the 21 quadrants with disagreement between mpMRI and PSMA PET/MRI, RPE showed true-positive lesions in 10 quadrants on PSMA PET/MRI and five quadrants on mpMRI. One quadrant negative on biopsy showed GS 4+3 (ISUP 3) cancer on RPE (true-positive on PSMA PET/MRI with PIRADS 1 on mpMRI).

Taking the discrepancies between biopsy results and RPE into account, the sensitivity and specificity of reader one for mpMRI would rise to 63.9% and 94.7%, and for PSMA PET/MRI to 72.1% and 96.8%, respectively.

Discussion

Per-quadrant accuracy for tumour localization before biopsy did not differ significantly for mpMRI and PSMA PET/MRI, with sensitivities of around 61% and 67%, respectively, and specificity of ≈ 93% for both methods. Interreader agreement for lesion localization was substantial for both modalities but slightly higher for PSMA PET/MRI compared to mpMRI (0.73 vs 0.65). PSMA PET/MRI semiquantitative parameters (SUV_{max} and $PSMA_{vol}$) had an almost perfect interreader agreement as well as lesion size on mpMRI, while for ADC it was only moderate. Furthermore, SUV_{max} and $PSMA_{vol}$ correlated with biopsy GS, but mpMRI semiquantitative parameters did not. Our findings suggest PSMA PET/MRI could be used to guide biopsy in patients with suspicious prostate cancer, with similar accuracy and reliability in comparison with mpMRI regarding lesion localization, but with a more robust assessment of lesion aggressiveness by semiquantitative parameters.

The relatively lower per-quadrant accuracy for primary tumour localization on PSMA PET/MRI compared to our previously published per-patient accuracy (83.3% vs 88.0%) (Ferraro et al. 2021) is in concordance with other results. Eiber et al. reported 98% tumour detection with PSMA PET/MRI on a patient basis but only 76% of sensitivity for lesion localization in prostate per sextants (Eiber et al. 2016), and Park et al. reported a sensitivity of around 85% using per-lobe localization (Park et al. 2018). Bodar et al. reported a significant drop in sensitivity and specificity in their cohort from 84.4 to 61.4% and from 97 to 88%, respectively, when using more stringent criteria of tumour localization with PSMA PET/CT using 12 prostate regions (Bodar et al. 2020). This drop in accuracy might also reflect the limitation of TTSB as a reference standard.

Furthermore, the current results also point out that TTSB as a reference standard has limitations. Incorporating the RPE results for all quadrants with discrepant findings was rising the specificity for both imaging modalities to around 95% (mpMRI) and 97% (PSMA PET/MRI). Also the sensitivity improved for both imaging methods, from around 61 to 64% for mpMRI and from around 67 to 72% for PSMA PET/MRI, respectively. Given that several patients did not have any evidence for significant PCa on imaging or biopsy, despite the initial PIRADS 3 lesions on the clinical read out of the mpMRI, we could not incorporate RPE systematically within this study. However, the observation reflects the limitation of TTSB, which despite being the most accurate way to study the prostate through biopsies still has a substantial disagreement

with RPE results (Crawford et al. 2013). Causes of false-positive and false-negative results on PSMA PET/MRI in this cohort were already published and discussed elsewhere (Ferraro et al. 2021).

MpMRI PIRADS version 2 interreader agreement has been extensively assessed in the literature. In a meta-analysis including 4095 patients, Greer et al. (2019) found substantial interreader agreement using score 4 as cutoff but observed fair to moderate agreement using score 3. They also found significant variation associated with reader experience. Similarly, we have observed a low interreader agreement on lesions classified as PIRADS 3, and in our cohort reader experienced affected specificity more than sensitivity. Furthermore, a high agreement of 82–85% on negative quadrants was already reported by Brembilla et al. (2020), which matches well our result of 82%.

PSMA PET interreader agreement is known to be high for primary tumour detection and agreement for T, N and M range from substantial to almost perfect in the literature (Basha et al. 2019; Fendler et al. 2017; Toriihara et al. 2020). Therefore, we expected it to be high in the pre-biopsy context for primary tumour localization, which is crucial in the biopsy-guidance setting. Our results indeed show substantial agreement for both primary tumour detection and its localization but also draw attention to some pitfalls on PSMA PET/MRI such as physiological uptake in the central zone (Pizzuto et al. 2018) or uptake close to the urethra, which can potentially mislead readers that lack MRI training despite of awareness of the potential pitfalls.

The full potential of semiquantitative measures on imaging is still under investigation. SUV_{max} correlation to GS has been shown before (Uprimny et al. 2017) as well as to presence of lymph node metastasis (Ferraro 2019). In fact, SUV_{max} reflects the tumour PSMA expression (Woythal et al. 2018), which correlates to tumour aggressiveness and has prognostic value (Paschalis et al. 2019; Hupe et al. 2018). In our cohort, both SUV_{max} and $PSMA_{vol}$ positively correlated with GS on TTSB. While an inverse correlation between mpMRI ADC value and GS can be demonstrated in large meta analysis (Shaish et al. 2017), ADC more strongly correlates with other cellularity metrics/differences in tumour architecture (Chatterjee et al. 2015). As expected, in our cohort however, neither ADC nor tumour size on mpMRI correlated significantly with GS. Furthermore, ADC had the lowest interreader agreement, suggesting overall that parameters derived from PSMA expression and tumour size are more robust for prediction of GS.

Important considerations must be made about PSMA PET/MRI. It is not an ionizing radiation-free modality, it is not widely available, and no study so far assessed its cost-effectiveness in the pre-biopsy setting of PCa. This study showed that PSMA PET/MRI can localize the primary tumour with similar accuracy to mpMRI read by a dedicated genitourinary radiologist and it has substantial interreader agreement. However, further studies are needed to determine which patients could benefit from it in clinical routine. Interestingly, in the present readout 11 of 39 patients that had a PIRADS $\geq$ 3 lesion on clinical read out were considered as not suspicious (PIRADS 1/2) by Reader 1. This probably reflects the higher accuracy of mpMRI read by a dedicated genitourinary radiologist compared to clinical reports, whose positive predictive value can vary widely (Westphalen et al. 2020). Interestingly, this seems to be less problematic on PSMA PET/MRI, since a nuclear medicine physician without specific MRI training with two years of experience was able to reach a moderate interreader agreement.

Limitations of this study include its retrospective nature, the lack of whole mount prostatectomy specimens as standard of reference and the quadrant-based approach. These limitations were partially mitigated by using TTSB with an extensive number of cores (median 43) and a careful readout by a nuclear physician and a radiologist together to define quadrant status as positive or negative based on matching histopathology and lesions delineated on the imaging readouts. Another drawback is the lack of validation for the 5-point score used for PSMA PET/MRI, which was chosen to allow a direct comparison between the two imaging modalities. Finally, inherent limitations of using score 3 as cutoff for positive quadrants must be acknowledged since its impact in accuracy was already shown for mpMRI (Wadera et al. 2021). However, we believe this is the most reasonable approach for patients imaged in the pre-biopsy setting, in which targeting a false-positive lesion would probably bring less harm than failing to target a csPCa lesion or dismissing from biopsy a patient with csPCa.

Conclusion

PSMA PET/MRI has similar accuracy and reliability to mpMRI regarding primary PCa localization. Semiquantitative parameters from PSMA PET/MRI correlated with tumour grade and were more reliable than the ones from mpMRI. Further studies are needed to determine which patients could benefit from pre-biopsy PSMA PET/MRI in clinical routine.

Supplementary Information

The online version contains supplementary material available at https://doi.org/10.1186/s41824-022-00135-4.

Additional file 1. Readout sheet layout, Table S1 and mpMRI protocol.

Acknowledgements
The authors acknowledge the technicians Marlena Hofbauer and Josephine Trinckauf and their team for the excellent work on high-quality PET images. DAF thanks the USZ ICT team for making it possible for her to do part of this work remotely.

Author contributions
IAB, OFD and DE contributed to study concept and design. UAF, AH, RL, NJR, JHR, JM and AM contributed to acquisition of data. DAF, IAB and ASB contributed to analysis and interpretation of data. DAF and IAB drafted the manuscript. DAF and ASB contributed to statistical analysis. All authors critically revised the manuscript for important intellectual content. IM and AB contributed to administrative, technical or material support. MTS, DE, OFD and IAB supervised the study. All authors read and approved the final manuscript.

Funding
The authors thank the Sick legat and the Iten-Kohaut foundation for their financial support. This study was financed in part by the Coordenação de Aperfeiçoamento de Pessoal de Nível Superior-Brasil (CAPES)-Finance Code 001. ASB was funded in part through the NIH/NCI Cancer Center Support Grant P30 CA008748 and the Peter Michael Foundation.

Availability of data and materials
The datasets generated during and/or analysed during the current study are available from the corresponding author on reasonable request.

Declarations

Ethics approval
This study was performed in line with the principles of the Declaration of Helsinki. Approval was granted by the Cantonal Ethics Committee of Zurich (Date: 03/23/2017/BASEC Nr: 2017-00016).

Consent to participate
Informed consent was obtained from all individual participants included in the study.

Competing interests

IAB has received research grants and speaker honorarium from GE Healthcare, research grants from Swiss Life, and speaker honorarium from Bayer Health Care and Astellas Pharma AG. MM received speaker fees from GE Healthcare. The Department of Nuclear Medicine holds an institutional Research Contract with GE Healthcare. NJR has provided consultancy services (advisory board member) to F. Hoffmann-La Roche AG. ASB received research grants from the Prof. Dr. Max Cloëtta Foundation, medAlumni UZH, and the Swiss Society of Radiology. All other authors declare no competing interests.

Author details

[1]Department of Nuclear Medicine, University Hospital Zürich , University of Zurich, Rämistrasse 100, 8091 Zurich, Switzerland. [2]Department of Radiology and Oncology, Faculdade de Medicina FMUSP, Universidade de São Paulo, São Paulo, Brazil. [3]University of Zurich, Zurich, Switzerland. [4]Diagnostic and Interventional Radiology, University Hospital Zurich, University of Zurich, Zurich, Switzerland. [5]Department of Radiology, Memorial Sloan Kettering Cancer Center, New York City, USA. [6]Department of Urology, University Hospital Zürich, University of Zurich, Zurich, Switzerland. [7]Department of Biomedical and Dental Sciences and Morpho-Functional Imaging, Nuclear Medicine Unit, University of Messina, Messina, Italy. [8]Department of Pathology and Molecular Pathology, University Hospital Zurich, University of Zurich, Zurich, Switzerland. [9]Department of Urology, University Hospital Basel, Basel, Switzerland. [10]Department of Nuclear Medicine, Kantonsspital Baden, Baden, Switzerland.

Received: 20 February 2022 Accepted: 3 April 2022
Published online: 18 July 2022

References

Ahdoot M et al (2020) MRI-targeted, systematic, and combined biopsy for prostate cancer diagnosis. N Engl J Med 382(10):917–928
Ahmed HU et al (2017) Diagnostic accuracy of multi-parametric MRI and TRUS biopsy in prostate cancer (PROMIS): a paired validating confirmatory study. Lancet 389(10071):815–822
American Joint Committee on Cancer, Amin MB (2017) AJCC cancer staging manual. Springer, New York
Basha MAA et al (2019) (68)Ga-PSMA-11 PET/CT in newly diagnosed prostate cancer: diagnostic sensitivity and interobserver agreement. Abdom Radiol (NY) 44(7):2545–2556
Bodar YJL et al (2020) Detection of prostate cancer with (18)F-DCFPyL PET/CT compared to final histopathology of radical prostatectomy specimens: is PSMA-targeted biopsy feasible? The DeTeCT trial. World J Urol 39:2439–2446
Brembilla G et al (2020) Interreader variability in prostate MRI reporting using prostate imaging reporting and data system version 2.1. Eur Radiol 30(6):3383–3392
Briganti A et al (2018) Active surveillance for low-risk prostate cancer: The European Association of Urology Position in 2018. Eur Urol 74(3):357–368
Chatterjee A et al (2015) Changes in epithelium, stroma, and lumen space correlate more strongly with gleason pattern and are stronger predictors of prostate ADC changes than cellularity metrics. Radiology 277(3):751–762
Crawford ED et al (2013) Clinical-pathologic correlation between transperineal mapping biopsies of the prostate and three-dimensional reconstruction of prostatectomy specimens. Prostate 73(7):778–787
de Rooij M et al (2016) Accuracy of magnetic resonance imaging for local staging of prostate cancer: a diagnostic meta-analysis. Eur Urol 70(2):233–245
Donati OF et al (2014) Diffusion-weighted MR imaging of upper abdominal organs: field strength and intervendor variability of apparent diffusion coefficients. Radiology 270(2):454–463
Eiber M et al (2016) Simultaneous (68)Ga-PSMA HBED-CC PET/MRI Improves the localization of primary prostate cancer. Eur Urol 70(5):829–836
Elkhoury FF et al (2019) Comparison of targeted vs systematic prostate biopsy in men who are biopsy naive: the prospective assessment of image registration in the diagnosis of prostate cancer (PAIREDCAP) study. JAMA Surg 154(9):811–818
Epstein JI et al (2016) The 2014 International Society of Urological Pathology (ISUP) consensus conference on gleason grading of prostatic carcinoma: definition of grading patterns and proposal for a new grading system. Am J Surg Pathol 40(2):244–252
Fendler WP et al (2017) (68)Ga-PSMA-11 PET/CT Interobserver Agreement for Prostate Cancer Assessments: an International multicenter prospective study. J Nucl Med 58(10):1617–1623
Ferraro DA et al (2019) Impact of (68)Ga-PSMA-11 PET staging on clinical decision-making in patients with intermediate or high-risk prostate cancer. Eur J Nucl Med Mol Imaging 47:652–664
Ferraro DA et al (2021) Diagnostic performance of (68)Ga-PSMA-11 PET/MRI-guided biopsy in patients with suspected prostate cancer: a prospective single-center study. Eur J Nucl Med Mol Imaging 48:3315–3324
Ferraro DA et al (2019) (68)Ga-PSMA-11 PET has the potential to improve patient selection for extended pelvic lymph node dissection in intermediate to high-risk prostate cancer. Eur J Nucl Med Mol Imaging
Futterer JJ et al (2015) Can clinically significant prostate cancer be detected with multiparametric magnetic resonance imaging? A systematic review of the literature. Eur Urol 58(6):1045–1053
Greer MD et al (2019) Interreader variability of prostate imaging reporting and data system version 2 in detecting and assessing prostate cancer lesions at prostate MRI. AJR Am J Roentgenol. https://doi.org/10.2214/AJR.18.20536
Grubmuller B et al (2018) PSMA ligand PET/MRI for primary prostate cancer: staging performance and clinical impact. Clin Cancer Res 24(24):6300–6307
Han S et al (2018) Impact of (68)Ga-PSMA PET on the management of patients with prostate cancer: a systematic review and meta-analysis. Eur Urol 74:179–190

Hofman MS et al (2020) Prostate-specific membrane antigen PET-CT in patients with high-risk prostate cancer before curative-intent surgery or radiotherapy (proPSMA): a prospective, randomised, multi-centre study. Lancet 395:1208–1216
Hupe MC et al (2018) Expression of prostate-specific membrane antigen (PSMA) on biopsies is an independent risk stratifier of prostate cancer patients at time of initial diagnosis. Front Oncol 8:623
Kanthabalan A et al (2016) Transperineal magnetic resonance imaging-targeted biopsy versus transperineal template prostate mapping biopsy in the detection of localised radio-recurrent prostate cancer. Clin Oncol (r Coll Radiol) 28(9):568–576
Kasivisvanathan V et al (2018) MRI-targeted or standard biopsy for prostate-cancer diagnosis. N Engl J Med 378(19):1767–1777
Landis JR, Koch GG (1977) The measurement of observer agreement for categorical data. Biometrics 33(1):159–174
Li M et al (2019) Comparison of PET/MRI with multiparametric MRI in diagnosis of primary prostate cancer: a meta-analysis. Eur J Radiol 113:225–231
Loeb S et al (2013) Systematic review of complications of prostate biopsy. Eur Urol 64(6):876–892
Mortezavi A et al (2018) Diagnostic accuracy of multiparametric magnetic resonance imaging and fusion guided targeted biopsy evaluated by transperineal template saturation prostate biopsy for the detection and characterization of prostate cancer. J Urol 200(2):309–318
Mottet N et al (2017) EAU-ESTRO-SIOG guidelines on prostate cancer. Part 1: Screening, diagnosis, and local treatment with curative intent. Eur Urol 71(4):618–629
Muehlematter UJ et al (2019) Diagnostic accuracy of multiparametric MRI versus (68)Ga-PSMA-11 PET/MRI for extracapsular extension and seminal vesicle invasion in patients with prostate cancer. Radiology 293(2):350–358
Park SY et al (2018) Gallium 68 PSMA-11 PET/MR imaging in patients with intermediate- or high-risk prostate cancer. Radiology 288(2):495–505
Park KJ et al (2020) Interreader agreement with prostate imaging reporting and data system version 2 for prostate cancer detection: a systematic review and meta-analysis. J Urol JUM(4):661–670
Paschalis A et al (2019) Prostate-specific membrane antigen heterogeneity and DNA repair defects in prostate cancer. Eur Urol 76:469–478
Pizzuto DA et al (2018) The central zone has increased (68)Ga-PSMA-11 uptake: "Mickey Mouse ears" can be hot on (68)Ga-PSMA-11 PET. Eur J Nucl Med Mol Imaging 45(8):1335–1343
Roach PJ et al (2018) The Impact of (68)Ga-PSMA PET/CT on management intent in prostate cancer: results of an australian prospective multicenter study. J Nucl Med 59(1):82–88
Shaish H, Kang SK, Rosenkrantz AB (2017) The utility of quantitative ADC values for differentiating high-risk from low-risk prostate cancer: a systematic review and meta-analysis. Abdom Radiol (NY) 42(1):260–270
Toriihara A et al (2020) Comparison of 3 interpretation criteria for (68)Ga-PSMA11 PET based on inter- and intrareader agreement. J Nucl Med 61(4):533–539
Turkbey B et al (2019) Prostate imaging reporting and data system version 2.1: 2019 update of prostate imaging reporting and data system version 2. Eur Urol 76(3):340–351
Uprimny C et al (2017) (68)Ga-PSMA-11 PET/CT in primary staging of prostate cancer: PSA and Gleason score predict the intensity of tracer accumulation in the primary tumour. Eur J Nucl Med Mol Imaging 44(6):941–949
Wadera A et al (2021) Impact of PI-RADS Category 3 lesions on the diagnostic accuracy of MRI for detecting prostate cancer and the prevalence of prostate cancer within each PI-RADS category: a systematic review and meta-analysis. Br J Radiol 94(1118):20191050
Westphalen AC et al (2020) Variability of the positive predictive value of PI-RADS for prostate MRI across 26 centers: experience of the society of abdominal radiology prostate cancer disease-focused panel. Radiology 296(1):76–84
Woythal N et al (2018) Immunohistochemical validation of PSMA expression measured by (68)Ga-PSMA PET/CT in primary prostate cancer. J Nucl Med 59(2):238–243

Publisher's Note

Springer Nature remains neutral with regard to jurisdictional claims in published maps and institutional affiliations.

Submit your manuscript to a SpringerOpen journal and benefit from:

- ► Convenient online submission
- ► Rigorous peer review
- ► Open access: articles freely available online
- ► High visibility within the field
- ► Retaining the copyright to your article

Submit your next manuscript at ► springeropen.com